

**Gene expression profiling in human hepatic and neuronal  
cells by Wasabi-derived isothiocyanates**

A dissertation presented

To

**THE UNITED GRADUATED SCHOOL  
OF AGRICULTURAL SCIENCES  
KAGOSHIMA UNIVERSITY**



In partial fulfillment for the degree of

**DOCTOR OF PHILOSOPHY**

**PHOEBE ZAPANTA TRIO**

December 2016

Kagoshima, Japan



## ACKNOWLEDGMENT

The recently concluded research study carried out in Kagoshima University and subsidized by Ministry of Education, Culture, Sports, Science and Technology-Japan (MEXT) under the supervision of Prof. De-Xing Hou would not be feasible without the support and assistance of various individuals.

First and foremost, my utmost gratitude to Prof. De-Xing Hou, my laboratory supervisor, for the unwavering mentoring, supervision and encouragement throughout the duration of the course. Thank you not only for the scientific knowledge and skills imparted but also for the nuggets of wisdom shared especially when I was ready to give up graduate school. Without your intervention, I would not be able to come up with the dissertation.

My deepest thanks to Prof. Fumio Hashimoto of Kagoshima University and Prof. Koji Nagao of Saga University, my co-supervisors, for the valuable technical comments and feedbacks.

My sincere thanks to Dr. Kozue Sakao of Kagoshima University, our laboratory assistant professor, for being available and accommodating in every consultation. Thank you for the positive criticisms and kind words whenever I am uncertain.

My heartfelt gratitude to Ayami Hisanaga, my tutor, for being a helping hand not only in all the academic procedures I underwent but also in transitioning to Japanese culture and environment.

Grateful to the Laboratory of Food Function and Nutrigenomics, my home away from home, for the opportunity to work and allowing me to conduct the research. Many

thanks to the past and present members of the laboratory for the ideas, time, and memories shared, help rendered, and patience. Also, to KU United Graduate School of Agricultural Sciences and ISO staff, for the assistance and entertaining our queries.

Thankful for friends here and abroad, for being the source of fun, great conversations, and sounding board. Also, for my church family for the prayers and comforts offered.

My overwhelming appreciation to my family, not only for the unending support and understanding towards my academic pursuits but also for challenging me to go through and finish every tough journey. Indeed, there's more to life beyond the comfort zone.

Above all to the Almighty Father for being a rock of stability in my life. All praises and honor are due unto Him.

Lastly, to anyone that I may have forgotten, my thank you and apology as well.

Phoebe Z. Trio

Kagoshima, December 2016



## ABSTRACT

Wasabi (*Wasabia japonica* (Miq.) Matsumara) is a member of Brassicaceae vegetables, and a popular condiment in Japanese households. Wasabi contains high amount of isothiocyanates (ITCs) such as 6-(Methylsulfinyl)hexyl isothiocyanate (6-MSITC), 6-(methylthio)hexyl isothiocyanate (6-MTITC) and sulforaphane (SFN). These ITCs have been reported to have antioxidant, anti-inflammatory, and anti-cancer activities, although the molecular mechanisms are not clear. Therefore, this study is designed to clarify the genome-wide gene expression profiles in hepatic cells, HepG2, and neuron cells, IMR-32 stimulated by the three ITCs, using microarray technology.

In HepG2 cells, comparative gene expression profiling was performed by treating the cells with ITCs, followed by DNA microarray analyses using HG-U133 plus 2.0 oligonucleotide array. Partial array data on selected gene products were confirmed by real-time polymerase chain reaction (PCR), and functional subsets of genes and biologically significant network were identified using Ingenuity Pathway Analysis (IPA). Array data showed that 6-MTITC had the highest number of differentially altered ( $\geq 2$ ) gene expressions, consist of 114 upregulated genes and 75 downregulated genes. Furthermore, IPA revealed that Nrf2-mediated pathway was the common significantly modulated pathway across the ITCs treatment, along with glutamate metabolism pathway. Interestingly, 6-MSITC was the most potent activator of Nrf2-mediated pathway. Thus, our data suggest that 6-MSITC could exert cytoprotective function through the activation of Nrf2-mediated antioxidant pathway.

Next, DNA microarray profiling was designed in neuron cells, IMR-32, treated with the three ITCs to profile the global changes at the transcript level. Among the three ITCs, 6-MSITC caused expression changes of most genes, of which 100 genes were upregulated and 163 genes were downregulated. Biological gene categorization using Gene Ontology (GO) revealed that most of the differentially expressed genes are associated with oxidative stress response. Pathway analysis by IPA further demonstrated that Nrf2-mediated antioxidant pathway was the top of the most modulated pathways by ITCs. Lastly, real-time PCR and Western blot analyses confirmed the gene expressions and protein products which were mainly targeted by ITCs. Therefore, these results suggest that Wasabi-derived ITCs might target the Nrf2-mediated antioxidant pathway to exert its neuroprotective function.

In summary, comparative DNA microarray profiling analysis unveiled that 6-MTITC was the most potent inducer of gene expressions changes in HepG2 cells, whereas 6-MSITC was the most effective inducer in IMR-32 cells. Despite this cell-type response discrepancies, 6-MSITC prevailed as the strongest inducer of antioxidant-associated genes, which was through the activation of the Nrf2-mediated pathway. Altogether, this study provided comprehensive information on how structural differences of Wasabi-ITCs contribute to its efficacy and impact specific targets.

## 要 旨

“ワサビ”はアブラナ科の植物で、日本人の食卓に人気の薬味調味料である。ワサビには、6-MSITC、6-MTITC、SFN などのイソチオシアネート化合物 (ITCs) が含まれている。これらの ITCs が抗酸化活性、抗炎症活性、抗がん活性を有することは多数報告されてきているが、詳細な分子メカニズムはまだ明らかではない。そこで本研究では、DNA マイクロアレイ解析技術を用いてこれらの ITCs によるヒト肝細胞 (HepG2) ならびにヒト神経芽細胞 (IMR-32) の遺伝子発現に及ぼす影響について網羅的解析を行った。

HepG2 細胞においては、3 種類の ITCs を処理したのち、包括的ヒトゲノム発現解析用アレイである HG-U133 plus 2.0 oligonucleotide array を用いて相対的な遺伝子発現プロファイリングを行った。一部の遺伝子発現のアレイデータはリアルタイム PCR により確認した。その結果、2 倍以上発現した遺伝子数は、6-MTITC が最大で、発現上昇を示した遺伝子は 114 個、発現減少を示した遺伝子は 75 個だった。さらに、遺伝子発現制御のネットワーク解析は、論文を根拠とした相互作用情報データベースである IPA ソフトウェアを用いて行った。その結果、主に 5 つの経路で制御されていることが明らかになった。その中に Nrf2 およびグルタミン酸代謝経路を介した遺伝子発現は 3 種類の ITCs に共通で、顕著に発現変動を引き起こすことが IPA 解析により明らかになった。興味深いことに 3 種類の ITCs とも一番強く Nrf2 経路を活性化した。これらの結果は、3 種類の ITCs が Nrf2 を介した抗酸化経路を活性化することでがんに対する化学的予防効果を発揮することを明らかにした。

次に、3種類のITCsで処理したヒト神経芽細胞IMR-32において、同様にヒトゲノム発現解析用マイクロアレイで遺伝子発現の変化を網羅的に解析した。3種類のITCsの中で6-MSITCが最も多くの遺伝子発現変動を引き起こし、発現上昇を示した遺伝子は100個、発現減少を示した遺伝子は163個だった。特定遺伝子の機能情報を検索するGene Ontology及びIPA解析により、変動を示した遺伝子のほとんどが酸化ストレス応答に関連するものであり、特にNrf2を介した抗酸化経路が最も活性化されていることが明らかになった。また、主なターゲット遺伝子の発現をリアルタイムPCR法で、そのタンパク質をウェスタンブロット法で確認した結果、これらのワサビITCsはNrf2を介した抗酸化経路を活性化することで神経細胞保護機能を発揮することを明らかにした。

総括として、本研究は、DNAマイクロアレイ解析技術を用いてヒト肝細胞ならびにヒト神経芽細胞の遺伝子発現に対するワサビイソチオシアネート化合物の影響について、その構造と活性の関係をゲノムレベルで明らかにした。さらに、遺伝子発現制御の経路解析でこれらの遺伝子の発現変動は、主に5つの経路で制御されており、特に、両細胞においてもNrf2を介した抗酸化経路が最も活性化されていることを明らかにした。これらの成果は、ワサビイソチオシアネート化合物の機能性に関する分子機構に新たな知見を与えるものである。

## LIST OF ABBREVIATIONS

4-MSITC	4-(methylsulfinyl)butyl isothiocyanate
6-MSITC	6-(methylsulfinyl)hexyl isothiocyanate
6-MTITC	6-(methylthio)hexyl isothiocyanate
ABCC1	ATP-binding cassette, sub-family C (CFTR/MRP), member 1
AITC	Allyl isothiocyanate
AKR1C1	<i>Aldo-keto</i> reductase family 1 member C1
AKR1C2	<i>Aldo-keto</i> reductase family 1 member C2
AKR1C3	<i>Aldo-keto</i> reductase family 1 member C3
ANOVA	Analysis of variance
ARE	Antioxidant response element
cDNA	Complementary DNA
CHX	Cycloheximide
COX-2	Cyclooxygenase-2
DMEM	Dulbecco's modified Eagle medium
DMSO	Dimethyl sulfoxide
DNAJB4	DnaJ (Hsp40) homolog, subfamily B, member 4
DNAJB6	DnaJ (Hsp40) homolog, subfamily B, member 6
DPPH	2,2-diphenyl-1-picrylhydrazyl
ECL	Enhanced chemiluminescence
EMEM	Eagles minimum essential medium
EpRE	Electrophile response element

FOSL1	V-fos FBJ murine osteosarcoma viral oncogene homolog ( <i>FOS</i> ), FOS-like antigen 1
FTH1	Ferritin heavy polypeptide 1
FTL	Ferritin light polypeptide
GCLC	Glutamate-cysteine ligase, catalytic subunit
GCLM	Glutamate-cysteine ligase, modifier subunit
GO	Gene Ontology
GOI	Gene of interest
GSH	Glutathione
GSR	Glutathione reductase
GST	Glutathione S-transferase
HO-1/HMOX-1	Heme oxygenase (decycling) 1
HPLC	High performance liquid chromatography
HRP	Horseradish peroxidase
HUVEC	Human umbilical endothelial cells
IFN- $\gamma$	Interferon- $\gamma$
IgG	Immunoglobulin G
iNOS	Inducible nitric oxide synthase
IPA	Ingenuity Pathway Analysis
IPKB	Ingenuity Pathway Knowledge Base
ITC	Isothiocyanate
Keap1	Kelch-like ECH-associated protein 1
LPS	Lipopolysaccharide

MNNG	<i>N</i> -methyl- <i>N'</i> -nitro- <i>N</i> -nitroguanidine
NFKB	Nuclear factor- $\kappa$ B
NQO1	Nicotinamide adenine dinucleotide phosphate (NAD[P]H) quinone oxidoreductase 1
Nrf2	Nuclear factors (erythroid-derived 2)-like 2
PCR	Polymerase chain reaction
PVDF	Polyvinylidene difluoride
ROS	Reactive oxygen species
SDS-PAGE	Sodium dodecyl sulfate polyacrylamide gel electrophoresis
SFN	Sulforaphane
SQSTM1	Sequestosome 1
TNF- $\alpha$	Tumor necrosis factor- $\alpha$
TXNRD1	Thioredoxin reductase 1
VDR/RXR	Vitamin D receptor/9- <i>cis</i> retinoic acid receptor

# LIST OF TABLES

## Chapter I

Table 1.1. Major Isothiocyanates components of <i>Wasabia japonica</i> Matsum. from ether extracts expressed as mg per 100 g fresh Wasabi .....	6
Table 1.2. Applications of DNA microarray gene expression profiling on phytochemicals in our laboratory .....	14

## Chapter II

Table 2.1. Primer sequences used for real-time PCR analysis .....	26
Table 2.2. Number of genes regulated by SFN, 6-MSITC and 6-MTITC in HepG2 cells .....	29
Table 2.3. Classification of genes targeted by ITCs in HepG2 .....	31
Table 2.4. Lists of genes involved in significantly modulated canonical pathways by SFN, 6-MSITC and 6-MTITC in HepG2 cells .....	33
Table 2.5. The differential expressions of genes involved in top modulated canonical pathways by Wasabi-derived ITCs .....	35

## Chapter III

Table 3.1. Primer sequences used for real-time PCR .....	57
Table 3.2. Number of genes regulated by Wasabi-derived isothiocyanates .....	60
Table 3.3. Classification of upregulated genes based on biological processes targeted by ITCs in IMR-32 cells .....	61
Table 3.4. Classification of downregulated genes based on biological processes targeted by ITCs in IMR-32 cells .....	69



Table 3.5. List of genes involve in significantly modulated canonical pathways by SFN, 6-MSITC and 6-MTITC in IMR-32 cells .....	83
Table 3.6. Genes coding for proteins involved in apoptosis regulation .....	85
Table 3.7. List of genes involved in Nrf2-mediated oxidative stress pathway by SFN, 6-MSITC and 6-MTITC in IMR-32 cells .....	96

#### **Chapter IV**

Table 4.1. Comparative classification of genes annotated for biological processes targeted by Wasabi-derived ITCs in HepG2 and IMR-32 cell lines .....	116
Table 4.2. Nrf-2 gene expression changes by SFN, 6-MSITC and 6-MTITC in HepG2 and IMR-32 cell lines .....	124

# LIST OF FIGURES

## Chapter I

Figure 1.1. Glucosinolates conversion into isothiocyanates .....	4
Figure 1.2. Metabolic mechanism of isothiocyanate via mercapturic pathway .....	5
Figure 1.3. Primary isothiocyanate components of Japanese Wasabi .....	7

## Chapter II

Figure 2.1. Venn diagram of microarray results by treatment of HepG2 with SFN, 6-MSITC, and 6-MTITC .....	30
Figure 2.2. Comparative canonical pathway analyses of differentially expressed genes in HepG2 hepatoblastoma stimulated with ITCs .....	32
Figure 2.3. Validation of differentially expressed genes in 6-MSITC-treated HepG2 cells from DNA microarray analyses by real-time PCR .....	39
Figure 2.4. Validation of differentially expressed genes in 6-MSITC-treated HepG2 cells from DNA microarray analysis by Western blot analysis .....	40
Figure 2.5. Nrf2-mediated pathway was found as significantly enriched pathway by IPA .....	42

## Chapter III

Figure 3.1. Chemical structure s of wasabi-derived ITCs used in the study .....	50
Figure 3.2. Cytotoxicity assay results of isothiocyanates in IMR-32 cells .....	59
Figure 3.3. Comparative canonical pathway analyses of differentially expressed genes in IMR-32 neuron cells stimulated with wasabi-derived ITCs .....	82

Figure 3.4. Validation of differentially expressed genes in wasabi-derived ITC-treated IMR-32 cells from DNA microarray analysis by real-time PCR .....	98
Figure 3.5. Effect of 6-MSITC on Nrf2 level and Nrf2-mediated induction of typical proteins .....	100
Figure 3.6. Effect of 6-MSITC on the stability of Nrf2 .....	101
Figure 3.7. Proposed mechanisms for the neuroprotective effects by wasabi-derived 6-MSITC in IMR-32 cells .....	107

## **Chapter IV**

Figure 4.1. Structure-gene expression profile relationship of SFN and SFN analogues .....	110
Figure 4.2. Comparative total number of genes regulated by ITCs in HepG2 and IMR-32 cells lines using Affymetrix HG UG133 plus 2.0 oligonucleotide arrays containing 54,000 probe sets ..	113
Figure 4.3. Comparative Venn diagram representation of HepG2 and IMR-32 cells gene expression profile from microarray data in response to Wasabi-derived ITCs .....	115
Figure 4.4. Wasabi-derived isothiocyanates multitargeted pathways .....	120
Figure 4.5. Comparative analyses of significantly modulated pathways by ITCs in HepG2 and IMR-32 cell lines .....	123

# TABLE OF CONTENTS

Acknowledgment .....	iii
Abstract .....	v
List of Abbreviations .....	ix
List of tables .....	xii
List of figures .....	xiv
Table of contents .....	xvi
<b>1. Introduction .....</b>	<b>1</b>
1.1. Overview of Wasabi .....	1
1.1.1. Botany of Japanese Wasabi .....	1
1.1.2. Isothiocyanates .....	2
1.1.3. Biological functions .....	7
1.2. Microarray analysis .....	10
1.2.1. Background .....	10
1.2.2. Transcriptional profiling .....	11
1.2.3. Application of transcriptional profiling .....	12
1.2.4. Bioinformatics tools for microarray data analysis .....	14
1.3. Thesis objectives .....	16
<b>2. DNA microarray profiling highlights Nrf2-mediated chemoprevention targeted     by Wasabi-derived isothiocyanates in HepG2 cells .....</b>	<b>18</b>
2.1. Abstract .....	18

2.2. Introduction .....	19
2.3. Materials and methods .....	22
2.3.1. Chemical reagents .....	22
2.3.2. Hepatoblastoma cell culture .....	22
2.3.3. Total RNA extraction .....	23
2.3.4. Microarray hybridization and transcript analyses .....	23
2.3.5. Pathway analyses and network generation .....	24
2.3.6. Reverse transcription and real-time PCR analyses .....	25
2.3.7. Western blot analyses .....	26
2.3.8. Statistical analyses .....	27
2.4. Results .....	28
2.4.1. Gene expression profile of HepG2 cells treated with ITCs .....	28
2.4.2. Grouping of genes targeted by Wasabi-derived ITCs .....	30
2.4.3. Identification of biologically significant pathways .....	31
2.4.4. Expression of genes associated with significantly modulated pathways ..	34
2.4.5. Confirmation of microarray results .....	38
2.4.6. Nrf2 pathway and network analysis .....	41
2.5. Discussions .....	43
<b>3. DNA microarray highlights Nrf2-mediated neuron protection targeted by Wasabi-derived isothiocyanates in IMR-32 cells .....</b>	<b>49</b>
3.1. Abstract .....	49
3.2. Introduction .....	50
3.3. Materials and methods .....	53

3.3.1. Materials and cell cultures .....	53
3.3.2. 3-(4,5-dimethylthiazol-2-yl)-2,5-diphenyltetrazolium bromide assay .....	54
3.3.3. Total RNA extraction .....	54
3.3.4. Microarray hybridizations and transcript analyses .....	55
3.3.5. Pathway analyses .....	55
3.3.6. Real-time PCR .....	56
3.3.7. Western blot analyses .....	57
3.3.8. Statistical analyses .....	58
3.4. Results .....	58
3.4.1. Gene profile analysis in IMR-32 cells treated by Wasabi-derived ITCs ...	58
3.4.2. Grouping of genes targeted by Wasabi-derived ITCs .....	60
3.4.3. Identification of biological pathways by IPA .....	81
3.4.4. Expression profiling of Nrf2-mediated genes by Wasabi-derived ITCs ....	84
3.4.5. Influence of 6-MSITC on Nrf2-mediated protein levels .....	99
3.4.6. Influence of 6-MSITC on Nrf2 protein at transcription and post transcription .....	100
3.5. Discussions .....	102
<b>4. Discussions and conclusions .....</b>	<b>108</b>
4.1. Discussions .....	108
4.1.1. Effect Wasabi-derived isothiocyanates on expression profile changes in HepG2 and IMR-32 cells.....	108
4.1.2. Influence of cell type variation on gene expression profiles following isothiocyanates treatment .....	111

4.1.3. Pathway network and global functional analyses by ITCs stimulation in HepG2 and IMR-32 cells .....	118
4.1.4. Nrf2-ARE pathway activation underlying mechanisms as the target of Wasabi-derived ITCS in hepatic and neuron cell models .....	124
4.2. Conclusions .....	126
<b>5. References .....</b>	<b>127</b>

# CHAPTER I

## Introduction

### 1.1. Overview of Wasabi

#### 1.1.1. Botany of Japanese Wasabi

Japanese horseradish, commonly called Wasabi, was introduced to Japan through the cultivation of native crucifer, *Wasabia japonica* (Miquel) Matsumura. Wasabi is a glabrous perennial crop of Cruciferae family and botanically close to genera Caramine, Cochelearia and Nasturtium (Chadwich *et al*, 1993; Hodge, 1974). Open woodland with cool running water from streams and springs is the natural habitat of this plant (Depree *et al*, 1999). It is more or less evergreen in color and forms sizeable clumps. Cluster of large, long-stemmed, heart-shaped leaves grow in its rhizome, which would eventually fall off, leaving the knobby scar characteristic on the thick, finger-size, greenish rhizome that are sold in the markets (Hodge, 1974).

Rhizome is the most valuable part of the plant. It is mainly utilized as a condiment for Japanese foods, especially for sashimi, sushi and some other noodle dishes due to its pungent taste (Chadwich *et al*, 1993). The pungent taste is owed primarily to the volatile components that is liberated and rapidly lost into the air when the plant tissue is damage, *e.g.* during the grating process of the rhizome (Depree *et al*, 1999). The leaves and petioles are traditionally pickled in 'sake' brine or soy sauce and served as side dish. Other parts are also used as material for making ice cream, salad dressing, crackers, and even in wine and cheese.



### **1.1.2. Isothiocyanates**

Like other cruciferous plants, the pungent taste of Wasabi originated from the breakdown products of a group of compound known as glucosinolates through the action of myrosinase (Fenwick *et al*, 1982). In intact plant cells, myrosinase is physically separated from glucosinolates (Holst & Williamson, 2004). However, when cruciferous vegetables are chopped or chewed, myrosinase can interact with glucosinolates, and subsequently hydrolyze into glucose and an unstable aglycone (Depree *et al*, 1999). The unstable aglycone further undergoes Lossen-type rearrangement under neutral pH to form isothiocyanates (ITCs) as illustrated in **Figure 1.1**.

ITCs are naturally occurring small molecules. They are a group of organo-sulfur containing chemical compound with a general formula of  $R-N=C=S$ , where R can be any alkyl or aryl group. Once formed, they are more stable in acidic condition than in neutral or alkaline environment. Also, ITCs are considered reactive compounds due to the electron-deficient central carbon atom which happens to be the target nucleophilic attack (Wu *et al*, 2009). ITCs can cross the gastrointestinal epithelium and capillary endothelium by passive diffusion when ingested (Wu *et al*, 2009). Then, they penetrate the cells of the tissues by rapid and reversible binding via the thiol group of the plasma protein localized in the plasma membrane. Intracellularly, ITCs can associate with glutathione (GSH) to form GSH conjugate, S-(N-alkyl/arylthiocarbamoyl) glutathione, in the presence of glutathione S-transferase (GST) before exported out of the cell by the transporter proteins (Shapiro *et al*, 1998). Once out of the cell,  $\gamma$ -glutamyl and glycylyl residues are cleaved consecutively with the aid  $\gamma$ -glutamyl transferase and dipeptidase,

respectively, which are both localized on the extracellular surface of the plasma membrane. The resulting cysteine derivative becomes acetylated by *N*-acetyl transferase in the liver, and is metabolized into  $N_{\alpha}$ -acetyl derivative or mercapturic acid (Clarke *et al*, 2011). Finally, the ITC metabolites are transported to the kidney and eliminated from the human body through urinary excretion (**Figure 1.2**). ITC metabolites can be quantified in the urine and were found to be highly correlated with cruciferous vegetables dietary intake (Seow *et al*, 1998).

However, due to its high volatility and susceptibility to hydrolysis, some ITCs are usually lost at large quantity during food processing. Thus, low ITCs but a much higher amount of glucosinolates are usually present in cooked cruciferous vegetables (Shapiro *et al*, 1998).

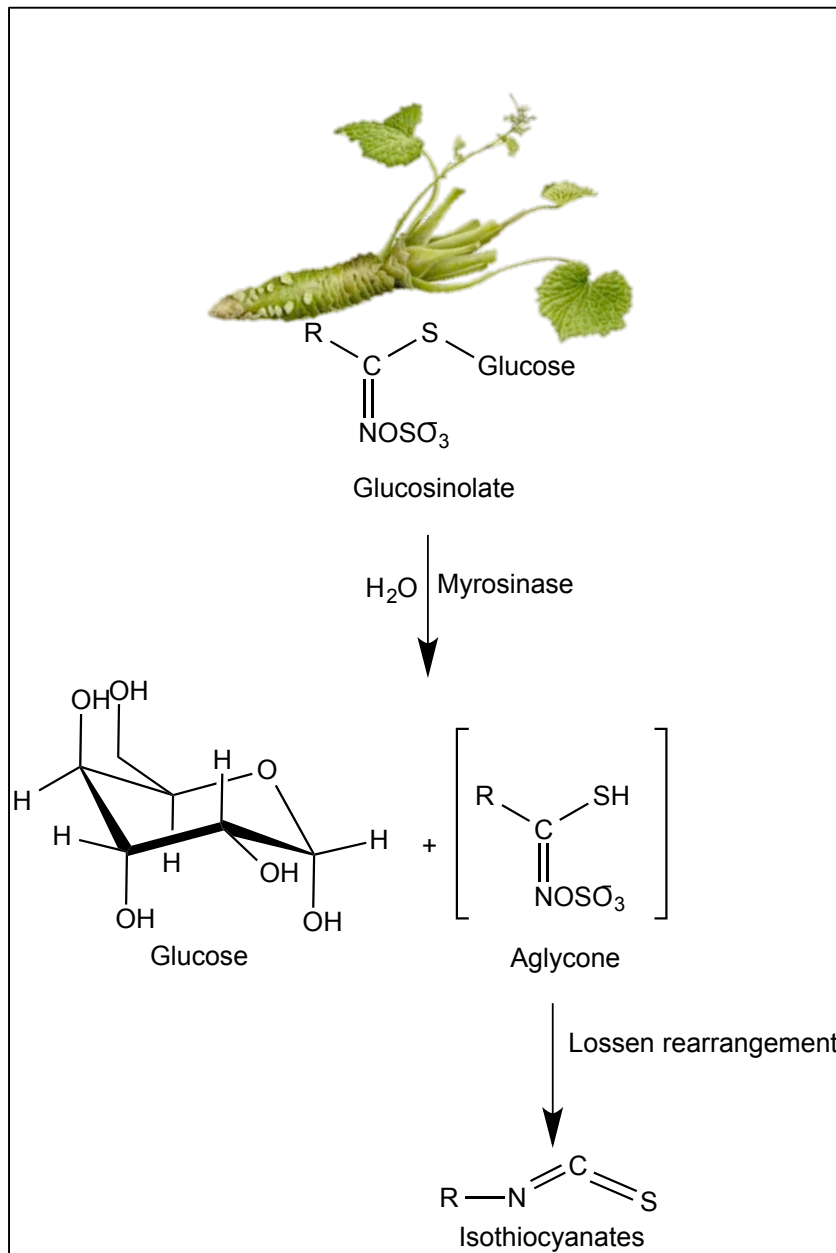


**Figure 1.1.** Chemical mechanism of isothiocyanate formation. Japanese Wasabi (*Wasabia japonica* (Miquel) Matsumura) contains glucosinolates that are hydrolyzed in glucose and unstable aglycone, through the action of myrosinase enzyme in the presence of  $\text{H}_2\text{O}$ . Unstable aglycone can undergo Lossen-type rearrangement under neutral pH to yield isothiocyanate which is responsible to the pungent taste of Wasabi.

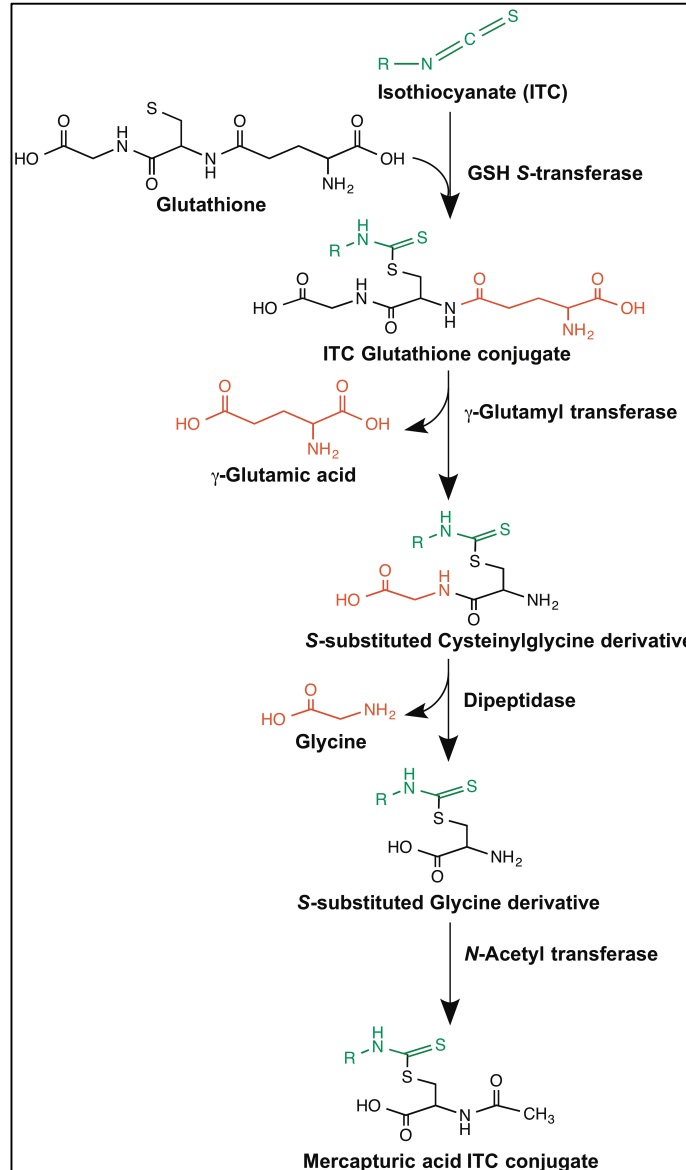


**Figure 1.2.** Metabolic mechanism of isothiocyanates (ITC) via the mercapturic pathway. In the cell, ITC can associate with glutathione (GSH) to form ITC-GSH conjugate with the aid of glutathione S-transferase before it is exported out of the cell by transporter proteins. Then extracellular consecutive cleavage of  $\gamma$ -glutamyl and glycyl residues from ITC-GSH conjugate can take place in the presence of  $\gamma$ -glutamyl transferase and dipeptidase, respectively. The resulting cysteine derivative becomes acetylated by *N*-acetyl transferase in the liver to form mercapturic acid-ITC conjugate before being transported to the kidney and excreted through the urine.

Allyl isothiocyanate (AITC) as indicated in **Table 1.1** is the primary cause of the pungent taste of Japanese Wasabi. Together with 6-(methylsulfinyl)hexyl isothiocyanate (6-MSITC) and 6-(methylthio)hexyl isothiocyanate (6-MTITC), they provide a distinct heat and flavor to Wasabi (Etoh *et al*, 1990; Ina *et al*, 1989). 6-MSITC exists not only in Wasabi but also in horseradish. Whereas, 6-MTITC, available in Wasabi alone, gives the fresh green taste characteristic. Wasabi-derived ITCs differ from each other on the number of carbon atoms on the alkyl backbone and the substituent atom at the sulfur atom of the methyl carbon end (**Figure 1.3**). Both 6-MSITC and 6-MTITC are considered sulforaphane (SFN) analogues, also known as 4-(methylsulfinyl)butyl isothiocyanate (4-MSITC).

**Table 1.1.** Major isothiocyanate components of *Wasabia japonica* Matsum.

from ether extracts expressed as mg per 100g fresh Wasabi.\*

<b>Isothiocyanates</b>	<b>Root</b>	<b>Stem</b>	<b>Leaf</b>
Allyl isothiocyanate	111.00	18.60	22.80
<i>n</i> -Butyl isothiocyanate	1.74	0.30	0.36
3-Butenyl isothiocyanate	1.83	0.06	0.27
4-Pentenyl isothiocyanate	3.90	0.66	0.78
5-Hexenyl isothiocyanate	1.02	0.30	0.57
5-(Methylthio)pentyl isothiocyanate	0.48	0.27	0.12
6-(Methylthio)hexyl isothiocyanate	1.89	2.64	1.14
7-(Methylthio)heptyl isothiocyanate	1.44	0.60	0.33
5-(Methylsulfinyl)pentyl isothiocyanate	2.17	0.30	0.42
6-(Methylsulfinyl)hexyl isothiocyanate	7.80	2.52	5.40
7-(Methylsulfinyl)heptyl isothiocyanate	1.41	0.45	1.08

\*Adapted from Etoh *et al*, 1990

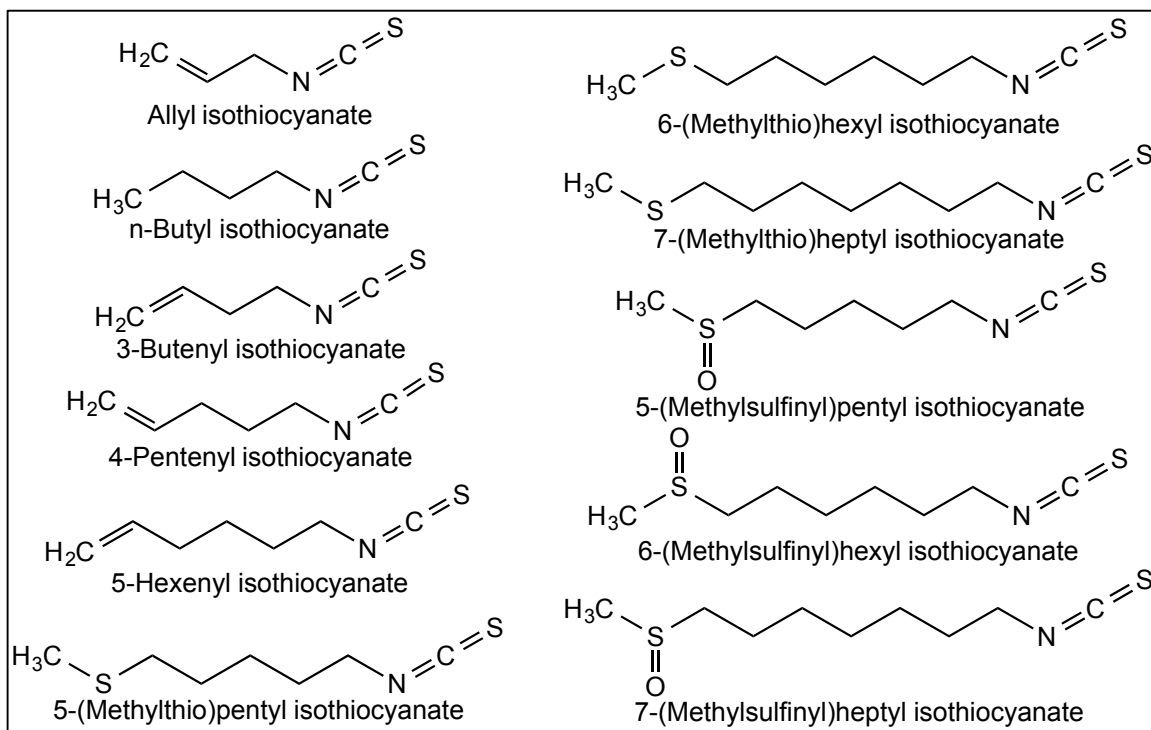


**Figure 1.3.** Primary isothiocyanate components of Japanese Wasabi.

### 1.1.3. Biological functions

Protective effect of ITC have been reported a few decades ago but until now, it has still continuously attracted various researchers. In fact, a growing number of naturally occurring bioactive ITCs has been reported ever since the first observance of  $\alpha$ -naphthyl ITC ability to reduce liver tumor development in Wistar rats at a dose dependent manner (Sidransky *et al*, 1966). For instance, SFN, a predominant ITC in broccoli and cabbage, became a widely known and studied ITC compound. Studies have showed that it demonstrated anti-proliferative, anti-cancer, antioxidative, anti-inflammatory, and neuroprotective functions in various adopted experimental models. In ovarian cancer cell line, SKOV3, and mouse ovarian cancer cell lines, C3 and T3, SFN displayed antiproliferative effects via the Akt signaling pathway (Chaudhuri *et al*, 2007).

Dietary SFN can even network with numerous signaling pathways associated with carcinogenesis and modify epigenetic events (Myzak *et al*, 2006; Atwell *et al*, 2015). SFN can also increase the resistance of RPE 19 cell against oxidative stress by upregulating antioxidant-related enzymes and downregulating inflammatory mediators and cytokines (Ye *et al*, 2013). Additionally, SFN displayed protective effects against neurodegenerative diseases by targeting the induction of various groups of cytoprotective proteins via activation of Nrf2 (Tarrozi *et al*, 2013).

As with Japanese Wasabi, evidence from several studies implies that its biological and pharmacological activities are contributed by the existence of high amount of ITC compounds. The major ITCs found in wasabi are considered powerful inhibitor of microbial growths compared with other ITCs from cruciferous plants. For instance, AITC and 6-MSITC can strongly inhibit the growth of *Staphylococcus aureus*, *Escherichia coli*, and *Helicobacter pylori* (NCTC11637, YS27 and YS50) even at a minute concentration (Isshiki & Tokouka, 1993; Ono *et al*, 1998; Shin *et al*, 2004). AITC can also exert anti-obesity activity through the suppression of adipogenesis or lipogenesis (Kim *et al*, 2015). On contrary, 6-MTITC can inhibit platelet aggregation mediated by arachidonic acid, promotes deaggregation in less than 30 minutes after intake, and is 10 times more potent than aspirin (Kumagai *et al*, 1994). Furthermore, protective effect of Wasabi powder against *N*-methyl-*N'*-nitro-*N*-nitroguanidine (MNNG)-induced gastrointestinal tumor was observed by Tanida *et al* (1991) in rats supplemented with 10% Wasabi powder. Other than its chemopreventive effect, Wasabi extract displayed anti-cancer potential in human MKN-28 stomach cancer cell model at 40  $\mu$ M which was attributed to the presence of 6-MSITC (Fuke *et al*, 1994). Beyond that,

6-MSITC is also responsible for the anti-inflammatory, anti-coagulant and anti-apoptosis activities of Wasabi as supported by its ability to suppress lipopolysaccharide (LPS)-induced macrophage activation, arachidonic- or adenosine diphosphate induced platelet activation and tumor cell proliferation in primary human umbilical endothelial cells (HUVECs) (Okamoto *et al*, 2013). Extensive studies from our laboratory supported Wasabi-derived 6-MSITC anti-inflammatory function by acting as a potent inhibitor of cyclooxygenase-2 (COX-2) induced by LPS or interferon- $\gamma$  (IFN- $\gamma$ ), and by suppressing iNOS expression via inhibition of Jak2 mediated JNK signaling cascade with the attendant to AP-1 activation in murine macrophage RAW264 (Uto *et al*, 2005a; Uto *et al*, 2007; Uto *et al*, 2005b). On top of that, genome-wide study of our research group using DNA microarray technology revealed that 6-MSITC exert anti-inflammatory function through regulation of chemokines, interleukins and interferons in mouse macrophages (Chen *et al*, 2010). Screening of Wasabi extract yielded a positive response for anti-diabetic and antioxidant activities. Wasabi extract showed higher lipogenic index (LI = 1.74) than anti-diabetic drug, troglitazone (LI = 1.43) (Babish *et al*, 2010). The extract can enhance adiponectin secretion and inhibit tumor necrosis factor- $\alpha$  (TNF- $\alpha$ )-stimulated lipolysis and IL-6 secretion comparable to troglitazone. However, conflicting results were reported regarding the degree of antioxidant capacity by Wasabi extract. Ryu *et al* (2007) and Lee (2008) stated that water extract of rhizome is superior in inhibiting 2,2-diphenyl-1-picrylhydrazyl (DPPH) radical formation over alcohol extract while Shin *et al* (2014) reported that alcohol extracts have higher DPPH radical scavenging activity as compared to water extract. Irrespective of the contradictory figures, evidence showed that Wasabi possesses antioxidant function. In summary, the



compendium of evidence showed that Wasabi not only served as a condiment in most Japanese households but can be also utilized for prevention and cure of some diseases due to its multiple biological properties. However, limited studies are available dealing with its global-wide mechanisms to exert pharmacological effects.

## **1.2. Microarray Analysis**

### **1.2.1. Background**

The advent of microarray analysis in the field of genomics during the early 1990s launched a new era of molecular biology research (Poustka *et al*, 1986). From its inception as a technique for comprehensive DNA mapping and sequencing into a successful methodological approach for transcript-level analyses, microarray analysis has expanded immensely with the incorporation of other technologies (Poustka *et al*, 1986; Cantor *et al*, 1992; Schena *et al*, 1995). Microarray analysis allowed researchers around the world to simultaneously perform experiment on ten to hundreds of thousands of immobilized probes with the aid of microarray chips (Berard *et al*, 2012). Microarray chips are prepared by amplifying DNA segments representing thousands of genes to be assayed using polymerase chain reaction (PCR) (Hedge *et al*, 2000). Complementary DNA (cDNA) binding probes are then mechanically spotted at high density onto a substrate, usually a glass slide, in predefined spatial location using a simple x-y-z stage robotic system.

Given the characteristic of microarray technology, studies on individual biological functions of a few related genes or proteins and most importantly global investigations

of cellular activity which were once considered non-traceable turned out feasible. Moreover, microarray studies can provide key insights underlining the growth and development of life as well as unearth genetic causes of diseases happening within the human body (Fahmideh *et al*, 2016). With the use of this technology biomarkers for breast cancer, oral cancer, ovarian cancer, prostate cancer and other types of cancer has been identified (Colombo *et al*, 2011; Choi *et al*, 2008; Konstantinopoulos *et al*, 2008; Sørensen and Ørntoft, 2010).

### **1.2.2. Transcriptional profiling**

To the multitude, the term microarray analysis is synonymous to transcript analysis. However, transcriptional profiling is just one of the most prevalent application of microarray analysis for it has the power to study complex phenomena such as cancer (Schena *et al*, 1995; DeRisi *et al*, 1996). Transcriptional profiling is capable of differential gene expression patterns or comparative mRNA level expression analysis between similar cells exposed to different stimuli or between different cellular phenotypes or developmental stages (Hedge *et al*, 2000).

Essentially, transcriptional profiling experimental procedure is based on similar analytical protocol of microarray technology. RNA is extracted from the given cellular sample of interest and total extracted RNA is reverse-transcribed into cDNA, followed by labeling with the use of fluorescent dye and hybridization of individual cDNA onto the microarray chip (Sørensen & Ørntoft, 2010). When hybridization is finished, samples are washed and is subjected to confocal laser scanning for the determination of transcript abundance (single-color system) or relative expression compared to a reference sample

with a different label (two-color system). This process simultaneously determines the relative expression level of all the genes represented in the array which is then transformed into a numerical value (Hedge *et al*, 2000; Xiang & Chen, 2000).

Despite some drawbacks such as amount of sample available for analysis, time, RNA degradation and chip production labor, microarray-based transcriptional profiling analysis is still a suitable tool since it provides broad coverage of the whole genomes on a single chip (Berard *et al*, 2012). Beside, chips of specific subsets of genes are already available commercially, and a lot extensive optimization and standardization of the method has taken place recently. Thus, going through the tedious process of preparation is no longer necessary.

### **1.2.3. Application of microarray technology**

Microarrays are significant in clinical setting since they can be used to diagnose diseases, drug discovery, toxicological research and immunology. Previous studies showed that microarray technology helped scientists classify different types of cancers based on the organs in which the tumors develops (Fahmideh *et al*, 2016). It enabled to predict which medication might be the best for the cancer of an individual person or why some unwanted side effects occur (Wiltgen & Tilz, 2007).

In medicinal chemistry, the emergence of microarray technology paved way for better understanding on how to utilize and improve certain drugs because it allowed researchers to quantitatively profile genes that are upregulated or downregulated by drugs or bioactive compounds. (Gerhold *et al* 2002; Freiberg *et al*, 2005). Now, drug mechanism can be more fully mapped out by examining how it affects the genome *in*

*vivo* and genomic response due to drug therapy can be used predict individual drug sensitivity and resistance (Wiltgen & Tilz, 2007). Another important application of microarray technology is on identification of molecular mechanisms of toxicity especially in neurotoxicity studies. Microarray can be a screening tool to classify genes and gene products that are associated in conferring resistance or sensitivity to toxic substances (Fahmideh *et al*, 2016).

In the field of nutrigenomic research, it has become the prominent analytical tool for exploring interaction between nutrients and bioactive compounds, and genes (Kawakami *et al*, 2013). The technology was first employed to investigate the effects of caloric restriction on aging (Lee *et al*, 1999). This approach not only produced clinically important data but also determine the impact of diet or of a single nutrient on a particular human pathology as supported by the succeeding studies. Other important aspects of nutrigenomics covered were effects of dietary protein in the gene expression of cells, mechanisms of polyunsaturated fatty acid in cancer and normal cells, and effects of low or high carbohydrate intakes at the transcriptomic level (Endo *et al*, 2002; Narayanan *et al*, 2003; Sparks *et al*, 2006). Our laboratory has also successfully investigated the molecular mechanisms of notable phytochemicals by microarray technology as summarized in **Table 1.2**. These studies indicated that despite the disadvantages associated with the technology, the application of microarray-based technology is still incredibly magnificent.

**Table 1.2.** Applications of DNA microarray gene expression profiling on phytochemicals  
in our laboratory.

<b>Phytochemical</b>	<b>Model</b>	<b>Findings</b>	<b>Method</b>	<b>Reference</b>
Anthocyanin	RAW264 cells	Targeted some pro-inflammatory genes to exert potential anti-inflammatory function	Agilent mouse oligonucleotide array	Chen <i>et al</i> , 2008
Baicalein	HepG2 cells	Activated Nrf2-ARE to induce hepatic drug metabolizing enzyme genes	Affymetrix Gene Chip Human U133 plus 2.0 Array	Qin <i>et al</i> , 2012
Myrcetin	HepG2 cells	Nrf2-mediated ARE activation	Affymetrix Gene Chip Human U133 plus 2.0 Array	Qin <i>et al</i> , 2013
Theasinensin A	RAW264 cells	Regulated the relevant expression networks of chemokines, interleukins, and interferons to exert its anti-inflammatory effects	Agilent mouse oligonucleotide array	Chen <i>et al</i> , 2011
6-MSITC	RAW264 cells	Regulated chemokines, interleukins and interferons	Agilent mouse oligonucleotide array	Chen <i>et al</i> , 2010

#### **1.2.4. Bioinformatics tools for microarray data analysis**

Compiled studies have established the power of microarray-based gene expression profiling to generate a long lists gene that are significantly altered at the transcript levels. However, in biological systems these changes do not occur independently, but rather in a highly coordinated and interweaved manner, making microarray data unanalyzable without statistical and informational technology. Thus, to fully exhaust DNA microarray generated data, elucidation of biological interdependency

is required through the support of bioinformatics tools. These could include fold-change analysis to identify significantly regulated genes, gene clustering and classification to identify global pattern of gene expression, and genetic network analysis to determine the biological meaning of both individual genes and group genes.

The most common approach of array data analysis is to compute statistical associations to biological concepts such as to biological function as categorized by Gene Ontology (GO). GO is a structured database by GO consortium whose purpose is to produce a dynamic, controlled vocabulary that is applicable to all eukaryotes even as the knowledge of gene and protein roles in the cells is evolving (Rhee *et al*, 2008). Three independent ontologies are accessible world-wide, consisting of biological process, molecular function and cellular component. Biological process denotes the biological objective to which the gene or gene product contributes and process is achieved through one or more ordered assemblies of molecular functions which could involve a chemical or physical transformation (Botstein *et al*, 2010). Molecular function refers to the biochemical activity of a gene product such as specific binding to ligands or structures without specifying where or when the event takes place. Cellular component is the location in the cell where a gene product is active which is based on the eukaryotic cell structure. However, not all terms are applicable to all organisms.

Although GO is a widely used tool, it lacks the detailed and directional molecular information available to Ingenuity Pathway Analysis (IPA). IPA is a web-based software application which continuously develop, maintained and updated regularly. This tool allows to search targeted information on genes, proteins, chemicals, diseases, and drugs, even to distinguish new targets or candidate biomarkers within the context of

biological systems (<http://www.ingenuity.com>). The data analysis and experimental modeling feature of the software is based on the comprehensive and manually curated content of the Ingenuity Pathway Knowledge Base (IPKB). At present, IPKB has approximately five million individual findings, mainly on relationships between molecules or between molecules and diseases or biological functions (Kramer *et al*, 2014). When IPKB findings are coupled with powerful algorithms, IPA provide more advanced analysis that could help identify the most significant pathways and even discover potential novel regulatory networks and causal relationships associated with the experimental data since it can draw direct and indirect interactions between genes and assign genes to specific biological functions, canonical pathways, and networks (<http://www.ingenuity.com>). The strong network building component feature of IPA permits also the formation and analysis of networks comprised of any gene of interest (GOI). For instance, IPA has been effective in detecting genes that are associated with cell growth and cell proliferation in unilateral traumatic brain injury model (White & Ford, 2015). In our previous study, IPA has been useful in identifying related networks of chemokines, interleukins and interferons which is responsible for the anti-inflammatory activity of theasinensin A (Chen *et al*, 2011).

### **1.3. Thesis Objectives**

The well-entrenched connection of diet and health gave birth to nutrigenomics which revolved on how to balance bioactive dietary compounds and how this compounds exert beneficial effects. These studies could lead to the improvement of our

well-being by providing us molecular biomarkers and also assist in discerning gene expression patterns brought by our whole diet or individual dietary constituents. However, to attain this purpose, the need of high throughput functional genomic technique such as microarray is crucial. Microarray technique is a robust and suitable technique for gene-diet interaction research studies for it permits scholars to identify the therapeutic function of a natural food component, and at the same time allows us to understand why and how some natural foods may induce varying gene responses. Therefore, this study was designed to contrast the global changes in transcript levels and the underlying genes targeted by Japanese Wasabi-derived ITCs in HepG2 with that of IMR-32 using microarray-based technology. ITCs are present in Japanese Wasabi at high quantities, and of different carbon chain backbone. Thus, the use of multiple ITCs samples with structural variabilities are designed to identify the impact of structural difference towards biological functions of Wasabi-derived ITCs. cDNA microarray is applied to acquire novel information regarding the effect of the particular Japanese Wasabi-derived ITCs at genome-wide level. Furthermore, different cell lines are chosen as *in vitro* models to demonstrate distinct gene expression patterns in response to ITCs stimulation in cells of hepatic versus neuronal origin. Therefore, HepG2 and IMR-32 are utilized to explore and determine cell-specific expression regulation of individual ITCs. Altogether, the approach of this study would provide novel information how structural differences of Japanese Wasabi-ITCs contribute to its efficacy and impact specific targets.



## Chapter II

### **DNA microarray profiling highlights Nrf2-mediated chemoprevention targeted by Wasabi-derived isothiocyanates in HepG2 cells**

#### **2.1. Abstract**

6-MSITC and 6-MTITC are sulforaphane (SFN, or 4-(methylsulfinyl)butyl isothiocyanate (4-MSITC)) analogues found in Japanese Wasabi. As reported previously, Wasabi-derived isothiocyanates (ITCs) are activators of nuclear factor (erythroid-derived 2)-like 2 (Nrf2)-antioxidant response element (ARE) pathway, and also inhibitors of pro-inflammatory cyclooxygenase-2 (COX-2). This study is the first to assess the global changes in transcript levels of Wasabi ITCs, comparing with SFN, in HepG2 cells. The comparative gene expression profiling was performed by treating HepG2 cells with ITCs, followed by DNA microarray analyses using HG-U133 plus 2.0 oligonucleotide array. Partial array data on selected gene products were confirmed by real-time polymerase chain reaction (PCR) and Western blotting. Ingenuity Pathway Analysis (IPA) software was used to identify functional subsets of genes and biologically significant network pathways. 6-MTITC showed the highest number of differentially altered ( $\geq 2$  folds) gene expression, of which 114 genes were upregulated and 75 were downregulated. IPA revealed that Nrf2-mediated pathway, together with glutamate metabolism, is the common significantly modulated pathway across treatments. Interestingly, 6-MSITC

exhibited the most potent effect toward Nrf2-mediated pathway. The data suggest that 6-MSITC could exert chemopreventive role against cancer through its underlying antioxidant activity via the activation of Nrf2-mediated subsequent induction of cytoprotective genes.

## 2.2. Introduction

SFN or 4-MSITC, a naturally occurring ITC compound found primarily from broccoli and a small amount from other cruciferous vegetables, is recognized nowadays as a multifaceted chemopreventive agent (Keum *et al*, 2004). It exhibits antiproliferative, anti-cancer, anti-inflammatory and antioxidative activities (Chaudhuri *et al*, 2007; Chung *et al*, 2015; Sun *et al*, 2015). Dietary SFN can interact with multiple pathways associated with carcinogenesis and modify epigenetic events as observed both *in vivo* and *in vitro* (Myzak *et al*, 2006; Atwell *et al*, 2015). The recent review of Fuentes *et al* (2015) highlighted the activation of Nrf2 and Nrf2 target genes, inhibition of nuclear factor- $\kappa$ B (NF $\kappa$ B)-mediated processes, and modulation of signaling pathways associated with cellular proliferation, angiogenesis and cancer stem cell self-renewal as the mechanisms involved in the anticarcinogenic and anti-cancer activities of SFN. Other than that, SFN also displayed protective effects against neurodegenerative diseases by targeting the induction of various groups of cytoprotective proteins via activation of Nrf2 (Tarrozi *et al*, 2013).

Recently, two other SFN analogues isolated from Japanese Wasabi (*Wasabia japonica* (Miq.) Matsumura), a widely available spice in Japan, have been characterized. They are 6-MSITC and 6-MTITC. These ITCs contributed to the anti-microbial, anti-

platelet, anti-inflammatory, and anti-obesity activities of Japanese Wasabi (Isshiki & Tokuoka, 1993; Kumagai *et al*, 1994; Nagai & Okunishi, 2009; Yamasaki *et al*, 2013). In particular, 6-MSITC mediated important inflammatory factors by suppressing COX-2, inducible nitric oxide synthase (iNOS), and pro-inflammatory cytokines (Uto *et al*, 2012). Likewise, in animal *in vitro* study, 6-MSITC showed neuroprotection via activation of glutathione-dependent antioxidant enzymes (Morrone *et al*, 2014). Moreover, both 6-MSITC and 6-MTITC were previously identified to enhance the ARE-driven nicotinamide adenine dinucleotide phosphate (NAD[P]H):quinone oxidoreductase 1 (NQO1) expression by stabilizing Nrf2 via enhanced Kelch-like ECH-associated protein 1 (Keap1) mediation that leads to the increase of nuclear Nrf2 levels (Hou *et al*, 2011; Korenori *et al*, 2013).

Nrf2 is a basic region leucine-zipper transcription factor, acting as the master regulator of the cellular antioxidant response via stimulation of over 250 genes (Itoh *et al*, 1997; Nguyen *et al*, 2000). Under normal condition, Nrf2 is localized into the cytoplasm where it is associated with Keap1, which acts as the reactive oxygen species (ROS)/electrophilic stress sensor (Jung & Kwak, 2010). Importance of Nrf2 in cancer prevention has been demonstrated in a number of animal model studies. Absence of *Nrf2* gene resulted to the increasing susceptibility of mice against chemically-induced skin cancer and decrease responsiveness to chemopreventive agents (Xu *et al*, 2006). Rise of tumor incidence was also found in the intestine of azoxymethane/dextran sulphate sodium-induced Nrf2-deficient mice when compared with the wild-type mice (Khor *et al*, 2008). Nrf2 protective mechanism against these chemical carcinogens can be attributed to its ability to reduce ROS generation and DNA damage (Frohlich *et al*, 2008). In

response to the increase of ROS, Nrf2 dissociates with Keap1 complex and translocates to the nucleus, where it binds with ARE to induce transcription of cytoprotective genes (Itoh *et al*, 1997; Nguyen *et al*, 2000).

Though 6-MSITC and 6-MTITC activated Nrf2/Keap1-ARE pathway through the similar mechanism, they have different inhibitory effects on the expression of pro-inflammatory mediator, COX-2, in lipopolysaccharide (LPS)-induced RAW264 cells (Uto *et al*, 2005; Uto *et al*, 2007). Moreover, their potency as inhibitor COX-2 was found to be dependent on the length of their methyl chains. This implies that an increase of methyl chain length in Wasabi-derived ITCs is important for their inhibitory activity. As a consequence, genome-wide transcriptional effects of 6-MSITC and 6-MTITC, as well as SFN, were investigated using DNA microarray technology in human hepatoblastoma HepG2 cells. DNA microarray is an appropriate tool to investigate the expressions of thousands of genes simultaneously in a given cell type or tissue sample (Barett & Kawasaki, 2003; Rushmore & Kong, 2002). In RAW264 and HepG2 cell models, the anti-inflammatory genes targeted by 6-MSITC and hepatic metabolic enzymes targeted by baicalein, respectively, were successfully profiled using DNA microarray technology (Chen *et al*, 2010; Qin *et al*, 2012).

This study is the first to carry out comparative gene expression profiling analyses in HepG2 cells treated with SFN, 6-MSITC or 6MTITC. The results showed that 6-MTITC has greater effect on gene regulation compared with that of SFN and 6-MSITC. Interestingly, analyses of the signaling pathways using IPA software revealed that 6-MSITC has the most potent influence towards modulation of Nrf2-mediated pathway. Furthermore, Wasabi-derived ITCs treatments of HepG2 cells significantly affected the

regulation of glutamate metabolism. Hence, these data suggest that Wasabi-derived ITCs can exert chemopreventive potential against cancer through the underlying antioxidant activity involving the activation of Nrf2 and subsequent induction of antioxidant proteins and metabolizing enzymes.

## **2.3. Materials and methods**

### **2.3.1. Chemical Reagents**

ITCs (SFN, 6-MSITC and 6-MTITC) were isolated from Japanese Wasabi and purified to 93.3 % purity by gas chromatography (Hou *et al*, 2000). All ITCs were dissolved in dimethyl sulfoxide (DMSO) for cell culture experiments. The antibodies against Nrf2 (C20), HO-1 (H105), NQO1 (C-19), HSP70 (D69),  $\alpha$ -tubulin (B-7), rabbit immunoglobulin G (IgG) and horseradish peroxidase-conjugated anti-goat secondary antibody were purchased from Santa Cruz Biotechnology (Texas, USA). AKR1C1 and AKR1C3 antibodies were obtained from Abcam (Cambridge, United Kingdom). Horseradish peroxidase-conjugated anti-rabbit and anti-mouse secondary antibodies were from Cell Signaling Technology (Massachusetts, USA).

### **2.3.2. Hepatoblastoma cell culture**

Human hepatoblastoma HepG2 cells (cell no. TKG0205) were obtained from Riken Bioresource Center Cell Bank (Ibaraki, Japan). HepG2 cells were grown in Dulbecco's

modified Eagle medium (DMEM) (Nissui, Seiyaku, Tokyo, Japan) containing 10 % FBS (Equitech-Bio, Texas, USA) under humidified 5 % CO<sub>2</sub> atmosphere at 37 °C.

### **2.3.3. Total RNA extraction**

HepG2 cells were pre-cultured for 24 hours in 10-cm dishes and then treated with 10 µM of ITCs (SFN, 6-MSITC or 6-MTITC) for another 9 hours. Total RNA was extracted using RNeasy Mini kit (Qiagen™, California, USA) following the manufacturer's instructions. RNA integrity was assessed using Agilent 2100 Bioanalyzer (California, USA).

### **2.3.4. Microarray hybridization and transcript analyses**

Microarray experiments were performed based on the protocol described by Qin *et al* (2012). In brief, total RNA of 400 ng was amplified using cDNA with Eukaryotic Poly-A RNA control kit (Affymetrix, California, USA) and GeneChip® One-cycle cDNA Synthesis kit (Affymetrix, California, USA) following the manufacturer's protocol. Then, cRNAs were biotin-labeled at 37 °C for 16 hours by GeneChip IVT Labeling kit (Affymetrix, California, USA). After that, they were hybridized at 45 °C for 16 hours onto Human Genome U133 (HG-U133) plus 2.0 oligonucleotide arrays (Affymetrix, California, USA) containing >54,000 gene targets. The array was washed and stained by GeneChip Hybridization, Wash and Stain kit (Affymetrix, California, USA) in Fluidics Station and then scanned using Affymetrix Launcher. The images were processed for visualization and normalization of each probe set to a common baseline using GeneSpring GX 10.1

(Agilent Technologies, California, USA). Gene Ontologies (GO, <http://geneontology.org>) was used for classification of gene products of greater than two-fold change. Gene products were grouped together based on biological processes, molecular functions, and signaling pathways.

### **2.3.5. Pathway analyses and network generation**

Pathway and global functional analyses were performed using IPA (Ingenuity® System, [www.ingenuity.com](http://www.ingenuity.com)). Gene accession numbers and the corresponding fold change of ITCs-treated HepG2 cells *versus* the control cells were uploaded into the IPA software. The analysis generated biological functions as well as pathways from the IPA library that is significant to the data set. Genes from the data sets associated with biological functions or canonical pathway of significance level less than 0.05 were used to map out molecular pathway networks. Network pathway is a graphical illustration of the molecular interaction between genes or gene products. Nodes represent the gene or gene products and lines represent the biological interaction between two nodes. All the lines are supported by at least one reference found in the literature, textbook or canonical information from the Ingenuity Pathway Knowledge Base (IPKB). Color intensity of the node indicates the degree of the up- (red) or downregulation (green). Various shapes of the nodes indicate the functional class of the gene products. Different labels below the lines describe the nature of the relationship between the nodes, *e.g.* E for expression, A for activation.

### **2.3.6. Reverse transcription and real-time PCR analyses**

Primers for the real-time PCR in the present study were generated based on the NCBI sequence database using the software PRIMER3 as elaborated in the previous study (Qin *et al*, 2012). Reverse transcription and real-time PCR were transformed with DyNamo SYBR Green two-Step qRT-PCR kit (Finnzymes Oy, Espoo, Finland) according to manufacturer's manual. Briefly, RNA was reversed to cDNA using Oligo dT and m-MuLV RNase at 37 °C for 30 minutes and the reaction was then terminated at 85 °C for 5 minutes. Real-time PCR was performed with the Roter-Gene-30000AKAA (Corbett Research, New South Wales, Australia) in triplicates using the standard curve. The  $T_m$  of PCR was determined according to each primer sequence (<https://www.finnzymes.fi/tm.detrmination.html>). The thermal cycling condition was hold at 95 °C for 15 minutes followed by 50-60 cycles of 30 seconds at 94 °C, 30 seconds corresponding  $T_m$  (Table 2.1) and 30 seconds at 72 °C (Qin *et al*, 2012). The results were represented by the relative expression level normalized with the control cells.



**Table 2.1.** Primer sequences used for real-time PCR analysis.

Gene name	Accession number	Direction	Sequences	T <sub>m</sub> (°C)
AKR1C1	S68290	Fw	5'-ATC CCT CCG AGA AGA ACC AT-3'	59
		Re	5'-ACA CCT GCA CGT TCT GTC TG-3'	
AKR1C3	AB018580	Fw	5'-AAG TAA AGC TTT GGA GGT CAC A-3'	59
		Re	5'-GGA CCA ACT CTC GTC GAT GAA-3'	
GCLC	NM_001498	Fw	5'-GAG CTG GGA GGA AAC CAA G-3'	61
		Re	5'-TGG TTT GGG TTT GTC CTT TC-3'	
GCLM	NM_002061	Fw	5'-GGG AAC CTG CTG AAC TGG-3'	61
		Re	5'-GCA TGA GAT ACA GTG CAT TCC-3'	
HO-1	NM_002133	Fw	5'-CCA CGC GGC CAG CAA CAA AGT GC-3'	60
		Re	5'-AAG CCT TCA GTG CCC ACG GTA AGG-3'	
NQO1	NM_000903	Fw	5'-AGT GCA GTG GTG TGA TCT CG-3'	60
		Re	5'-GGT GGA GTC ACG CCT GTA AT-3'	
TXNRD1	NM_003330	Fw	5'-ATC AGG AGG GCA GAC TTC AA-3'	61
		Re	5'-CCC ACA TTC ACA CAT GTT CC-3'	

### 2.3.7. Western blot analyses

HepG2 cells were seeded into 6-cm dishes and pre-cultured for 24 hours. Ten micromolar of ITC (SFN, 6-MSITC or 6-MTITC) was added and co-cultured for another 9 hours. Cells were harvested by lysis and extraction buffer, and homogenized twice in an ultrasonicator for 10 seconds and then incubated for 30 minutes under ice bath (Hou *et al*, 2000). The homogenates were centrifuged after at 14,000 g for 15 minutes at 4 °C. The protein concentration was determined by protein assay kit (Bio-Rad Laboratories, California, USA).

Forty microgram of protein lysates were run on 10-15 % SDS-PAGE and electrophoretically transferred to polyvinylidene difluoride (PVDF) membrane (Amersham Pharmacia Biotech, Little Chalfont, UK). The membrane was incubated with specific antibody overnight at 4 °C, followed by incubation for 1 hour with HRP-conjugated secondary antibody. Bound antibodies were detected using enhanced chemiluminescence (ECL) system and the relative amounts of protein associated with specific antibody were quantified using Lumi Vision Imager Software (TAITEC Co., Fukuoka, Japan).

### **2.3.8. Statistical Analyses**

Differences of array data among the treatments and control were analyzed using analyses of variance (ANOVA) test followed by *post hoc* analyses using Fisher's least significant difference (LSD). A probability of  $p < 0.005$  were considered to be statistically significant.

The genes from the microarray data set that meet the cut-off value of  $\geq 2$ -fold change and  $p < 0.0005$  were considered for IPA analysis. Fischer's right tail *t*-test was used to determine that the canonical pathway assigned to a given data set is not a product of chance alone. The  $p < 0.05$  were considered to be statistically significant.

Data obtained from the real-time PCR and Western blot were assessed for statistical significance using Student's *t*-test. Values with statistical probability of  $p < 0.05$  were considered significant.

## 2.4. Results

### 2.4.1. Gene expression profile of HepG2 cells treated with ITCs

Previous studies indicated that HepG2 cells treated with ITCs ranging from 5-20  $\mu\text{M}$  concentrations could result to increasing cellular response (Hou *et al*, 2011; Korenori *et al*, 2013). Upregulation of the antioxidant-associated protein expressions were observed at a dose of 10  $\mu\text{M}$  between 6-12 hours without cytotoxicity (Qin *et al*, 2012). Thus, 10  $\mu\text{M}$  concentration and 9-hour treatment condition was chosen for microarray analysis. mRNA profiling was carried out using Affymetrix HG UG133 plus 2.0 oligonucleotide arrays, which contains >54,000 gene probes, as described in 'Section 2.3.4'. Vehicle controls were cells treated with 0.2% v/v DMSO. Hepatocyte cells treated with DMSO was previously reported to exhibit negligible effect on the number of differentially altered genes in hepatocytes cells (Sumida *et al*, 2011). Hybridization signal comparison of the three ITC-treated mRNA samples with that of the control mRNA revealed that SFN, 6-MSITC and 6-MTITC differentially ( $p < 0.005$ ) regulated the expressions of 105, 144 and 189 genes, respectively (Table 2.2). Of these, 85 were upregulated and 20 genes were downregulated by SFN. For 6-MSITC, up- and downregulated genes were 66 and 78 genes, respectively. Whereas, 6-MTITC upregulated 114 genes and downregulated 75 genes. Detailed evaluation revealed that 6-MTITC exhibited the strongest influence on upregulated gene and 6-MSITC for downregulated genes. Nevertheless, 6-MSITC had the least contribution to the regulation of induced genes and SFN showed the least for the repressed genes. Overall, 6-MSITC and 6-MTITC treatments had a greater effect on the number of repressed genes with that of SFN treatment. Moreover, Venn diagram of microarray results in Figure 2.1 depicted

the number of uniquely differentially altered genes for each ITC treatment in comparison to the number of commonly altered genes. Of the altered genes, 57 were common among the three treatments, 10 were unique for SFN, 48 unique for 6-MSITC and 30 unique for 6-MTITC. The SFN and 6-MSITC treatments shared 10 genes, 6-MSITC and 6-MTITC treatments shared 56 genes, and SFN and 6-MTITC treatments shared 3 genes. Antioxidant-related genes was found as the most common genes between the three ITC treatments. Whereas, example of the unique genes in Wasabi-treated group were *PRKAB2* and *BCL10*, identified to be associated with cancer metabolic pathway and cell proliferation or survival. These data suggest that the structural differences of ITCs may influence the variability of the expression patterns, and Wasabi-derived ITCs had greater effect than SFN on the gene expression in HepG2 cells.

**Table 2.2.** Number of genes regulated by SFN, 6-MSITC and 6-MTITC in HepG2 cells.

<b>Fold change</b>	<b>SFN</b>	<b>6-MSITC</b>	<b>6-MTITC</b>
≥ 4	3	5	7
≥ 3 to < 4	10	9	13
≥ 2 to < 3	72	52	94
<i>Subtotal</i>	85	66	114
≥ -4	0	2	1
≥ -3 to < -4	0	9	8
≥ -2 to < -3	20	67	66
<i>Subtotal</i>	20	78	75
<b>Total</b>	<b>105</b>	<b>144</b>	<b>189</b>

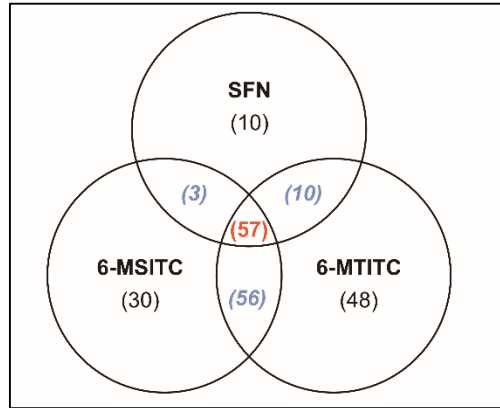


**Figure 2.1.** Venn diagram of microarray results by treatment of HepG2 with SFN, 6-MSITC and 6-MTITC. The overlapping circles depict the number of differentially regulated gene common or partially common to each ITC treatment. Non-overlapping circles indicated the unique altered genes to each ITC treatment.

#### **2.4.2. Grouping of genes targeted by Wasabi-derived ITCs**

All differentially ( $\geq 2$  folds) expressed genes were subjected to GO analyses to understand the function of genes targeted by SFN, 6-MSITC and 6-MTITC. Genes were grouped based on their biological or molecular functions. In biological processes, the gene that were identified with known annotation information were associated with apoptosis, cell cycle, cell proliferation, immune response, metabolic process, stress response and regulation of transcription (Table 2.3). Under molecular function, the gene groups highly affected by the three ITCs were found to be related to antioxidant, catalytic, ligase, oxidoreductase, signal transduction, transcription activator, transcription cofactor, transcription factor, transcription regulator and transferase activities (Table 2.3).

**Table 2.3.** Classification of genes targeted by ITCs in HepG2 cells.

<b>Category</b>	<b>SFN</b>	<b>6-MSITC</b>	<b>6-MTITC</b>
<i>Biological process</i>			
Apoptosis	7	14	17
Cell cycle	2	2	6
Cell proliferation	5	10	12
Immune response	7	7	8
Metabolic process	12	21	23
Stress response	6	8	14
Regulation of transcription	13	26	36
<i>Molecular function</i>			
Antioxidant activity	1	1	2
Catalytic activity	4	7	8
Ligase activity	3	4	5
Oxidoreductase activity	6	9	7
Signal transduction	3	8	7
Transcription activator	2	6	4
Transcription cofactor	1	1	4
Transcription factor	6	12	16
Transcription regulator	2	4	5
Transferase activity	5	12	16

### **2.4.3. Identification of biologically significant pathways**

Pathway analyses were done on datasets using IPKB to identify biologically significant networks and pathways associated with the regulation of Wasabi-derived ITCs, and to compare the potency of influence of each ITC. From pathway analysis using IPA software, various pathways within the threshold level of 0.05 were discovered. In Figure 2.2, the five statistically significant canonical pathways were displayed with respect to SFN regulation. Interestingly, the signaling pathway modulated by SFN, 6-MSITC and 6-MTITC with the highest significance score were gene subsets associated with Nrf2-mediated pathway. Four other significantly affected pathways with respect to SFN treatment were Notch signaling, glutamate metabolism, glutathione metabolism and vitamin D receptor (VDR)/9-*cis* retinoic acid receptor (RXR) activation. Among the three

treatments, 6-MSITC treatment had the utmost effects on Nrf2-mediated pathway with  $P$ -value of  $7.76 \times 10^{-6}$ , followed by 6-MTITC ( $P = 8.32 \times 10^{-4}$ ), and SFN ( $P = 5.50 \times 10^{-4}$ ) (Table 2.4). Additionally, 6-MSITC had the highest number of differentially regulated genes (9) by two-fold and above that are associated with Nrf2-mediated pathway. Meanwhile, out of 185 total genes linked to Nrf2-mediated pathway, 7 and 5 genes were identified to be up-regulated by  $\geq 2$  folds for 6-MTITC and SFN, respectively. However, the level of significance for glutathione metabolism and VDR/RXR activation by 6-MSITC and 6-MTITC treatments were greater than 0.05, indicating that the modulated pathway cannot be classified accurately

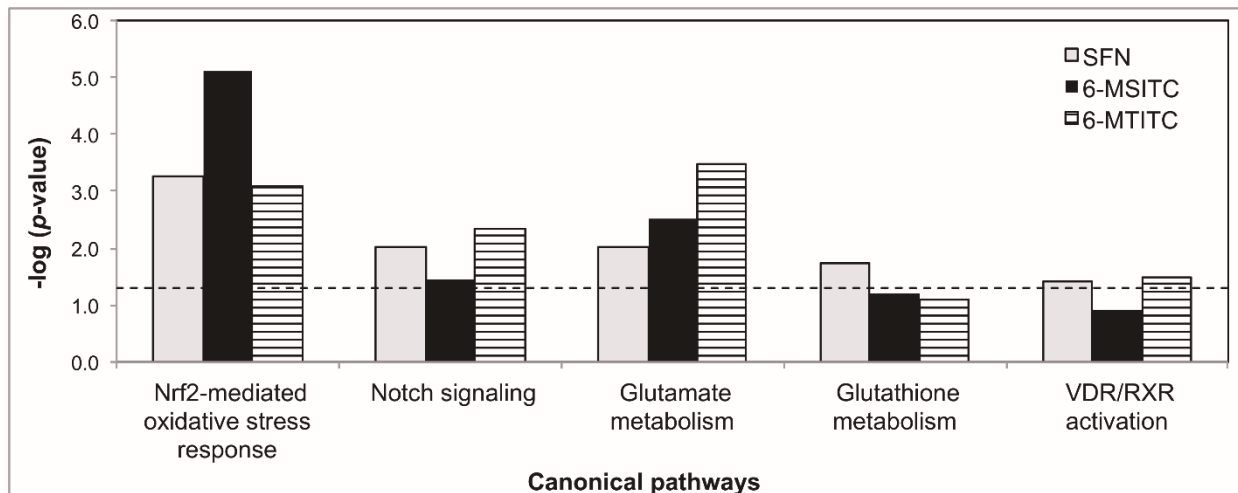


**Figure 2.2.** Comparative canonical pathway analyses of differentially expressed genes in HepG2 hepatoblastoma cells stimulated with ITCs. Differentially upregulated and downregulated genes were evaluated for canonical pathway analyses using IPA software as described in “**Section 2.3.5**”. Only five of the top most significant pathways with respect to SFN were shown here. List of corresponding significant pathways is indicated below and their respective level of significance ( $p < 0.05$ ) denoted by the length of the bars.

**Table 2.4.** List of genes involved in significantly modulated canonical pathways by SFN, 6-MSITC and 6-MTITC in HepG2 cells.

<b>ITCs</b>	<b>Canonical pathways</b>	<b>p-value</b>	<b>Ratio*</b>	<b>Regulated genes</b>
SFN	Nrf2-mediated oxidative stress response	$5.52 \times 10^{-4}$	0.027	<i>DNAJB4, FOS, GCLC, GCLM, SQSTM1</i>
	Notch signaling	$9.59 \times 10^{-3}$	0.049	<i>HEY1, JAG1</i>
	Glutamate metabolism	$9.59 \times 10^{-3}$	0.026	<i>GCLC, GCLM</i>
	Glutathione metabolism	$1.77 \times 10^{-2}$	0.020	<i>GCLC, GCLM</i>
	VDR/RXR activation	$3.72 \times 10^{-2}$	0.025	<i>KLF4, SPP1</i>
6-MSITC	Nrf2-mediated oxidative stress response	$7.68 \times 10^{-6}$	0.049	<i>ABCC1, DNAJB4, DNAJC6, FOS, FOSL1, GCLC, GCLM, HMOX1, SQSTM1</i>
	Notch signaling	$3.47 \times 10^{-2}$	0.049	<i>HEY1, JAG1</i>
	Glutamate metabolism	$3.13 \times 10^{-3}$	0.038	<i>ABAT, GCLC, GCLM</i>
	Glutathione metabolism	$6.17 \times 10^{-2}$	0.020	<i>GCLC, GCLM</i>
	VDR/RXR activation	$1.22 \times 10^{-1}$	0.025	<i>SPP1, VDR</i>
6-MTITC	Nrf2-mediated oxidative stress response	$8.34 \times 10^{-4}$	0.038	<i>DNAJB4, FOS, FOSL1, GCLC, GCLM, HMOX1, SQSTM1</i>
	Notch signaling	$4.53 \times 10^{-3}$	0.073	<i>DTX4, HEY1, JAG1</i>
	Glutamate metabolism	$8.34 \times 10^{-4}$	0.051	<i>ABAT, GAD1, GCLC, GCLM</i>
	Glutathione metabolism	$7.76 \times 10^{-2}$	0.020	<i>GCLC, GCLM</i>
	VDR/RXR activation	$3.16 \times 10^{-2}$	0.038	<i>KLF4, SPP1, VDR</i>

\**Ratio* is the number of statistically differentially regulated genes divided by the number of genes associated to the pathways.



#### **2.4.4. Expression of genes associated with significantly modulated pathways**

To investigate the influence of Wasabi-derived ITCs-regulated gene subsets on the biologically significant pathways, the expression levels of genes associated with each pathway were profiled in Table 2.5. For Nrf2-mediated pathway, the gene products were found to be ATP-binding cassette, sub-family C (CFTR/MRP), member 1 (*ABCC1*), DnaJ (Hsp40) homolog, subfamily B, member 4 (*DNAJB4*), DnaJ (Hsp40) homolog, subfamily C, member 6 (*DNAJC6*), v-fos FBJ murine osteosarcoma viral oncogene homolog (*FOS*), FOS-like antigen 1 (*FOSL1*), glutamate-cysteine ligase, catalytic subunit (*GCLC*), glutamate-cysteine ligase, modifier subunit (*GCLM*), heme oxygenase (decycling) 1 (*HMOX1* or *HO-1*), and sequestosome 1 (*SQSTM1*). Gene-by-gene inspection revealed that the presence of *DNAJB4*, *FOS*, *GCLC*, and *GCLM* were common across three ITC treatments. However, *ABCC1* and *DNAJC6* were induced only as a result of stimulating the cell with 6-MSITC. Moreover, treatment of 6-MTITC induced the highest fold changes on the stress related genes, albeit the increase was not significant from that of 6-MSITC.

**Table 2.5.** The differential expressions of genes involved in top modulated canonical pathways by Wasabi-derived ITCs.

Signaling pathway	Gene symbol	Gene title	Fold change			Accession no.
			SFN	6-MSITC	6-MTITC	
Nrf2-mediated oxidative stress response	<i>ABCC1</i>	ATP-binding cassette, subfamily C (CFTR/MRP), member 1	↑ 1.66	↑ 1.73	↑ 1.70	AI539710
	<i>ABCC1</i>	ATP-binding cassette, subfamily C (CFTR/MRP), member 1	↑ 1.84	↑ 2.20	↑ 1.90	NM_004996
	<i>DNAJB4</i>	DnaJ (Hsp40) homolog, subfamily B, member 4	↑ 2.35	↑ 2.80	↑ 2.91	BG252490
	<i>DNAJB4</i>	DnaJ (Hsp40) homolog, subfamily B, member 4	↑ 2.19	↑ 2.73	↑ 2.72	NM_007034
	<i>DNAJC6</i>	DnaJ (Hsp40) homolog, subfamily C, member 6	↑ 1.99	↑ 2.20	↑ 2.07	AV729634
	<i>DNAJC6</i>	DnaJ (Hsp40) homolog, subfamily C, member 6	↑ 1.03	↑ 1.01	↓ 1.01	NM_014787
	<i>FOS</i>	V-fos FBJ murine osteosarcoma viral oncogene homolog	↑ 3.16	↑ 3.89	↑ 4.14	BC004490
	<i>FOSL1</i>	FOS-like antigen 1	↑ 1.90	↑ 2.40	↑ 2.35	BG251266
	<i>GCLC</i>	Glutamate-cysteine ligase, catalytic subunit	↑ 2.02	↑ 2.28	↑ 2.33	BF676980
	<i>GCLC</i>	Glutamate-cysteine ligase, catalytic subunit	↑ 2.33	↑ 2.51	↑ 2.50	NM_001498
	<i>GCLC</i>	Glutamate-cysteine ligase, catalytic subunit	↑ 1.97	↑ 2.40	↑ 2.59	BC022487

Signaling pathway	Gene symbol	Gene title	Fold change			Accession no.
			SFN	6-MSITC	6-MTITC	
	<i>GCLM</i>	Glutamate-cysteine ligase, modifier subunit	↑ 2.29	↑ 2.40	↑ 2.48	NM_002061
	<i>GCLM</i>	Glutamate-cysteine ligase, modifier subunit	↑ 2.37	↑ 2.05	↑ 2.59	AI753488
	<i>HMOX1</i>	Heme oxygenase (decycling) 1 (HO-1)	↑ 1.55	↑ 2.22	↑ 2.27	NM_002133
	<i>SQSTM1</i>	Sequestosome 1	↑ 2.12	↑ 2.37	↑ 2.41	NM_003900
	<i>SQSTM1</i>	Sequestosome 1	↑ 2.33	↑ 2.46	↑ 2.21	N30649
	<i>SQSTM1</i>	Sequestosome 1	↑ 1.03	↑ 1.07	↑ 1.32	U46752
	<i>SQSTM1</i>	Sequestosome 1	↑ 1.00	↑ 1.25	↑ 1.18	U46752
	<i>SQSTM1</i>	Sequestosome 1	↓ 1.04	↓ 1.05	↓ 1.01	AI041019
	<i>SQSTM1</i>	Sequestosome 1	↑ 1.35	↑ 1.56	↑ 1.38	AW293441
Notch signaling	<i>DTX4</i>	Deltex 4 homolog (Drosophila)	↓ 1.66	↓ 1.73	↓ 1.95	AV728526
	<i>HEY1</i>	airy/enhancer-of-split related with YRPW motif 1	↑ 2.40	↑ 3.43	↑ 3.23	NM_012258
	<i>HEY1</i>	Hairy/enhancer-of-split related with YRPW motif 1	↑ 2.37	↑ 3.36	↑ 3.23	R61374
	<i>JAG1</i>	Jagged 1 (Alagille syndrome)	↑ 1.49	↑ 1.24	↑ 1.41	BF056748
	<i>JAG1</i>	Jagged 1 (Alagille syndrome)	↑ 2.76	↑ 3.59	↑ 4.02	U61276
	<i>JAG1</i>	Jagged 1 (Alagille syndrome)	↑ 2.04	↑ 2.42	↑ 2.44	U73936
	<i>JAG1</i>	Jagged 1 (Alagille syndrome)	↑ 1.97	↑ 2.23	↑ 2.33	U77914
	<i>JAG1</i>	Jagged 1 (Alagille syndrome)	↑ 1.83	↑ 1.87	↑ 2.06	AI457817
Glutamate metabolism	<i>ABAT</i>	4-Aminobutyrate aminotransferase	↓ 1.54	↓ 2.11	↓ 1.94	AF237813
	<i>ABAT</i>	4-Aminobutyrate aminotransferase	↓ 1.58	↓ 1.98	↓ 2.02	AF237813
	<i>GAD1</i>	Glutamate decarboxylase 1 (brain, 67kDa)	↓ 1.42	↓ 1.80	↓ 2.02	NM_000817
	<i>GAD1</i>	Glutamate decarboxylase 1 (brain, 67kDa)	↓ 1.13	↓ 1.33	↓ 1.18	NM_013445

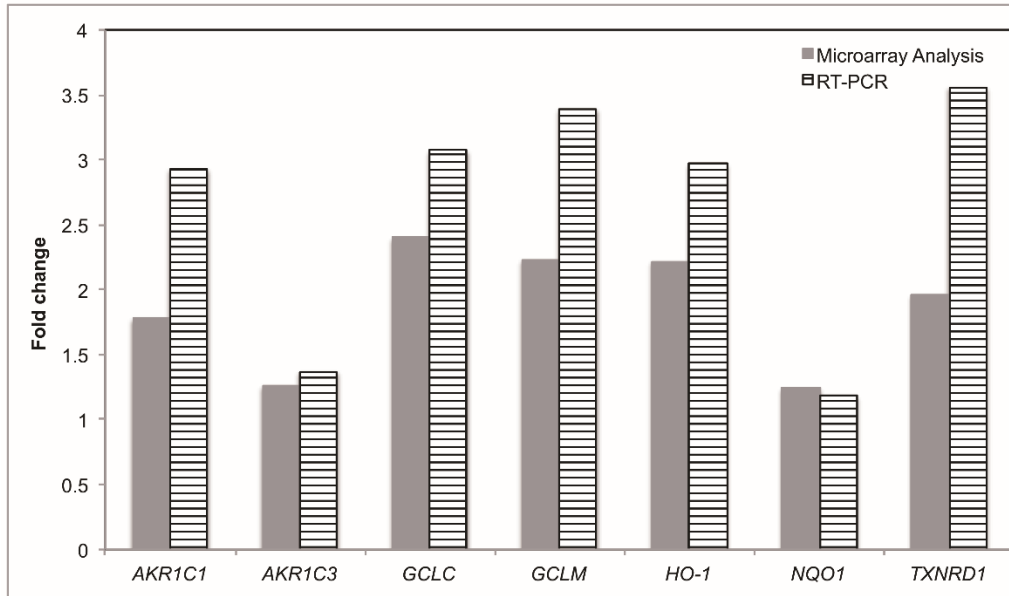
Signaling pathway	Gene symbol	Gene title	Fold change			Accession no.
			SFN	6-MSITC	6-MTITC	
Glutathione metabolism	<i>GAD1</i>	Glutamate decarboxylase 1 (brain, 67kDa)	↓ 1.20	↓ 1.24	↓ 1.49	NM_013445
	<i>GCLC</i>	Glutamate-cysteine ligase, catalytic subunit	↑ 2.02	↑ 2.28	↑ 2.33	BF676980
	<i>GCLC</i>	Glutamate-cysteine ligase, catalytic subunit	↑ 2.33	↑ 2.51	↑ 2.50	NM_001498
	<i>GCLC</i>	Glutamate-cysteine ligase, catalytic subunit	↑ 1.97	↑ 2.40	↑ 2.59	BC022487
	<i>GCLM</i>	Glutamate-cysteine ligase, modifier subunit	↑ 2.29	↑ 2.40	↑ 2.48	NM_002061
	<i>GCLM</i>	Glutamate-cysteine ligase, modifier subunit	↑ 2.37	↑ 2.05	↑ 2.59	AI753488
	<i>GCLC</i>	Glutamate-cysteine ligase, catalytic subunit	↑ 2.02	↑ 2.28	↑ 2.33	BF676980
	<i>GCLC</i>	Glutamate-cysteine ligase, catalytic subunit	↑ 2.33	↑ 2.51	↑ 2.50	NM_001498
	<i>GCLC</i>	Glutamate-cysteine ligase, catalytic subunit	↑ 1.97	↑ 2.40	↑ 2.59	BC022487
	<i>GCLM</i>	Glutamate-cysteine ligase, modifier subunit	↑ 2.29	↑ 2.40	↑ 2.48	NM_002061
	<i>GCLM</i>	Glutamate-cysteine ligase, modifier subunit	↑ 2.37	↑ 2.05	↑ 2.59	AI753488
	VDR/RXR activation	<i>KLF4</i>	Kruppel-like factor 4 (gut)	↑ 1.26	↑ 1.56	↑ 1.55
<i>KLF4</i>		Kruppel-like factor 4 (gut)	↑ 2.38	↑ 1.98	↑ 2.52	BF514079
<i>SPP1</i>		Secreted phosphoprotein 1 (osteopontin, bone sialoprotein I, early T-lymphocyte activation 1)	↑ 3.21	↑ 2.64	↑ 2.82	M83248
<i>SPP1</i>		Secreted phosphoprotein	↓ 1.02	↑ 1.07	↑ 1.12	AB019562

Signaling pathway	Gene symbol	Gene title	Fold change			Accession no.
			SFN	6-MSITC	6-MTITC	
		1 (osteopontin, bone sialoprotein I, early T-lymphocyte activation 1)				
	VDR	Vitamin D (1,25-dihydroxyvitamin D3) receptor	↓ 1.38	↓ 1.26	↓ 1.53	AA454701
	VDR	Vitamin D (1,25-dihydroxyvitamin D3) receptor	↓ 1.55	↓ 2.24	↓ 2.11	NM_000376
	VDR	Vitamin D (1,25-dihydroxyvitamin D3) receptor	↓ 1.77	↓ 2.70	↓ 2.86	AA772285
	VDR	Vitamin D (1,25-dihydroxyvitamin D3) receptor	↓ 1.13	↓ 1.30	↓ 1.33	AA904259

#### 2.4.5. Confirmation of microarray results

Seven genes associated with Nrf2-mediated pathway were selected to confirm the results of microarray analyses by real-time PCR (Figure 2.3). Each of these genes has a corresponding primer that was designed according to the NCBI sequence database using Primer 3 software (Qin *et al*, 2012). 6-MSITC was used as a representative for the confirmatory analysis since it displayed the most significant regulation associated with Nrf2-mediated pathway across ITC treatments. Most of the chosen genes exhibited a similar expression pattern between the microarray and real-time PCR data. For instance, real-time PCR data showed that *HO-1* was upregulated by 2.97 folds relative to the control level, whereas microarray analysis data revealed 2.22-fold change. 6-MSITC also induced *GCLC* gene expression by 3.07 in real-time PCR, while in microarray analysis an increase of 2.04 folds. On the other hand, *GCLM* mRNA expression increased by 3.39 folds in real-time PCR while 2.23 folds in microarray analysis. *NQO1* gene whose

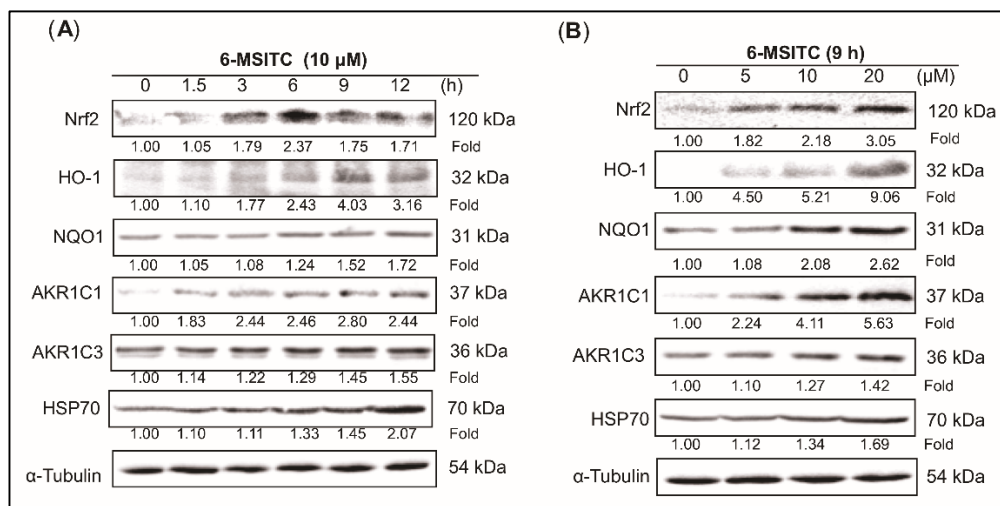
expression in microarray analysis was not differentially significant remained not significant in real-time PCR. However, *TXNRD1* gene induction was found higher in microarray analysis (1.96 folds) than in real-time PCR (3.56 folds).



**Figures 2.3.** Validation of differentially expressed genes in 6-MSITC-treated HepG2 cells from DNA microarray analyses by real-time PCR. DNA microarray results were compared to real-time PCR results for selected genes. Real-time PCR was performed using DyNAmo™ SYBR® Green 2-Step qRT-PCR Kit as described in “**Section 2.3.6**”. Fold changes represented the ratio between the treated samples values to that of the untreated samples. Expression changes are depicted as fold change (*y*-axis). Gene symbols are shown below.

Next, the involvement of 6-MSITC in the Nrf2-mediated pathway, as revealed from the signaling pathway analyses of microarray data, was verified at the translational level. Hence, HepG2 cells were treated with 10  $\mu$ M of 6-MSITC from 0–24 hours and then

detected the protein levels by Western blotting. As shown in Figure 2.4A, 6-MSITC caused a time-dependent induction of Nrf2 protein together with Nrf2-dependent proteins HO-1, NQO1, AKR1C1, AK1C3, and Hsp70. For HO-1 and AKR1C1, an early induction was observed, whereas NQO1, AKR1C3 and HSP70 were induced at the later time. Meanwhile, dose-course experiment increased Nrf2, HO-1, NQO1, and AKR1C1 protein levels significantly as the ITC concentration was increased (Figure 2.4B). However, a gradual increase was found in the protein expressions of AKR1C3 and HSP70.



**Figures 2.4.** Validation of differentially expressed genes in 6-MSITC-treated HepG2 cells from DNA microarray analyses by Western blot analysis. **(A)** HepG2 cells were treated with 10 μM of 6-MSITC for 0–12 hours. **(B)** HepG2 cells were treated for 9 h with 0–20 μM of 6-MSITC. Nrf2, HO-1, NQO1, AKR1C1, AKR1C3, HSP70, and α-tubulin were detected using Western blot analysis with their respective antibodies. The induction fold of the protein was calculated as the intensity of the treatment relative to that of control normalized to α-tubulin by densitometry. The blots shown were the examples of three separate experiments.

#### **2.4.6. Nrf2 pathway and network analysis**

The connectivity pathways were constructed using IPA software built pathway tools to analyze the Nrf2-associated gene expressions by ITCs with Nrf2 as focus molecule. The analyses were performed to evaluate the molecular interactions as responses to ITCs stimulation in reference to the prevailing studies collated under IPKB database. Growing out nodes downstream of Nrf2 molecules generated the pathways. Only nodes affected by ITC treatment and their interactions are shown.

Figures 2.5A-C revealed the schematic network pathways among Nrf2-mediated genes that responded to SFN, 6-MSITC and 6-MTITC treatments. Network pathway shows that there was no significant regulation in the gene expressions of *Keap1* and *Nrf2* between the three treatments. Interestingly, under this network pathway, the genes upregulated by SFN were mostly metabolizing enzymes. Whereas, Wasabi-derived ITCs, 6-MSITC and 6-MTITC, showed that they can upregulate genes involved not only in metabolism, but also in antioxidation (e.g. *HO-1*, *SQSTM1*), detoxification (e.g. *ABCC1*) and stress response (e.g. *DNAJB4*, *DNAJC6*). Altogether, the Nrf2 network pathway analyses showed that the activation of *Nrf2* by Wasabi-derived ITCs can result to the induction of multiple groups of genes downstream.



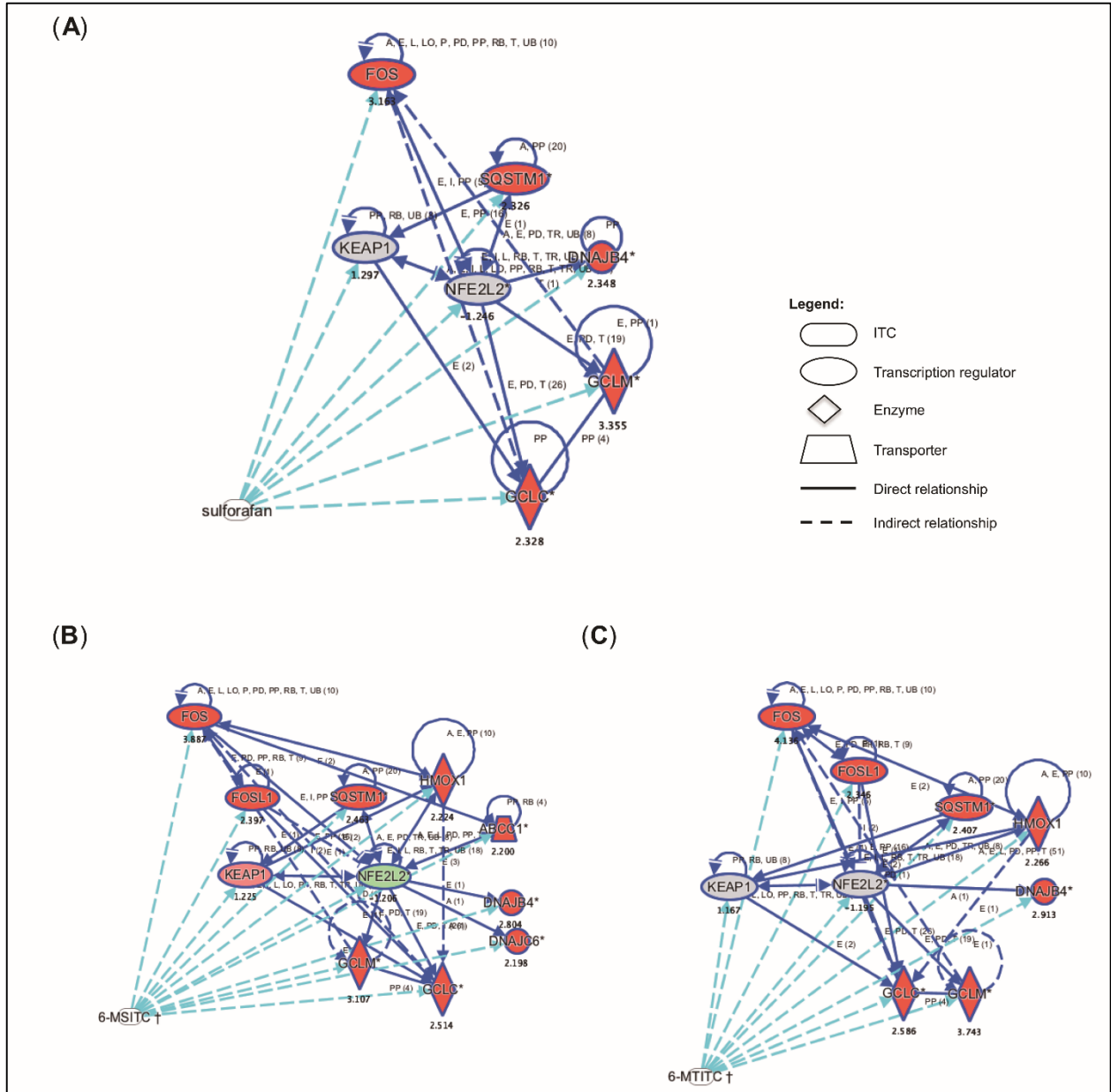


**Figure 2.5.** Nrf2-mediated pathway was found as significantly enriched pathway by IPA. Schematic flow charts were shown with the differentially regulated genes and molecular interaction of **(A)** SFN, **(B)** 6-MSITC and **(C)** 6-MTITC towards Nrf2 and Nrf2-associated genes.

## 2.5. Discussions

ITC is a group of organosulfur compound known for their wide array of bioactive functions. In particular, SFN is effective in improving bronchoprotective response in asthmatics, ameliorating memory impairment, attenuating muscle inflammation and inhibiting thyroid cancer cell growth (Brown *et al*, 2015; Dwivedi *et al*, 2015; Sun *et al*, 2015; Wang *et al*, 2015). SFN exerts these pharmacological effects by inducing antioxidant redox system, downregulating inflammation-associated genes, and inducing apoptosis in cancer cells (Sumida *et al*, 2011; Ye *et al*, 2013; Bergantin *et al*, 2014). Although the chemopreventive mechanism of SFN is well-characterized, pharmacologic role of Wasabi-derived ITCs is limited to reduction of cell proliferation and phase 1 enzymes, suppression of cell adhesion, reduction of cytokines and chemokines, and activation of antioxidant system (Kuno *et al*, 2010; Okamoto & Akita 2013; Morroni *et al*, 2013). Nevertheless, none of these studies addressed the comparative effects of SFN and Wasabi-derived ITCs, especially their degree of potency as chemopreventive agents, at a genome-wide expression level. Thus, this is the first study to assess the global changes in transcript levels of the two major ITCs from Japanese Wasabi (6-MSITC and 6-MTITC), as well as SFN, in human hepatoblastoma HepG2 cells.

DNA microarray analysis identified 105, 144 and 189 differentially expressed genes in response to SFN, 6-MSITC and 6-MTITC treatments, respectively (Table 2.2). These genes were associated with various functions such as stress and immune response, cell cycle and proliferation, metabolic process and apoptosis. Out of the three ITC treatments, the 10  $\mu$ M treatment of 6-MTITC for 9 hours was found to alter the most number of gene expressions. 6-MSITC gene response was 23 % lower than 6-MTITC

while SFN was 44 % lower. This suggests that the effect of the three ITCs towards gene expression regulation may be dictated by the carbon chain length between the ITC group and the sulfinyl sulfur of the methyl group. 6-MSITC is a methylthioalkyl ITC containing S=O substituent attached to methyl group, whereas, 6-MTITC is a methylsulfinylalkyl ITC without oxygen atom attached to the sulfur atom of the methyl group (Ina *et al*, 1989; Etoh *et al*, 1990). On the other hand, SFN is two-carbon chain lesser than 6-MSITC and 6-MTITC. However, it will be also interesting to investigate the effect of long carbon chain or aromatic naturally occurring ITCs on gene expression profile of HepG2 cells to fully distinguish the variance. Also, Venn diagram shown in Figure 2.1 indicated the unique genes altered by Wasabi-derived ITCs in comparison with the common genes regulated by the three ITCs. Detailed evaluation of the types of unique and common genes revealed that they are cancer-driver genes (unique) and antioxidant activity-associated genes (common). Thus, this could imply that Japanese Wasabi-derived ITCs exhibit synergistic effect via the gene-gene interaction, but needs to be further clarified in the proceeding study.

The list of differentially regulated genes (Table 2.2) coupled with the canonical pathways generated from IPA software (Figure 2.2) revealed that the gene expression profiles of SFN, 6-MSITC and 6-MTITC modulated Nrf2-mediated pathway. While 6-MTITC has the highest differentially regulated genes, 6-MSITC emerged as the most potent inducer of pathway associated with Nrf2-mediated response. This indicates that the differentially regulated genes of 6-MSITC are mainly controlled by transcription factor Nrf2, known to be involved in antioxidant stress response (Qin *et al*, 2013). Furthermore, the enrichment of glutamate metabolism is also a strong reflection of the induction of

phase 2 enzyme response. Indeed, gene expression profile of HepG2 cells treated with 6-MSITC induced gene transcripts targeted by Nrf2 activation (Table 2.4). Similarly, Nrf2-mediated response was also reported as the topmost significantly upregulated pathway in Wasabi-derived ITCs-treated IMR-32 cells (Trio *et al*, 2016). Though a higher number of genes were differentially altered in IMR-32 than HepG2 cells, Wasabi-derived ITCs still remained the potent regulator of gene expression in both cells. Thus, this implies that ITCs exhibit similar stimulation effect in the two cell lines. Additionally, this also signifies that 6-MSITC combats oxidative stress via the underlying antioxidant activity. Among the three gene expression profiles, 6-MSITC profiles affected the highest number of genes linked to Nrf2-mediated pathway. This is in agreement with the recent finding that an increase on the length of the carbon chain separating the ITC group and sulfinyl sulfur from 4 to 6 carbon atoms of ITC compounds positively influences Nrf-2 activation (Elhalem *et al*, 2014). Moreover, lengthening of the carbon chain displayed beneficial cytotoxic effect to normal cells while maintaining its cytotoxicity to cancer cells. The genes induced by 6-MSITC associated with the Nrf2 signaling were *ABCC1*, *DNAJB4*, *DNAJC6*, *GCLC*, *GCLM*, *HMOX1* and *SQSTM1* (Table 2.5). They are known to contain electrophile response element (EpRE, or ARE) and belong to the important gene categories of chaperone proteins, metabolizing enzymes, detoxifying and antioxidant proteins, demonstrating the modulatory effects of 6-MSITC on Nrf2-ARE pathway (Wild *et al*, 1999; Solis *et al*, 2002; Hou *et al*, 2011). Interestingly, upregulated gene transcripts under the chaperone protein category are all heat shock proteins. For example, *DNAJB4* has been reported to suppress tumor in non-small cell lung cancer model via inhibition of cell proliferation and promotion of apoptosis (Tsai *et al*, 2006). This indicates that induction of

heat shock proteins by 6-MSITC as a response to oxidative stress may assist the repair or degradation of damaged proteins. As previously mentioned, one of the significantly induced pathways by Wasabi-derived ITCs also include glutamate metabolism. Glutamate metabolism is anticipated since phase 2 genes (*GCLM* and *GCLC*) are among the significantly induced genes. Additionally, downregulation of 4-aminobutyrate aminotransferase (*ABAT*) and glutamate decarboxylase 1 (brain, 67kDa) (*GAD1*) genes by Wasabi-derived ITCs were also linked to glutamate metabolism. However, the molecular mechanism of how these upregulated genes by Wasabi-derived ITCs is linked to glutamate metabolism in hepatic cancer cell model will require further study.

Wasabi-derived ITCs was also found to exhibit protective effects up to the translational level. Using 6-MSITC as a Wasabi-derived ITCs representative, the Nrf2 activation was confirmed to be translated to the protein level. The treatment of 6-MSITC induced a higher level of Nrf2 expression. As a result, Nrf2 activation was followed by increased expression of cytoprotective proteins such as HO-1, NQO1, AKR1C1, AKR1C3 and HSP70 (Figure 2.3). These data further demonstrated that Wasabi-derived ITCs exert the antioxidant effects in HepG2 cells by activating Nrf2-mediated pathway up to the protein level. This result is also in agreement with the previous report where activation of Nrf2 by 6-MSITC was found to lead to the induction of ARE-dependent NQO1 expression (Hou *et al*, 2011). Both Wasabi-derived ITCs have the similar potency with respect to antioxidant protein induction, but 6-MTITC has a higher maximal attainable induction response than 6-MSITC. Thus, this indicates that 6-MTITC is a stronger antioxidant protein inducer per concentration equivalent than 6-MSITC in HepG2 cells (Figure 3A; Itoh *et al*, 1997). With respect to time-response effect, 6-MTITC was found to have an

early effective response than 6-MSITC as indicated by an early induction of the antioxidant proteins. Thus, this could deduce that 6-MSITC has a longer effective window than 6-MTITC because 6-MSITC continuously increased the expression of antioxidant protein whereas 6-MTITC inducing efficacy started to decline after 9 hours.

Experimental evidence indicated that Nrf2 play a major role in cancer prevention. This has been proven in various studies using different Nrf2 inducers applied to various cancer cell and animal models. For instance, upregulation of HO-1 expression via Nrf2 activation in animal model study is effective in inhibiting the development of skin tumor (Xu *et al*, 2006). In the study, the Nrf2 was identified as the focus molecule and the molecules highly regulated by Wasabi-derived ITCs downstream of Nrf2 were emphasized. This gene network regulation has been observed also in SFN-treated mice (Hu *et al*, 2006). The microarray data support that 6-MSITC could regulate a wide array of drug metabolism enzymes, and Nrf2 was found to be the central gene in this gene network regulation, indicating the anticarcinogenic potential of 6-MSITC and the underlying molecular mechanism involved the enhancement of the cellular defense system.

In conclusion, the results of the DNA microarray analyses revealed for the first time the expression profiles of Wasabi-derived ITCs in human hepatoblastoma HepG2 cells. 6-MTITC has the most number of differentially expressed genes across three ITC treatments, indicating the positive effect of carbon chain-length increase towards gene regulation. Interestingly, 6-MSITC emerged as the most potent inducer of Nrf2-mediated pathway, suggesting the important role of the sulfinyl sulfur group and the carbon chain length in liver cancer cell model. Further, glutamate metabolism also showed to be

regulated by 6-MSITC. Altogether, these data suggest that 6-MSITC exerts cytoprotective role through its underlying antioxidant activity via the activation of Nrf2 and subsequent induction of antioxidant proteins and metabolizing enzymes.

## CHAPTER III

### DNA microarray highlights Nrf2-mediated neuron protection targeted by Wasabi-derived isothiocyanates in IMR-32 cells

#### 3.1. Abstract

6-(Methylsulfinyl)hexyl isothiocyanate (6-MSITC), 6-(methylthio)hexyl isothiocyanate (6-MTITC), and sulforaphane (SFN) are isothiocyanate (ITC) bioactive compounds from Japanese Wasabi. Previous *in vivo* studies highlighted the neuroprotective potential of ITCs since they enhance the production of antioxidant-related enzymes. Thus, in this present study, a genome-wide DNA microarray analysis was designed to profile gene expression changes in a neuron cell line, IMR-32, stimulated by these ITCs. Among these ITCs, 6-MSITC caused the expression changes of most genes (263), of which 100 genes were upregulated and 163 genes were downregulated. Gene categorization showed that most of the differentially expressed genes are involved in oxidative stress response, and pathway analysis further revealed that Nrf2-mediated oxidative stress pathway is the top of the ITC-modulated signaling pathway. Finally, real-time polymerase chain reaction (PCR) and Western blotting confirmed the gene expression and protein products of the major targets by ITCs. Taken together, Wasabi-derived ITCs might target the Nrf2-mediated oxidative stress pathway to exert neuroprotective effects.



### 3.2. Introduction

Wasabi (*Wasabia japonica* (Miq.) Matsumura), commonly known as Japanese horseradish, is a member of the Brassicaceae vegetables. Its rhizome has a pungent flavor, which is popularly used as a spice among Japanese households. Studies have shown that Wasabi has multifarious functions such as antimicrobial, anticoagulation, anti-inflammatory, anti-obesity, and anticancer (Isshiki & Tokuoka, 1993; Kumagai *et al*, 1994; Nagai & Okunishi, 2009; Yamasaki *et al*, 2013; Hsuan *et al*, 2016). These activities can be attributed to a group of bioactive compounds identified as ITCs (Ono *et al*, 1996). They include sulforaphane (SFN), 6-MSITC, and 6-MTITC (Figure 3.1). Previous study revealed that a structure–activity relationship of Wasabi ITCs was present for the inhibition of cyclooxygenase 2 (COX-2) expression with a dependence on the methyl chain length of Wasabi ITCs (Uto *et al*, 2005). The longer the methyl chain length of Wasabi ITCs, the stronger the inhibition of COX-2 expression.

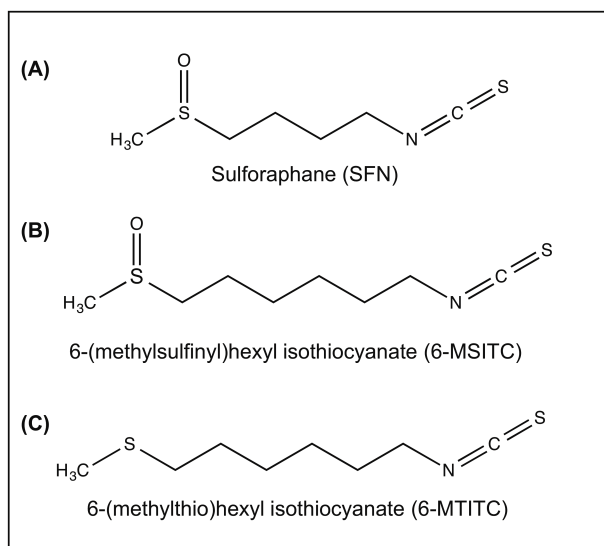


**Figure 3.1.** Chemical structures of Japanese Wasabi-derived ITCs used in the study. (A) Sulforaphane, SFN; (B) 6-(methylsulfinyl)hexyl isothiocyanate (6-MSITC); and (C) 6-(methylthio)hexyl isothiocyanate (6-MTITC).

Recently, Tarozzi *et al* (2013) have provided a review highlighting the potential of SFN against neurodegenerative diseases by implicating the activation of nuclear factor E2 related factor 2 (Nrf2) *cis*-acting antioxidant responsive element (ARE) pathway (Tarozzi *et al*, 2013). SFN pretreatment could protect disruption of blood–cerebrospinal fluid barrier and shield astrocytes and neuron cells from toxic effects caused by various oxidants through the increase of intracellular glutathione (GSH) and the induction of nicotinamide adenine dinucleotide phosphate (NAD[P]H) quinone oxidoreductase 1 (NQO1) via the activation of Nrf2 pathway (Xiang *et al*, 2012; Danilov *et al*, 2009; Mizuno *et al*, 2011). Similarly, in quinone-induced dopaminergic cell death model, SFN exerted protective function by mediating the toxic accumulation of quinones via induction of NQO1 expression (Han *et al*, 2007). Other than providing long-term protection against oxidative damage via upregulation of the antioxidant redox system, SFN can also downregulate the expressions of inflammation-associated genes (Ye *et al*, 2013). Collection of these studies proved that SFN is a budding neuroprotective agent but little is known yet about its analogs found in Japanese Wasabi. To date, animal study, following Parkinson’s disease mouse model, demonstrated that 6-MSITC reduced motor dysfunction induced by 6-hydroxydopamine via reducing oxidative stress and apoptotic cell death (Morromi *et al*, 2014). Also, 6-MSITC prevented oxidative stress cytotoxicity by raising the intracellular GSH content through the increase of  $\gamma$ -glutamylcysteine synthetase induced by the activation of Nrf2/ARE pathway in an oxidative stress-induced animal model (Mizuno *et al*, 2011). However, the exact molecular mechanism of interaction of Wasabi-derived ITCs toward neuroprotection at the cellular level has not yet been ascertained.

Nrf2 is a basic region leucine zipper transcription factor that activates the Nrf2/ARE pathway. It acts as the master regulator of the cellular antioxidant response via modulating the expressions of over 250 genes (Petri *et al*, 2012). Impaired Nrf2 leads to a dysfunctional Nrf2 pathway that decreases cellular defense against oxidative stress (Ramsey *et al*, 2007). The overproduction of oxidative stress could contribute to cell death, which is associated with the progression of neurodegenerative diseases. In *tert*-butyl hydroquinone-induced astrocytes, the cells from Nrf2 deficient mice were more sensitive to oxidative stress than the cells from wild-type mice (Lee *et al*, 2003). Hence, upregulation of Nrf2 activity is an attractive approach to combat the increase of oxidative stress during the development of neurodegeneration. Interestingly, *in vivo* studies revealed that Nrf2 inducers reduced toxic-induced cellular damage in the brain of wild-type mice but not in Nrf2 knockout mice (Shih *et al*, 2005; Calkins *et al*, 2009). For instance, SFN administration in rats exposed to traumatic brain injury attenuated oxidative stress and neuronal damage via upregulation of Nrf2-dependent antioxidant enzymes such as heme oxygenase 1 (HO-1) and NQO1 (Hong *et al*, 2010). HO-1 catalyzes heme degradation to form carbon monoxide (CO), free iron ( $\text{Fe}^{2+}$ ), and biliverdin that immediately undergoes enzymatic reduction to form bilirubin, a potent antioxidant and protector of neuron cells against oxidative stress even at minute concentration (Otterbein *et al*, 2003). NQO1 catalyzes the two electron reduction of quinones and diverts the participation of these agents from one electron oxidoreduction and oxidative stress (Siegel *et al*, 2004). Therefore, further understanding of how Nrf2/ARE pathway prevents the progress of neurodegenerative diseases through the use of these bioactive agents is important.

DNA microarray can investigate the expressions of thousands of genes simultaneously in a given cell type or tissue sample (Barret & Kawasaki, 2003; Rushmore & Kong, 2002). In the previous investigation, the anti-inflammatory genes and associated signaling pathways targeted by 6-MSITC were successfully clarified by employing DNA microarray technology to macrophages (Chen *et al*, 2010). In this present study, to clarify the molecular mechanism of Wasabi-derived ITCs on neuroprotection at the cellular level, the DNA microarray analysis was carried out to profile gene expression changes in a neuronal model cell line, IMR-32, stimulated by these ITCs. Moreover, Ingenuity Pathway Analysis (IPA) was used to map out cellular signaling pathways for these ITC regulated gene expressions.

### **3.3. Materials and methods**

#### **3.3.1. Materials and cell cultures**

ITCs (SFN, 6-MSITC, and 6-MTITC) were purified from Wasabi by reversed-phase high performance liquid chromatography (HPLC) to 99.3% purity and dissolved in dimethyl sulfoxide for cell culture experiments (Hou *et al*, 2000). The antibodies against Nrf2 (C20), Keap1 (E20), NQO1 (C19), HSP70 (D69), GAPDH, rabbit IgG, and horseradish peroxidase (HRP)-conjugated anti-goat secondary antibody were purchased from Santa Cruz Biotechnology (Texas, USA). AKR1C1, AKR1C3, and TXNRD1 antibodies were obtained from Abcam (Cambridge, UK). HRP-conjugated anti-rabbit and anti-mouse secondary antibodies were from Cell Signaling Technology (Massachusetts, USA).

Human neuroblastoma IMR-32 cells (cell no. TKG0207) were obtained from Riken Bioresource Center Cell Bank (Ibaraki, Japan). IMR-32 cells were grown in

Eagle's Minimum Essential Medium (EMEM, Nissui Seiyaku, Tokyo, Japan) supplemented with 2 mM L-glutamine (Nacalai Tesque, Kyoto, Japan), 1% v/v MEM non-essential amino acid solution (Nacalai Tesque, Kyoto, Japan), and 10% v/v fetal bovine serum (Equitech-Bio, Texas, USA) under a humidified 5% CO<sub>2</sub> atmosphere at 37 °C.

### **3.3.2. 3-(4,5-dimethylthiazol-2-yl)-2,5-diphenyltetrazolium bromide (MTT) assay**

Toxicity of ITCs on IMR-32 cells was checked by incubating the cells with 0-20 µM concentrations of ITCs and then assessed the viability using MTT assay. In brief, IMR-32 cells were seeded onto the 96-well plate ( $1 \times 10^4$  cells/well). After 24-hour preculture, the cells were treated with 0-20 µM concentration of ITCs for 12 hours. Then, 5 mg/mL of MTT was added to each well and incubated for another 4 hours. After incubation, 100 µL of stop solution was then added to each well and the absorbance was then measured at 595 nm after thorough pipetting to disperse the generated blue formazan.

### **3.3.3. Total RNA extraction**

IMR-32 cells were precultured in 10 cm dishes for 24 hours and then treated by 10 µM of ITCs (SFN, 6-MSITC, and 6-MTITC) in 0.2% dimethyl sulfoxide for another 9 hours. Total RNA was extracted using RNeasy Mini Kit (Qiagen™, Hilden, Germany), following the manufacturer's instructions. RNA integrity was assessed using Agilent 2100 Bioanalyzer (Agilent Technologies, California, USA).

### **3.3.4. *Microarray hybridization and transcript analyses***

Four hundred nanograms of total RNA were used to generate cDNA with Eukaryotic Poly-A RNA Control Kit (Affymetrix, California, USA) and GeneChip® One-cycle cDNA Synthesis Kit (Affymetrix, California, USA), following the manufacturer's protocol. After cleanup of double-stranded cDNA by Sample Cleanup Module Kit (Affymetrix, California, USA), cRNAs were biotin-labelled at 37 °C for 16 hours by GeneChip IVT Labeling Kit (Affymetrix, California, USA). Following the cleanup and quantification, the fragmented and biotin-labeled cRNAs were hybridized at 45 °C for 16 hours to the Affymetrix GeneChip (Human Genome U133 Plus 2.0 oligonucleotide arrays) containing approximately more than 54,000 probe sets. The GeneChip was washed and stained by GeneChip Hybridization, Wash, and Stain kit in Fluidics Station (Affymetrix, California, USA). The hybridized fluorescence was scanned using Affymetrix Launcher. The images were processed for visualization and normalization of each probe set to a common baseline using GeneSpring GX 10.1 (Agilent Technologies, California, USA). Gene products of fold change greater than 2 were further analyzed using Gene Ontology (GO) software (<http://www.geneontology.org>) for biological processes, molecular functions, and signaling pathways.

### **3.3.5. *Pathway analyses***

Pathway and global functional analysis were performed using IPA (Ingenuity® Systems; [www.ingenuity.com](http://www.ingenuity.com)). A data set containing gene accession numbers and the corresponding fold change of ITC-treated cells versus control was uploaded into the software and were mapped out using GO.

GO analysis generated the biological functions as well as pathways from the

IPA library that is significant to the data set. Genes from the data sets associated with biological functions or canonical pathway with level of significance ( $p$ ) less than 0.05 were used to map out molecular networks. Resulting networks were ranked based on the scores generated from Fisher's exact test to indicate the probability of each biological function and/or canonical pathway was not due to chance alone.

### **3.3.6. Real-time PCR**

The primers (Table 3.1) used for real-time PCR in the present study, including *AKR1C1*, *AKR1C3*, *NQO1*, *GSR*, *TXNRD1*, and *GCLM*, were designed according to the NCBI sequence database using the software Primer3. Reverse transcription and real-time PCR were performed with DyNAmo SYBR® Green 2-Step qRT-PCR Kit (Finnzymes Oy, Espoo, Finland) according to manufacturer's manual. Briefly, 200 ng of RNA was reversed to cDNA using Oligo dT and M-MuLV RNase at 37 °C for 30 minutes, and the reaction was then terminated at 85 °C for 5 minutes. Real-time PCR was performed with the Roter-Gene-3000 AKAA (Corbett Research, New South Wales, Australia) in triplicates using the standard curve. The  $T_m$  of PCR was determined according to each primer sequence (<https://www.finnzymes.com/tm.determination.html>). Each PCR contained 250 ng of reversed transcripts, 75 ng of each primer, and 10  $\mu$ L of Master Mix (Finnzymes Oy, Espoo, Finland). The thermal cycling condition was held at 95 °C for 15 minutes followed by 55 cycles of 30 seconds at 94 °C, 30 seconds at corresponding  $T_m$  (Table 3.1), and 30 seconds at 72 °C. The result was represented by relative expression level normalized with control cells.

**Table 3.1.** Primer sequences used for real-time PCR.

Gene symbol	Direction	Primer sequences	T <sub>m</sub> (°C)
<i>AKR1C1</i>	Fw	5'-ATC CCT CCG AGA AGA ACC AT-3'	59
	Re	5'-ACA CCT GCA CGT TCT GTC TG-3'	
<i>AKC1C3</i>	Fw	5'-AAG TAA AGC TTT GGA GGT CAC A-3'	59
	Re	5'-GGA CCA ACT CTC GTC GAT GAA-3'	
<i>NQO1</i>	Fw	5'-AGT GCA GTG GTG TGA TCT CG-3'	59
	Re	5'-GGT GGA GTC ACG CCT GTA AT-3'	
<i>GSR</i>	Fw	5'-GAT CCC AAG CCC ACA ATA GA-3'	59
	Re	5'-CTT AGA ACC CAG GGC TGA CA-3'	
<i>TXNRD1</i>	Fw	5'-ATC AGG AGG GCA GAC TTC AA-3'	61
	Re	5'-CCC ACA TTC ACA CAT GTT CC-3'	
<i>GCLM</i>	Fw	5'-GGG AAC CTG CTG AAC TGG-3'	61
	Re	5'-GCA TGA GAT ACA GTG CAT TCC-3'	

### 3.3.7. Western blot analyses

IMR-32 cells were seeded into a 10-cm dish and precultured for 24 hours. Ten micromolars of ITC (SFN, 6-MSITC, or 6-MTITC) were added and co-cultured for another 12 hours. Cells were harvested by lysis buffer, and then homogenized in an ultrasonicator for 10 seconds twice and incubated on ice for 30 minutes (Hou *et al*, 2000). After the homogenates were centrifuged at 14,000 × *g* for 15 minutes at 4 °C, the protein concentration was determined by protein assay kit (Bio-Rad Laboratories, California, USA). Forty micrograms of protein lysates were run on 10%–15% sodium dodecyl sulfate polyacrylamide gel electrophoresis (SDS-PAGE) and electrophoretically transferred to polyvinylidene difluoride (PVDF) membrane (Amersham Pharmacia Biotech, Little Chalfont, UK). The membrane was incubated with specific antibody overnight at 4 °C and further incubated for 1 hour with HRP-conjugated secondary antibody. Bound antibodies were detected using the ECL system and the relative amounts of proteins associated with specific antibody were quantified using Lumi Vision Imager software (TAITEC Co., Fukuoka, Japan).



### **3.3.8. Statistical analyses**

All experiments were done for at least three trials. The differences between the sample treatment and the control were statistically analyzed using Student's *t*-test. A statistical probability of  $p < 0.05$  was considered significant.

## **3.4. Results**

### **3.4.1. Gene profile analysis in IMR-32 cells treated by Wasabi-derived ITCs**

IMR-32 cells were treated with 0–20  $\mu\text{M}$  of SFN, 6-MSITC, or 6-MTITC for 12 hours (Chen *et al*, 2010; Korenori *et al*, 2013). The cytotoxicity assay results (Figure 3.2) showed that there was no significant decrease in the number of viable cells in such treatment, indicating that less than 20  $\mu\text{M}$  of these ITCs is the safe concentration for treating IMR-32 cells. Moreover, this concentration has been found to induce cytoprotective genes (Thimmulappa *et al*, 2002). Thus, gene profiling was performed using the cells treated by 10  $\mu\text{M}$  of SFN, 6-MSITC, or 6-MTITC for 9 hours. Cell mRNA was prepared, and mRNA profiling was carried out using Affymetrix HG UG133 plus 2.0 oligonucleotide arrays containing approximately over 54,000 probe sets as elaborated in the “**Section 3.3.4**”.

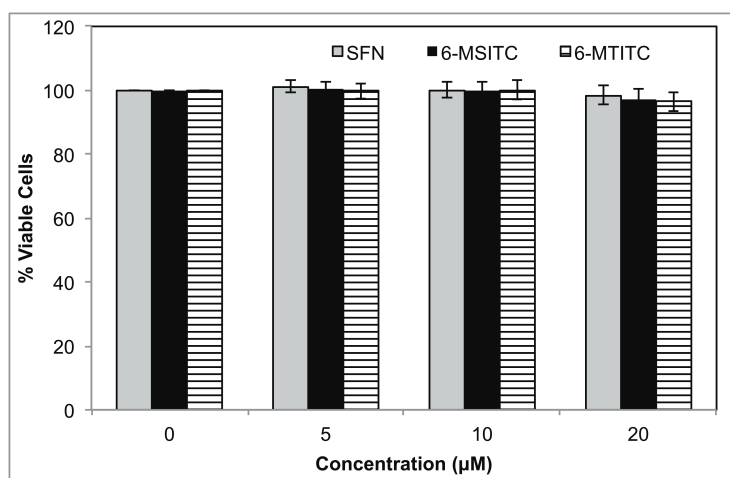


**Figure 3.2.** Cytotoxicity assay results of isothiocyanates in IMR-32 cells. Data showed no significant decrease in the number of viable cells after treatment with 0–20 μM of SFN, 6-MSITC, or 6-MTITC for 12 hours.

As summarized in Table 3.2, the total number of gene expression mediated by 6-MSITC (263 genes) and 6-MTITC (233 genes) were more than twice higher than SFN (108 genes). Detailed evaluation manifested that 6-MSITC had the strongest regulation on gene expression (100 upregulated and 163 downregulated genes), followed by 6-MTITC (98 upregulated and 135 downregulated genes) and SFN (67 upregulated and 41 downregulated genes). Moreover, total number of the genes downregulated by 6-MSITC and 6-MTITC were more than that of the genes upregulated while SFN acted by contrast.

**Table 3.2.** Number of genes regulated by Wasabi-derived isothiocyanates.

<b>Fold change</b>	SFN	6-MSITC	6-MTITC
≥ 4	16	21	22
≥ 3 to < 4	7	12	12
≥ 2 to < 3	44	67	64
<i>Subtotal</i>	<i>67</i>	<i>100</i>	<i>98</i>
≥ -4	40	3	2
≥ -3 to < -4	1	13	10
≥ -2 to < -3	0	147	123
<i>Subtotal</i>	<i>41</i>	<i>163</i>	<i>135</i>
<b>Total</b>	<b>108</b>	<b>263</b>	<b>233</b>

### **3.4.2. Grouping of genes targeted by Wasabi-derived ITCs**

To understand the function of the genes targeted by SFN, 6-MSITC, and 6-MTITC, all genes that were differentially expressed (at least 2 folds) were subjected to GO analyses for classification based on biological processes, molecular functions, or cellular component. Majority of the upregulated genes with known annotation information was associated with various categories such as metabolic processes, transcription, transport, oxidoreductase, signal transduction, and stress response (Table 3.3). For downregulated genes, most of the subsets (2-fold change) were related to binding, CNS-specific function, signal transduction, transcription, transferase activity, and transport (Table 3.4). A total of 14, 17, and 18 differentially expressed genes were identified from SFN, 6-MSITC, and 6-MTITC treatments, respectively, that were associated with oxidative stress response. Consequently, gene profile analyses revealed that most of the differentially expressed genes induced by SFN, 6-MSITC, and 6-MTITC are linked to the oxidative stress response.

**Table 3.3.** Classification of upregulated genes based on biological processes targeted by ITCs in IMR-32 cells.

Gene categories	Gene symbol	Gene description	Fold change <sup>1</sup>		
			SFN	6-MSITC	6-MTITC
Apoptosis	<i>CLU</i>	Clusterin	NS	↑ 2.47	↑ 2.77
	<i>PDCD2</i>	Programmed cell death 2	↑ 2.03	NS	NS
	<i>PPP3R1///WDR92</i>	Protein phosphatase 3 (formerly 2B), regulatory subunit B, $\alpha$ isoform /// WD repeat domain 92	NS	NS	↑ 2.29
	<i>TNFRSF1A</i>	Tumor necrosis factor receptor superfamily, member 1A	↑ 2.86	↑ 4.57	↑ 4.26
Adhesion	<i>ITGB5</i>	Integrin, $\beta$ 5	NS	↑ 2.10	↑ 2.08
Autophagy	<i>ABCB6</i>	ATP-binding cassette, sub-family B (MDR/TAP), member 6	↑ 3.50	↑ 3.16	↑ 3.17
Binding	<i>PHC3</i>	Polyhomeotic homolog 3 (Drosophila)	↑ 2.13	NS	↑ 2.54
	<i>UNKL</i>	Unkempt homolog (Drosophila)-like	↑ 2.71	↑ 3.13	↑ 3.15
Catabolic process	<i>UCHL1</i>	Ubiquitin carboxyl-terminal esterase L1 (ubiquitin thiolesterase)	↑ 2.01	↑ 2.55	↑ 2.57
Cell cycle	<i>SESN2</i>	Sestrin 2	NS	↑ 2.02	↑ 2.03
Cell growth	<i>OSGIN1</i>	Oxidative stress induced growth inhibitor 1	↑ 3.21	↑ 4.35	↑ 4.39
CNS specific function	<i>ADCYAP1</i>	Adenylate cyclase activating polypeptide 1 (pituitary)	↑ 2.15	NS	NS
	<i>GSTM3</i>	Glutathione S-transferase M3 (brain)	↑ 2.06	↑ 2.12	↑ 2.05

<sup>1</sup> NS – no significant change; fold change is <2

Gene categories	Gene symbol	Gene description	Fold change <sup>1</sup>		
			SFN	6-MSITC	6-MTITC
	<i>NEFH</i>	Neurofilament, heavy polypeptide 200kDa	↑ 4.90	↑ 7.35	↑ 6.77
	<i>PAFAH1B1</i>	Platelet-activating factor acetylhydrolase, isoform Ib, $\alpha$ subunit 45kDa	NS	↑ 2.01	NS
DNA repair	<i>ASF1A</i>	ASF1 anti-silencing function 1 homolog A ( <i>S. cerevisiae</i> )	↑ 2.59	↑ 2.32	↑ 2.88
Metabolic process	<i>ASNS</i>	Asparagine synthetase	↑ 2.10	↑ 2.37	↑ 2.88
	<i>BAG3</i>	BCL2-associated athanogene 3	NS	↑ 2.68	↑ 2.32
	<i>BLVRB</i>	Biliverdin reductase B (flavin reductase (NADPH))	NS	↑ 2.01	NS
	<i>C14orf37</i>	Chromosome 14 open reading frame 37	↑ 2.23	↑ 2.06	↑ 2.21
	<i>ENPP2</i>	Ectonucleotide pyrophosphatase/phosphodiesterase 2 (autotaxin)	↑ 3.08	↑ 2.76	↑ 2.61
	<i>FBXO9</i>	F-box protein 9	NS	NS	↑ 2.10
	<i>FECH</i>	Ferrochelatase (protoporphyrin)	↑ 2.54	↑ 2.40	↑ 2.45
	<i>FLJ25076</i>	Similar to CG4502-PA	NS	↑ 2.02	↑ 2.05
	<i>KIAA0746</i> /// <i>SERINC2</i>	KIAA0746 protein /// serine incorporator 2	NS	NS	↑ 2.07
	<i>LRP8</i>	Low density lipoprotein receptor-related protein 8, apolipoprotein e receptor	NS	↑ 2.02	↑ 2.07
	<i>ME1</i>	Malic enzyme 1, NADP(+)-dependent, cytosolic	↑ 8.95	↑ 11.68	↑ 12.75
	<i>NEDD4</i>	Neural precursor cell expressed, developmentally down-regulated 4	NS	↑ 2.19	NS

Gene categories	Gene symbol	Gene description	Fold change <sup>1</sup>		
			SFN	6-MSITC	6-MTITC
	<i>P4HA2</i>	Procollagen-proline, 2-oxoglutarate 4-dioxygenase (proline 4-hydroxylase), ✓ polypeptide II	↑ 2.08	↑ 3.35	↑ 3.29
	<i>PCK2</i>	Phosphoenol pyruvate carboxykinase 2 (mitochondrial)	↑ 2.12	↑ 2.26	↑ 2.26
	<i>PSAT1</i>	Phosphoserine aminotransferase 1	NS	NS	↑ 2.00
	<i>RBCK1</i>	RanBP-type and C3HC4-type zinc finger containing 1	NS	↑ 2.01	NS
	<i>TKT</i>	Transketolase (Wernicke-Korsakoff syndrome)	↑ 2.05	NS	NS
Oxido-reductase	<i>AKR1C1</i>	Aldo-keto reductase family 1, member C1 (dihydrodiol dehydrogenase 1; 20- $\alpha$ (3- $\alpha$ )-hydroxysteroid dehydrogenase)	↑ 10.60	↑ 11.02	↑ 12.02
	<i>AKR1C2</i>	Aldo-keto reductase family 1, member C2 (dihydrodiol dehydrogenase 2; bile acid binding protein; 3- $\alpha$ hydroxysteroid dehydrogenase, type III)	↑ 11.00	↑ 11.96	↑ 12.23
	<i>AKR1C3</i>	Aldo-keto reductase family 1, member C3 (3- $\alpha$ hydroxyl steroid dehydrogenase, type II)	↑ 103.64	↑ 103.85	↑ 109.70
	<i>GCLM</i>	Glutamate-cysteine ligase, modifier subunit	↑ 8.44	↑ 11.88	↑ 11.69
	<i>GSR</i>	Glutathione reductase	↑ 3.63	↑ 3.50	↑ 3.45

Gene categories	Gene symbol	Gene description	Fold change <sup>1</sup>		
			SFN	6-MSITC	6-MTITC
	<i>HMOX1</i>	Heme oxygenase (decycling) 1	↑ 11.50	↑ 59.14	↑ 54.63
	<i>LOC100130069</i> /// <i>PLOD1</i>	Procollagen-lysine 1, 2-oxoglutarate 5-di oxygenase 1 /// hypothetical protein LOC100130069	NS	↑ 2.86	↑ 2.20
	<i>NQO1</i>	NAD(P)H dehydrogenase, quinone 1	↑ 27.37	↑ 27.67	↑ 28.41
	<i>SRXN1</i>	Sulfiredoxin 1 homolog (S. cerevisiae)	↑ 6.56	↑ 7.80	↑ 7.90
	<i>TXNRD1</i>	Thioredoxin reductase 1	↑ 4.82	↑ 4.82	↑ 4.77
Signal transduction	<i>DDIT4</i>	DNA-damage-inducible transcript 4	↑ 2.00	↑ 2.40	↑ 2.47
	<i>DGKQ</i>	Diacylglycerol kinase, τ 110kDa	↑ 2.20	NS	NS
	<i>F2RL2</i>	Coagulation factor II (thrombin) receptor-like 2	NS	↑ 2.18	NS
	<i>PRKACB</i>	Protein kinase, cAMP-dependent, catalytic, β	↑ 2.43	↑ 2.45	↑ 2.31
	<i>SRC</i>	V-src sarcoma (Schmidt-Ruppin A-2) viral oncogene homolog (avian)	NS	NS	↑ 2.16
	<i>VEGFA</i>	Vascular endothelial growth factor A	NS	NS	↑ 2.03
	<i>WNT5A</i>	Wingless-type MMTV integration site family, member 5A	↑ 13.35	↑ 12.60	↑ 12.60
	<i>WNT5B</i>	Wingless-type MMTV integration site family, member 5B	↑ 2.09	↑ 2.58	↑ 2.26
Stress response	<i>DNAJB1</i>	DnaJ (Hsp40) homolog, subfamily B, member 1	NS	↑ 2.60	↑ 2.74

Gene categories	Gene symbol	Gene description	Fold change <sup>1</sup>		
			SFN	6-MSITC	6-MTITC
	<i>DNAJB4</i>	DnaJ (Hsp40) homolog, subfamily B, member 4	↑ 4.30	↑ 5.34	↑ 5.39
	<i>DUSP10</i>	Dual specificity phosphatase 10	↑ 2.21	NS	↑ 2.13
	<i>HSPA1A</i> /// <i>HSPA1B</i>	Heat shock 70kDa protein 1A /// heat shock 70kDa protein 1B	↑ 2.32	↑ 6.59	↑ 6.44
	<i>HSPB1</i>	Heat shock 27kDa protein 1	NS	↑ 2.44	↑ 2.38
	<i>MAFF</i>	V-maf musculoaponeurotic fibrosarcoma oncogene homolog F (avian)	↑ 2.21	↑ 2.90	↑ 2.78
	<i>SERPINH1</i>	Serpin peptidase inhibitor, clade H (heat shock protein 47), member 1, (collagen binding protein 1)	NS	↑ 2.55	↑ 2.53
Transferase activity	<i>SQSTM1</i>	Sequestosome 1	↑ 3.36	↑ 4.66	↑ 5.00
	<i>MGAT4B</i>	Mannosyl ( $\alpha$ -1,3-)-glycoprotein $\beta$ -1,4-N-acetylglucosaminyl transferase, isozyme B	NS	↑ 2.22	NS
	<i>RPS6KA2</i>	Ribosomal protein S6 kinase, 90kDa, polypeptide 2	NS	↑ 2.07	↑ 2.17
	<i>ST8SIA2</i>	ST8 $\alpha$ -N-acetylneuraminide $\alpha$ -2,8-sialyl transferase 2	NS	↑ 2.13	↑ 2.05
Transcription	<i>ATF3</i>	Activating transcription factor 3	NS	↑ 2.14	↑ 2.04
	<i>BACH1</i>	BTB and CNC homology 1, basic leucine zipper transcription factor 1	NS	↑ 2.08	↑ 2.24



Gene categories	Gene symbol	Gene description	Fold change <sup>1</sup>		
			SFN	6-MSITC	6-MTITC
	<i>CTDP1</i>	CTD (carboxy-terminal domain, RNA polymerase II, polypeptide A) phosphatase, subunit 1	NS	↑ 2.45	NS
	<i>EED</i>	Embryonic ectoderm development	NS	NS	↑ 2.04
	<i>ETV5</i>	Ets variant gene 5 (ets-related molecule)	↑ 2.87	↑ 2.85	↑ 2.94
	<i>HNRNPD</i>	Heterogeneous nuclear ribonucleoprotein D (AU-rich element RNA binding protein 1, 37kDa)	NS	↑ 2.85	↑ 2.65
	<i>JDP2</i>	Jun dimerization protein 2	2.14	NS	NS
	<i>KEAP1</i>	Kelch-like ECH-associated protein 1	NS	↑ 2.24	↑ 2.11
	<i>LASS6</i>	LAG1 homolog, ceramide synthase 6	NS	↑ 2.26	↑ 2.07
	<i>MAFG</i>	V-maf musculoaponeurotic fibrosarcoma oncogene homolog G (avian)	↑ 2.22	↑ 2.62	↑ 2.24
	<i>MSX1</i>	Msh homeobox 1	NS	↑ 2.38	NS
	<i>PIR</i>	Pirin (iron-binding nuclear protein)	↑ 2.24	↑ 2.04	
	<i>TFE3</i>	Transcription factor binding to IGHM enhancer 3	↑ 2.20	↑ 2.68	↑ 2.53
	<i>TRIM16</i>	Tripartite motif-containing 16	↑ 6.59	↑ 6.71	↑ 7.43
	<i>ZNF230</i>	Zinc finger protein 230	NS	↑ 2.02	NS
	<i>ZNF451</i>	Zinc finger protein 451	NS	↑ 2.29	↑ 2.44
Translation	<i>CPEB2</i>	Cytoplasmic polyadenylation element binding protein 2	↑ 3.34	↑ 4.99	↑ 4.24

Gene categories	Gene symbol	Gene description	Fold change <sup>1</sup>		
			SFN	6-MSITC	6-MTITC
Transport	<i>AMBP</i>	$\alpha$ -1-microglobulin/bikunin precursor	↑ 2.99	↑ 2.17	↑ 3.01
	<i>FTH1</i>	Ferritin, heavy polypeptide 1	↑ 2.74	↑ 3.41	↑ 3.48
	<i>FTL</i>	Ferritin, light polypeptide	↑ 2.59	↑ 2.88	↑ 2.86
	<i>LIN7A</i>	Lin-7 homolog A (C. elegans)	NS	↑ 2.14	NS
	<i>LOC442497</i> /// <i>SLC3A2</i>	Solute carrier family 3 (activators of dibasic and neutral amino acid transport), member 2 /// hypothetical protein LOC442497	↑ 2.13	↑ 2.51	↑ 2.44
	<i>LOC100127887</i> /// <i>SYT2</i>	Synaptotagmin II /// hypothetical protein LOC100127887	NS	↑ 2.35	↑ 2.25
	<i>SLC1A4</i>	Solute carrier family 1 (glutamate/neutral amino acid transporter), member 4	NS	↑ 2.46	↑ 2.50
	<i>SLC7A5</i>	Solute carrier family 7 (cationic amino acid transporter, y <sup>+</sup> system), member 5	↑ 2.12	↑ 2.46	↑ 2.44
	<i>SLC7A11</i>	Solute carrier family 7, (cationic amino acid transporter, y <sup>+</sup> system) member 11	↑ 19.05	↑ 27.07	↑ 28.27
	<i>TMEM37</i>	Transmembrane protein 37	NS	↑ 2.67	↑ 2.47
Unknown	<i>ARRDC3</i>	Arrestin domain containing 3	↑ 2.51	↑ 3.27	↑ 3.45
	<i>C15orf37</i>	Chromosome 15 open reading frame 37	NS	NS	↑ 2.07
	<i>C17orf91</i>	Chromosome 17 open reading frame 91	↑ 2.22	↑ 5.36	↑ 6.63
	<i>C20orf39</i>	Chromosome 20 open reading frame 39	↑ 2.01	↑ 2.81	↑ 2.86

Gene categories	Gene symbol	Gene description	Fold change <sup>1</sup>		
			SFN	6-MSITC	6-MTITC
	<i>C2orf59</i> /// <i>hLOC5414</i> <i>71</i>	Chromosome 2 open reading frame 59 /// hypothetical LOC541471	↑ 4.58	↑ 5.51	↑ 5.81
	<i>CLIP4</i>	CAP-GLY domain containing linker protein family, member 4	↑ 2.08	↑ 2.02	↑ 2.31
	<i>FLJ33297</i>	Hypothetical gene supported by AK090616	↑ 3.56	↑ 2.78	↑ 3.27
	<i>FLJ35767</i>	FLJ35767 protein	↑ 2.60	↑ 2.50	↑ 2.40
	<i>FTHP1</i>	Ferritin, heavy polypeptide pseudogene 1	NS	↑ 2.14	↑ 2.23
	<i>GPATCH2</i>	G patch domain containing 2	NS	NS	↑ 2.03
	<i>GPC1</i>	Glypican 1	↑ 2.67	↑ 3.53	↑ 3.49
	<i>KIAA1549</i>	KIAA1549	↑ 2.46	↑ 2.28	↑ 2.40
	<i>KRCC1</i>	Lysine-rich coiled-coil 1	NS	↑ 3.10	↑ 3.05
	<i>LOC</i> <i>100129129</i>	Hypothetical protein LOC100129129	NS	↑ 2.42	↑ 2.14
	<i>LOC134145</i>	Hypothetical protein LOC134145	NS	↑ 2.09	NS
	<i>LRIG1</i>	Leucine-rich repeats and immune globulin-like domains 1	↑ 2.13	NS	↑ 2.14
	<i>LRRC51</i>	Leucine rich repeat containing 51	NS	↑ 2.07	NS
	<i>LRRC7</i>	Leucine rich repeat containing 7	↑ 2.19	↑ 2.40	↑ 2.46
	<i>MAP1A</i>	Microtubule- associated protein 1A	↑ 2.72	↑ 3.33	↑ 3.12
	<i>MGC24039</i>	Hypothetical protein MGC24039	NS	↑ 2.06	NS
	<i>MIAT</i>	Myocardial infarction associated transcript (non-protein coding)	↑ 4.23	↑ 3.12	↑ 4.66
	<i>MUC19</i>	Mucin 19, oligomeric	↑ 2.17	NS	NS
	<i>PALM3</i>	Paralemmin-3	NS	↑ 2.39	↑ 2.23
	<i>PANX2</i>	Pannexin 2	NS	NS	↑ 2.04

Gene categories	Gene symbol	Gene description	Fold change <sup>1</sup>		
			SFN	6-MSITC	6-MTITC
	<i>RNF146</i>	Ring finger protein 146	NS	↑ 2.10	NS
	<i>RHBDD2</i>	Rhomboid domain containing 2	↑ 2.07	↑ 2.52	↑ 3.20
	<i>RHBDD3</i>	Rhomboid domain containing 3	NS	↑ 2.12	NS
	<i>TMEM20</i>	Transmembrane protein 20	↑ 2.58	↑ 2.40	↑ 2.53
	<i>TRIM4</i>	Tripartite motif-containing 4	NS	↑ 2.33	↑ 2.24
	<i>ZFAND2A</i>	Zinc finger, AN1-type domain 2A	NS	↑ 2.11	↑ 2.19
		Transcribe locus	↑ 14.26	↑ 2.74	↑ 12.91

**Table 3.4.** Classification of downregulated genes based on biological processes targeted by ITCs in IMR-32 cells.

Gene categories	Gene symbol	Gene description	Fold change		
			SFN	6-MSITC	6-MTITC
Apoptosis	<i>CXCR4</i>	Chemokine (C-X-C motif) receptor 4	NS	↓ 3.17	↓ 3.49
	<i>ELMO1</i>	Engulfment and cell motility 1	NS	↓ 2.03	NS
	<i>GJA1</i>	Gap junction protein, $\alpha$ 1, 43kDa	NS	↓ 3.01	NS
	<i>IHPK2</i>	Inositol hexaphosphate kinase 2	NS	↓ 2.08	↓ 2.21
	<i>RP6-213 H19.1</i>	Serine/threonine protein kinase MST4	NS	↓ 2.12	NS
Binding	<i>ADARB1</i>	Adenosine deaminase, RNA-specific, B1 (RED1 homolog rat)	NS	↓ 2.02	NS
	<i>BICD1</i>	Bicaudal D homolog 1 (Drosophila)	NS	↓ 4.03	↓ 3.32
	<i>CALB1</i>	Calbindin 1, 28kDa	NS	↓ 2.19	NS
	<i>CCDC136</i>	Coiled-coil domain containing 136	NS	↓ 3.71	↓ 3.00
	<i>CLPB</i>	ClpB caseinolytic peptidase B homolog (E. coli)	NS	↓ 2.16	NS

Gene categories	Gene symbol	Gene description	Fold change		
			SFN	6-MSITC	6-MTITC
	<i>DNAJC12</i>	DnaJ (Hsp40) homolog, subfamily C, member 12	NS	↓ 2.07	↓ 2.09
	<i>ENDOD1</i>	Endonuclease domain containing 1	NS	↓ 2.23	↓ 2.10
	<i>FBXO43</i>	F-box protein 43	NS	↓ 2.13	↓ 2.15
	<i>FRMD3</i>	FERM domain containing 3	NS	↓ 3.00	↓ 2.41
	<i>GCA</i>	Grancalcin, EF-hand calcium binding protein	NS	↓ 2.14	NS
	<i>GIGYF2</i>	GRB10 interacting GYF protein 2	NS	↓ 2.13	↓ 2.26
	<i>HIST1H2BG</i>	Histone cluster 1, H2bg	NS	↓ 2.02	↓ 2.31
	<i>HNRNPR</i>	Heterogeneous nuclear ribonucleoprotein R	NS	NS	↓ 2.15
	<i>HOOK1</i>	Hook homolog 1 (Drosophila)	↓ 2.02	↓ 2.08	NS
	<i>INTS7</i>	Integrator complex subunit 7	NS	↓ 2.03	↓ 2.00
	<i>KIF21B</i>	Kinesin family member 21B	NS	↓ 2.12	NS
	<i>LOC100133197///PDXK</i>	Pyridoxal (pyridoxine, vitamin B6) kinase /// similar to Pyridoxal (pyridoxine, vitamin B6) kinase	↓ 2.14	NS	↓ 2.27
	<i>LRRC34</i>	Leucine rich repeat containing 34	↓ 2.90	↓ 4.45	↓ 4.08
	<i>LTBP1</i>	Latent transforming growth factor β binding protein 1	NS	NS	↓ 2.31
	<i>MMACHC</i>	Methylmalonic aciduria (cobalamin deficiency) cblC type, with homocystinuria	NS	↓ 2.19	↓ 2.37
	<i>NAV2</i>	Neuron navigator 2	NS	↓ 2.12	↓ 2.18
	<i>PLS1</i>	Plastin 1 (I isoform)	NS	↓ 2.40	↓ 2.46
	<i>PTCD3</i>	Pentatricopeptide repeat domain 3	NS	↓ 2.12	NS
	<i>RRP15</i>	Ribosomal RNA processing 15 homolog (S. cerevisiae)	NS	↓ 2.03	NS
	<i>SFRS2IP</i>	Splicing factor, arginine/serine-rich 2, interacting protein	NS	↓ 2.17	NS

Gene categories	Gene symbol	Gene description	Fold change		
			SFN	6-MSITC	6-MTITC
	<i>SSFA2</i>	Sperm specific antigen 2	NS	↓ 2.04	NS
	<i>SYNCRIP</i>	Synaptotagmin binding, cytoplasmic RNA interacting protein	NS	NS	↓ 2.16
	<i>TACC2</i>	Transforming, acidic coiled-coil containing protein 2	NS	NS	↓ 2.03
	<i>TJP2</i>	Tight junction protein 2 (zona occludens 2)	NS	↓ 2.03	↓ 2.28
	<i>ZYG11A</i>	Zyg-11 homolog A (C. elegans)	NS	↓ 2.05	NS
Biogenesis	<i>MINA</i>	MYC induced nuclear antigen	NS	↓ 2.16	NS
Catabolic process	<i>OLA1</i>	Obg-like ATPase 1	NS	↓ 2.46	↓ 2.07
	<i>USP18</i>	Ubiquitin specific peptidase 18	↓ 2.27	↓ 2.90	↓ 2.39
Catalytic activity	<i>HDCC2</i>	HD domain containing 2	NS	↓ 2.14	NS
	<i>LYPLAL1</i>	Lysophospholipase-like 1	NS	↓ 2.35	↓ 2.25
Cell adhesion	<i>CD9</i>	CD9 molecule	NS	↓ 2.72	↓ 2.56
	<i>CDH10</i>	Cadherin 10, type 2 (T2-cadherin)	↓ 2.07	NS	NS
	<i>ITGA4</i>	Integrin, α4 (antigen CD49D, α4 subunit of VLA-4 receptor)	NS	↓ 2.19	↓ 2.24
	<i>ITGA9</i>	Integrin, α9	NS	NS	↓ 2.12
	<i>MLLT4</i>	Myeloid/lymphoid or mixed-lineage leukemia (trithorax homolog, Drosophila); translocated to, 4	NS	↓ 2.09	NS
Cell cycle	<i>ANAPC5</i>	Anaphase promoting complex subunit 5	NS	↓ 2.07	NS
Cell proliferation	<i>DLG1</i>	Discs, large homolog 1 (Drosophila)	NS	NS	↓ 2.03
	<i>FIGF</i>	C-fos induced growth factor (vascular endothelial growth factor D)	NS	↓ 2.36	↓ 2.64
Cellular process	<i>DTNBP1</i>	Dystrobrevin binding protein 1	↓ 2.05	NS	NS
	<i>MMD</i>	Monocyte to	NS	↓ 2.28	↓ 2.10

Gene categories	Gene symbol	Gene description	SFN	Fold change	
				6-MSITC	6-MTITC
CNS specific function		macrophage differentiation-associated			
	<i>TUBGCP5</i>	Tubulin, $\gamma$ complex associated protein 5	NS	↓ 2.12	NS
	<i>CCDC50</i>	Coiled-coil domain containing 50	NS	↓ 2.32	NS
	<i>CUGBP2</i>	CUG triplet repeat, RNA binding protein 2	NS	NS	↓ 2.01
	<i>NEUROD1</i>	Neurogenic differentiation 1	NS	↓ 2.06	↓ 2.03
	<i>NGEF</i>	Neuronal guanine nucleotide exchange factor	NS	↓ 2.04	NS
	<i>PDGFC</i>	Platelet derived growth factor C	NS	↓ 2.03	NS
	<i>PRCD</i>	Progressive rod-cone degeneration	NS	↓ 2.09	NS
	<i>PSEN2</i>	Presenilin 2 (Alzheimer disease 4)	NS	↓ 2.23	NS
Developmental process	<i>SLIT3</i>	Slit homolog 3 (Drosophila)	NS	↓ 2.02	↓ 2.04
	<i>C1orf107</i>	Chromosome 1 open reading frame 107	NS	NS	↓ 2.50
	<i>COL1A1</i>	Collagen, type I, $\alpha$ 1	↓ 2.01	NS	↓ 2.27
	<i>DONSON</i>	Downstream neighbor of SON	NS	NS	↓ 2.03
	<i>JPH1</i>	Junctophilin 1	NS	↓ 2.13	↓ 2.57
	<i>SGCD</i>	Sarcoglycan, $\delta$ (35kDa dystrophin-associated glycoprotein)	NS	↓ 2.10	NS
Inflammatory response	<i>PTX3</i>	Pentraxin-related gene, rapidly induced by IL-1 $\beta$	NS	↓ 2.17	NS
Metabolic process	<i>ACACA</i>	Acetyl-Coenzyme A carboxylase $\alpha$	↓ 2.01	↓ 2.26	↓ 2.03
	<i>ADAMTS5</i>	ADAM metalloproteinase with thrombospondin type 1 motif, 5 (aggrecanase-2)	NS	↓ 2.67	↓ 2.51
	<i>B3GAT2</i>	$\beta$ -1,3-glucuronyl transferase 2 (glucuronosyl transferase S)	NS	↓ 2.74	↓ 2.56

Gene categories	Gene symbol	Gene description	Fold change		
			SFN	6-MSITC	6-MTITC
Oxido-reductase	<i>CA12</i>	Carbonic anhydrase XII	NS	↓ 2.09	NS
	<i>CTSC</i>	Cathepsin C	NS	↓ 2.45	NS
	<i>FAHD2A</i>	Fumarylacetoacetate hydrolase domain containing 2A	NS	↓ 2.16	↓ 2.16
	<i>FBXO9</i>	F-box protein 9	NS	↓ 2.54	NS
	<i>IDI2</i>	Isopentenyl-diphosphate delta isomerase 2	NS	↓ 2.22	NS
	<i>MGC4172</i>	Short-chain dehydrogenase/reductase	NS	NS	↓ 2.21
	<i>MICAL2</i>	Microtubule associated monooxygenase, calponin and LIM domain containing 2	NS	NS	↓ 2.03
	<i>PHKA2</i>	Phosphorylase kinase, $\alpha$ 2 (liver)	NS	↓ 2.07	↓ 2.69
	<i>PHOSPHO2</i>	Phosphatase, orphan 2	NS	↓ 2.63	↓ 2.73
	<i>POP5</i>	Processing of precursor 5, ribonuclease P/MRP subunit (S. cerevisiae)	NS	↓ 2.29	↓ 2.13
Response to stimuli	<i>RDH13</i>	Transcribed locus /// Retinol dehydrogenase 13 (all-trans/9-cis)	NS	↓ 2.09	NS
	<i>SORL1</i>	Sortilin-related receptor, L(DLR class) A repeats-containing	↓ 2.16	↓ 2.25	NS
	<i>STAR</i>	Steroidogenic acute regulatory protein	NS	NS	↓ 2.00
	<i>IFI44</i>	Interferon-induced protein 44	NS	↓ 3.39	↓ 3.18
	<i>PLSCR1</i>	Phospholipid scramblase 1	NS	↓ 2.49	↓ 2.54
Signal transduction	<i>ANGPT1</i>	Angiopoietin 1	NS	↓ 2.46	↓ 2.07
	<i>ANK2</i>	Ankyrin 2, neuronal	NS	NS	↓ 2.03
	<i>ARL4A</i>	ADP-ribosylation factor-like 4A	NS	↓ 2.05	NS
	<i>CENTD1</i>	Centaurin, $\delta$ 1	NS	↓ 2.47	↓ 2.78
	<i>GKAP1</i>	G kinase anchoring protein 1	NS	NS	↓ 2.69



Gene categories	Gene symbol	Gene description	Fold change		
			SFN	6-MSITC	6-MTITC
	<i>GNG12</i>	Guanine nucleotide binding protein (G protein), $\gamma$ 12	NS	↓ 2.32	NS
	<i>GTPBP4///IDI2</i>	GTP binding protein 4 /// isopentenyl-diphosphate $\delta$ isomerase 2	NS	↓ 2.17	NS
	<i>IGFBP3</i>	Insulin-like growth factor binding protein 3	NS	NS	↓ 2.16
	<i>IGFBP5</i>	Insulin-like growth factor binding protein 5	NS	NS	↓ 2.34
	<i>IGSF1</i>	Immunoglobulin superfamily, member 1	↓ 2.10	NS	↓ 2.03
	<i>LETM1</i>	Leucine zipper-EF-hand containing transmembrane protein 1	↓ 2.09	NS	NS
	<i>MAP2K6</i>	Mitogen-activated protein kinase kinase 6	NS	↓ 2.04	NS
	<i>PDE8B</i>	Phosphodiesterase 8B	NS	↓ 2.27	NS
	<i>PDGFRA</i>	Platelet-derived growth factor receptor, $\alpha$ polypeptide	NS	↓ 2.19	↓ 2.02
	<i>PHLDB2</i>	Pleckstrin homology-like domain, family B, member 2	NS	↓ 2.51	↓ 2.50
	<i>PPP2R2B</i>	Protein phosphatase 2 (formerly 2A), regulatory subunit B, $\beta$ isoform	↓ 2.05	↓ 2.25	↓ 2.38
	<i>RAB30</i>	RAB30, member RAS oncogene family	↓ 2.10	NS	NS
	<i>RAB31</i>	RAB31, member RAS oncogene family	NS	↓ 2.22	NS
	<i>RAB7L1</i>	RAB7, member RAS oncogene family-like 1	NS	↓ 2.13	NS
	<i>RGS5</i>	Regulator of G-protein signaling 5	NS	↓ 2.18	↓ 2.13
	<i>SHANK2</i>	SH3 and multiple ankyrin repeat domains 2	NS	NS	↓ 2.03
	<i>SPA17</i>	Sperm autoantigenic protein 17	NS	↓ 2.23	NS

Gene categories	Gene symbol	Gene description	Fold change		
			SFN	6-MSITC	6-MTITC
Transcription	<i>SSTR2</i>	Somatostatin receptor 2	NS	↓ 2.02	↓ 2.14
	<i>VAV3</i>	Vav 3 guanine nucleotide exchange factor	NS	↓ 2.08	↓ 2.12
	<i>WDR67</i>	WD repeat domain 67	↓ 2.31	↓ 3.01	↓ 2.81
	<i>ASCC3</i>	Activating signal cointegrator 1 complex subunit 3	NS	↓ 2.31	↓ 2.01
	<i>ASXL3</i>	Additional sex combs like 3 (Drosophila)	NS	↓ 2.64	↓ 2.78
	<i>ATF7IP2</i>	Activating transcription factor 7 interacting protein 2	NS	↓ 3.47	↓ 2.84
	<i>ATOH8</i>	Atonal homolog 8 (Drosophila)	↓ 2.30	↓ 3.15	↓ 2.67
	<i>BCL11A</i>	B-cell CLL/lymphoma 11A (zinc finger protein)	NS	↓ 2.03	NS
	<i>C5orf41</i>	Chromosome 5 open reading frame 41	NS	NS	↓ 2.14
	<i>CASZ1</i>	Castor zinc finger 1	↓ 2.67	↓ 2.86	↓ 3.01
	<i>CBX5</i>	Chromobox homolog 5 (HP1 $\alpha$ homolog, Drosophila)	NS	↓ 2.19	↓ 2.19
	<i>DLX3</i>	Distal-less homeobox 3	NS	↓ 2.01	↓ 2.01
	<i>EPC1</i>	Enhancer of polycomb homolog 1 (Drosophila)	↓ 2.28	↓ 2.00	↓ 2.65
	<i>ESRRG</i>	Estrogen-related receptor $\gamma$	↓ 2.05	↓ 4.64	↓ 4.40
	<i>EYA2</i>	Eyes absent homolog 2 (Drosophila)	NS	↓ 2.01	NS
	<i>GRHL1</i>	Grainyhead-like 1 (Drosophila)	↓ 2.54	NS	NS
	<i>HELLS</i>	Helicase, lymphoid-specific	NS	NS	↓ 2.16
	<i>INSM1</i>	Insulinoma-associated 1	NS	↓ 2.03	NS
	<i>ISL1</i>	ISL LIM homeobox 1	NS	↓ 2.08	NS
	<i>KLF15</i>	Kruppel-like factor 15	NS	↓ 2.15	↓ 2.53
	<i>LHX6</i>	LIM homeobox 6	NS	↓ 2.14	↓ 2.25
	<i>LHX9</i>	LIM homeobox 9	↓ 2.33	↓ 2.80	↓ 3.57
	<i>MYT1</i>	Myelin transcription factor 1	NS	NS	↓ 2.14
<i>NFE2L3</i>	Nuclear factor (erythroid-derived 2)-like 3	NS	↓ 3.58	↓ 2.73	

Gene categories	Gene symbol	Gene description	Fold change		
			SFN	6-MSITC	6-MTITC
	<i>NR4A2</i>	Nuclear receptor subfamily 4, group A, member 2	NS	NS	↓ 2.08
	<i>PER2</i>	Period homolog 2 (Drosophila)	NS	↓ 2.96	↓ 2.96
	<i>PPARGC1A</i>	Peroxisome proliferator-activated receptor $\gamma$ , coactivator 1 $\alpha$	NS	↓ 2.43	↓ 2.45
	<i>PRDM13</i>	PR domain containing 13	NS	NS	↓ 2.33
	<i>PSMG4</i>	Proteasome (prosome, macropain) assembly chaperone 4	↓ 2.10	↓ 3.32	↓ 3.04
	<i>SYNPO2</i>	Synaptopodin 2	NS	↓ 2.70	↓ 2.93
	<i>TAF4B</i>	TAF4b RNA polymerase II, TATA box binding protein (TBP)-associated factor, 105kDa	NS	↓ 2.25	↓ 2.10
	<i>TAF5L</i>	TAF5-like RNA polymerase II, p300/CBP-associated factor (PCAF)-associated factor, 65kDa	NS	↓ 2.28	NS
	<i>TFDP1</i>	Transcription factor Dp-1	NS	↓ 2.00	NS
	<i>TRERF1</i>	Transcriptional regulating factor 1	↓ 2.28	↓ 3.40	↓ 2.49
	<i>TXNIP</i>	Thioredoxin interacting protein	NS	NS	↓ 2.17
	<i>ZNF114</i>	Zinc finger protein 114	NS	↓ 2.02	NS
	<i>ZNF529</i>	Zinc finger protein 529	↓ 2.15	↓ 2.45	↓ 2.24
	<i>ZNF789</i>	Zinc finger protein 789	↓ 2.29	NS	NS
Transferase activity	<i>CMPK2</i>	Cytidine monophosphate (UMP-CMP) kinase 2, mitochondrial	NS	↓ 2.25	↓ 2.39
	<i>CRLS1</i>	Cardiolipin synthase 1	NS	↓ 2.05	NS
	<i>DGCR14</i>	DiGeorge syndrome critical region gene 14	↓ 2.01	NS	NS
	<i>DTYMK/// LOC 727761</i>	Deoxythymidylate kinase (thymidylate kinase) /// similar to Deoxythymidylate kinase (thymidylate kinase)	↓ 2.07	NS	NS

Gene categories	Gene symbol	Gene description	Fold change		
			SFN	6-MSITC	6-MTITC
	<i>FGFR2</i>	Fibroblast growth factor receptor 2 (bacteria-expressed kinase, keratinocyte growth factor receptor, craniofacial dysostosis 1, Crouzon syndrome, Pfeiffer syndrome, Jackson-Weiss syndrome)	↓ 2.14	↓ 2.86	↓ 2.33
	<i>FLJ25006</i>	Hypothetical protein FLJ25006	↓ 2.30	↓ 2.79	↓ 2.77
	<i>FLT4</i>	Fms-related tyrosine kinase 4	↓ 2.00	NS	NS
	<i>GLT8D1</i>	Glycosyltransferase 8 domain containing 1	NS	↓ 2.13	NS
	<i>MAGI1</i>	Membrane associated guanylate kinase, WW and PDZ domain containing 1	NS	NS	↓ 2.03
	<i>MAT2A</i>	Methionine adenosyl transferase II, $\alpha$	NS	↓ 2.01	NS
	<i>NAT1</i>	N-acetyltransferase 1 (arylamine N-acetyl transferase)	NS	NS	↓ 2.06
	<i>NUAK1</i>	NUAK family, SNF1-like kinase, 1	NS	↓ 2.09	↓ 2.03
	<i>TRNT1</i>	TRNA nucleotidyl transferase, CCA-adding, 1	NS	NS	↓ 2.15
Translation	<i>NTRK1</i>	Neurotrophic tyrosine kinase, receptor, type 1	↓ 2.13	NS	↓ 2.05
	<i>PELO</i>	Pelota homolog (Drosophila)	NS	NS	↓ 2.18
	<i>RPL22L1</i>	Ribosomal protein L22-like 1	NS	↓ 2.13	↓ 2.36
Transport	<i>ATP5S</i>	ATP synthase, H <sup>+</sup> transporting, mitochondrial F0 complex, subunit s (factor B)	NS	↓ 2.77	↓ 3.08
	<i>CHML</i>	Choroideremia-like (Rab escort protein 2)	NS	↓ 2.02	NS
	<i>CLCN4</i>	Chloride channel 4	NS	↓ 2.63	↓ 2.39
	<i>CTHRC1</i>	Collagen triple helix repeat containing 1	NS	↓ 2.19	NS

Gene categories	Gene symbol	Gene description	Fold change		
			SFN	6-MSITC	6-MTITC
	<i>ITPR2</i>	Inositol 1,4,5-triphosphate receptor, type 2	NS	↓ 2.27	NS
	<i>KCNK3</i>	Potassium channel, subfamily K, member 3	↓ 3.75	↓ 2.19	↓ 2.40
	<i>KCNN2</i>	Potassium intermediate/small conductance calcium-activated channel, subfamily N, member 2	NS	↓ 2.81	↓ 2.20
	<i>OSBPL7</i>	Oxysterol binding protein-like 7	NS	NS	↓ 2.01
	<i>PGAP1</i>	Post-GPI attachment to proteins 1	↓ 2.13	NS	NS
	<i>RABEPK</i>	Rab9 effector protein with kelch motifs	↓ 2.12	NS	↓ 2.24
	<i>SLC44A1</i>	Solute carrier family 44, member 1	NS	↓ 2.55	↓ 3.32
	<i>SLC6A15</i>	Solute carrier family 6, member 15	NS	↓ 2.00	↓ 2.01
	<i>SYT13</i>	Synaptotagmin XIII	NS	NS	↓ 2.31
	<i>TTYH2</i>	Tweety homolog 2 (Drosophila)	NS	↓ 2.24	↓ 2.46
Unknown	<i>ARGLU1</i>	Arginine and glutamate rich 1	NS	↓ 2.16	↓ 2.16
	<i>ARPP-21</i>	Cyclic AMP-regulated phosphoprotein, 21 kD	NS	NS	↓ 2.00
	<i>ATG16L2</i>	ATG16 autophagy related 16-like 2 (S. cerevisiae)	↓ 2.08	NS	NS
	<i>C10orf128</i>	Chromosome 10 open reading frame 128	NS	↓ 2.06	NS
	<i>C10orf56</i>	Chromosome 10 open reading frame 56	NS	↓ 2.12	NS
	<i>C10orf78</i>	Chromosome 10 open reading frame 78	NS	↓ 2.21	NS
	<i>C14orf162</i>	Chromosome 14 open reading frame 162	NS	NS	↓ 2.38
	<i>C1orf114</i>	Chromosome 1 open reading frame 114	↓ 2.22	NS	NS
	<i>C1orf21</i>	Chromosome 1 open reading frame 21	NS	↓ 2.40	NS
	<i>C1orf62</i>	Chromosome 1 open reading frame 62	NS	↓ 2.44	↓ 2.71
	<i>C1orf79</i>	Chromosome 1 open reading frame 79	↓ 2.02	NS	NS
	<i>C4orf30</i>	Chromosome 4 open reading frame 30	NS	NS	↓ 2.71

Gene categories	Gene symbol	Gene description	Fold change		
			SFN	6-MSITC	6-MTITC
	<i>C6orf124</i> /// <i>LOC</i> <i>729439</i>	Chromosome 6 open reading frame 124 /// similar to HGC6.4	NS	↓ 2.07	NS
	<i>C6orf162</i>	Chromosome 6 open reading frame 162	NS	↓ 2.06	NS
	<i>C9orf135</i>	Chromosome 9 open reading frame 135	NS	↓ 2.02	NS
	<i>DKFZP434</i> <i>B2016</i>	Similar to hypothetical protein LOC284701	NS	NS	↓ 2.02
	<i>DKFZp667</i> <i>G2110</i>	Hypothetical protein DKFZp667G2110	NS	↓ 2.02	NS
	<i>DKFZp761</i> <i>H2121</i>	Hypothetical protein DKFZp761H2121	NS	↓ 2.10	↓ 2.00
	<i>DPY19L2P2</i>	Dpy-19-like 2 pseudogene 2 ( <i>C. elegans</i> )	NS	↓ 2.50	↓ 2.50
	<i>FAM19A4</i>	Family with sequence similarity 19 (chemokine (C-C motif)-like), member A4	NS	NS	↓ 2.05
	<i>FLJ13305</i>	Hypothetical protein FLJ13305	NS	↓ 2.25	NS
	<i>FLJ20323</i>	Hypothetical protein FLJ20323	NS	↓ 2.02	NS
	<i>KBTBD4</i>	Kelch repeat and BTB (POZ) domain containing 4	↓ 2.09	NS	NS
	<i>LOC</i> <i>100131067</i>	Hypothetical protein LOC100131067	NS	NS	↓ 2.27
	<i>LOC</i> <i>100134445</i>	Hypothetical protein LOC100134445	↓ 2.04	NS	NS
	<i>LOC150759</i>	Hypothetical protein LOC150759	NS	NS	↓ 2.03
	<i>LOC157627</i>	Hypothetical LOC157627	NS	NS	↓ 2.11
	<i>LOC203107</i>	Hypothetical protein LOC203107	NS	↓ 2.50	↓ 2.75
	<i>LOC283174</i>	Hypothetical LOC283174	NS	↓ 2.00	NS
	<i>LOC285878</i> /// <i>VSTM2A</i>	V-set and transmembrane domain containing 2A /// hypothetical protein LOC285878	NS	↓ 2.06	NS
	<i>LOC344595</i>	Hypothetical LOC344595	NS	↓ 2.77	NS
	<i>LOC375295</i>	Hypothetical gene supported by BC013438	NS	↓ 2.20	NS

Gene categories	Gene symbol	Gene description	Fold change		
			SFN	6-MSITC	6-MTITC
	<i>LOC388969</i>	Hypothetical LOC388969	NS	↓ 2.13	↓ 2.11
	<i>LOC401321</i>	Hypothetical LOC401321	NS	↓ 2.07	NS
	<i>LOC63920</i>	Transposon-derived Buster3 transposase-like	NS	↓ 2.11	↓ 2.28
	<i>LOC642236</i>	Similar to FRG1 protein (FSHD region gene 1 protein)	NS	↓ 2.10	NS
	<i>LOC643749</i>	Hypothetical LOC643749	NS	↓ 2.20	NS
	<i>LOC728903</i> ///MGC 21881	Hypothetical locus MGC21881 /// hypothetical LOC728903	NS	↓ 2.49	↓ 2.35
	<i>LOC730200</i>	Hypothetical LOC730200	NS	↓ 3.48	↓ 3.61
	<i>MCM3APAS</i>	Minichromosome maintenance complex component 3 associated protein antisense	NS	↓ 2.70	↓ 2.23
	<i>MIRHG1</i>	MicroRNA host gene (non-protein coding) 1	NS	↓ 2.40	NS
	<i>N4BP2L1</i>	NEDD4 binding protein 2-like 1	NS	↓ 2.04	NS
	<i>NBPF10</i> /// <i>NBPF11</i>	Neuroblastoma breakpoint family, member 11 /// neuroblastoma breakpoint family, member 10	NS	↓ 2.01	NS
	<i>SVIP</i>	Small VCP/p97- interacting protein	NS	↓ 2.10	NS
	<i>TM7SF3</i>	Transmembrane 7 superfamily member 3	NS	NS	↓ 2.46
	<i>TMEM111</i>	Transmembrane protein 111	NS	NS	↓ 2.13
	<i>TRIM37</i>	Tripartite motif-containing 37	NS	NS	↓ 2.23
	<i>VSTM2A</i>	V-set and transmembrane domain containing 2A	NS	↓ 2.06	NS
	<i>WDR17</i>	WD repeat domain 17	↓ 2.19	↓ 2.11	↓ 2.42

Gene categories	Gene symbol	Gene description	Fold change		
			SFN	6-MSITC	6-MTITC
	<i>WFIKKN2</i>	WAP, follistatin/kazal, immunoglobulin, kunitz and netrin domain containing 2	NS	NS	↓ 2.15
	<i>ZFAND2B</i>	Zinc finger, AN1-type domain 2B	↓ 2.21	↓ 2.22	NS

### 3.4.3. Identification of the biological pathways by IPA

To identify the biologically relevant networks and pathways within the differentially expressed genes of IMR-32 cells, pathway analyses were done using Ingenuity Pathways Knowledge Base (IPKB) on the datasets. Numerous pathways with significant threshold ( $p < 0.05$ ) were obtained from these analyses. The first five most statistically significant canonical pathways with respect to these ITCs are illustrated in Figure 3.3. Interestingly, gene profiles of SFN, 6-MSITC, and 6-MTITC treatment shared identical top two canonical pathways including Nrf2-mediated oxidative stress response and TR/RXR activation (Figure 3.3). Furthermore, the genes associated with each pathway that are modulated by ITCs were summarized in Table 3.5. 6-MSITC and 6-MTITC were found to cause greater number of differentially expressed genes (2-fold change) than SFN. These results imply that 6-MSITC and 6-MTITC have greater influence in the gene expression regulation of IMR- 32 cells than SFN.



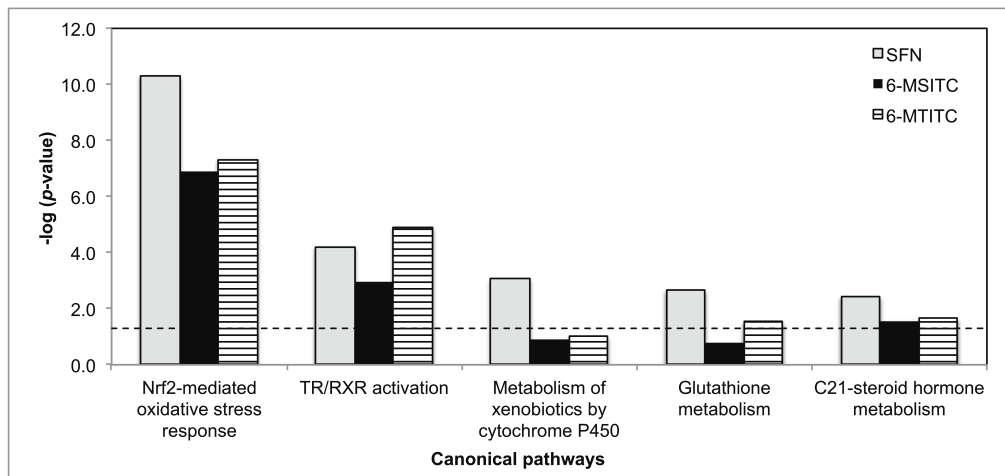


**Figure 3.3.** Comparative canonical pathway analyses of differentially expressed genes in IMR-32 neuron cells stimulated with Wasabi-derived ITCs. Differentially upregulated and downregulated genes were evaluated for canonical pathway analyses using IPA software as elaborated in “**Section 3.3.5**”. Only five of the top most significant pathways with respect to Wasabi-derived ITCs are shown here. The list of corresponding significant pathways is indicated below and their respective level of significance ( $p < 0.05$ ) denoted by the length of the bars.

**Table 3.5.** List of genes involved in significantly modulated canonical pathways by SFN, 6-MSITC and 6-MTITC in IMR-32 cells

ITCs	Canonical pathways	p-value	Regulation	No. of genes	Regulated genes
SFN	Nrf2-mediated oxidative stress response	5.01E-11	↑	12	<i>BACH1, DNAJB4, FTH1, FTL, GCLM, GSR, GSTM3, HMOX1, MAFF, NQO1, SQSTM1, TXNRD1</i>
	TR/RXR activation	6.03E-05	↑	5	<i>AKR1C1, AKR1C2, AKR1C3, ME1, SYT2</i>
	Metabolism of xenobiotics by cytochrome P450	8.71E-04	↑	4	<i>AKR1C1, AKR1C2, AKR1C3, GSTM3</i>
	Glutathione metabolism	2.19E-03	↑	3	<i>GCLM, GSR, GSTM3</i>
	C21-steroid hormone metabolism	3.72E-03	-	2	<i>AKR1C1, AKR1C3</i>
6-MSITC	Nrf2-mediated oxidative stress response	1.23E-07	↑	14	<i>BACH1, DNAJB1, DNAJB4, FTH1, FTL, GCLM, GSR, HMOX1, KEAP1, MAFF, MAFG, NQO1, SQSTM1, TXNRD1</i>
	TR/RXR activation	1.12E-03	↑	6	<i>ACACA, AKR1C1, AKR1C2, AKR1C3, ME1, SYT2</i>
	Wnt/β-catenin signaling	6.61E-03	↓	7	<i>GJA1, KREMEN1, PPP2R2B, PPP2R2C, SRC, WNT5A, WNT5B</i>
	PTEN signaling	8.91E-03	↓	5	<i>FOXO6, IKBKB, ITGA4, MAGI1, PDGFRA</i>
	Ephrin receptor signaling	1.05E-02	↑	7	<i>ANGPT1, CXCR4, FIGF, GNG12, ITGA4, NGEF, SRC</i>
6-MTITC	Nrf2-mediated oxidative stress response	4.68E-08	↑	14	<i>BACH1, DNAJB1, DNAJB4, FTH1, FTL, GCLM, GSR, HMOX1, KEAP1, MAFF, MAFG, NQO1, SQSTM1, TXNRD1</i>
	TR/RXR activation	1.23E-05	↑	8	<i>ACACA, AKR1C1, AKR1C2, AKR1C3,</i>

ITCs	Canonical pathways	p-value	Regulation	No. of genes	Regulated genes
	Hepatic Fibrosis/ Hepatic stellate cell activation	2.51E-04	-	8	<i>ME1, PPARGC1A, RXRA, SYT2, COL1A1, FGFR2, FIGF, FLT4, IGFBP5, PDGFRA, TNFRSF1A, VEGFA</i>
	Axonal guidance signaling	1.00E-03	↑	13	<i>CXCR4, FIGF, ITGA4, PLXNA2, PRKACB, SEMA6B, SHANK2, SHC1, SLIT2, SLIT3, VEGFA, WNT5A, WNT5B</i>
	Estrogen receptor signaling	3.24E-03	↑	6	<i>HNRNPD, PCK2, PPARGC1A, SHC1, SRC, TAF4B</i>

#### 3.4.4. Expression profiling of Nrf2-mediated genes by Wasabi-derived ITCs

To investigate the neuroprotective effects of SFN, 6-MSITC, and 6-MTITC, the genes coding for proteins involved in apoptosis regulations were investigated. However, microarray data revealed that the expressions of pro-apoptosis genes were unaltered by ITC treatment (Table 3.6). Also, pre-experiment data showed that ITCs could protect IMR-32 cells from oxidative stress induced by H<sub>2</sub>O<sub>2</sub>. This implies that ITCs do not induce neuronal cell death. Thus, the effects of SFN, 6-MSITC, and 6-MTITC on the expression of genes mediated by Nrf2 pathway were profiled (Table 3.7). They were classified into five categories including (a) the genes coding upstream regulators, (b) the genes coding antioxidant proteins, (c) the genes coding metabolizing enzymes and detoxifying protein genes, (d) the genes coding chaperone and stress response protein genes, and (e) the genes coding ubiquitination and proteosomal degradation protein. The gene expression of most of the antioxidant proteins and metabolizing enzymes from 6-MSITC and 6-MTITC treatment were found to be higher than SFN. These are ferritin heavy polypeptide 1

(*FTH1*), ferritin light polypeptide (*FTL*), glutathione reductase (*GSR*), *HO-1*, *NQO1*, sequestosome 1 (*SQSTM1*), and thioredoxin reductase 1 (*TXNRD1*) for the antioxidant proteins and enzymes. *Aldo–keto* reductase family 1 member C1, C2, C3 (*AKR1C1*, *AKR1C2*, *AKR1C3*), and glutamate-cysteine ligase modifier subunit (*GCLM*) were identified for metabolizing enzymes. 6-MSITC and 6-MTITC were found to have greater capacity to induce the expressions of genes associated with the Nrf2 pathway in neuron cells.

**Table 3.6** Genes coding for proteins involved in apoptosis regulation.

Categories	Gene Symbol	Gene Title	Fold change		
			SFN	6-MSITC	6-MTITC
Caspase	<i>CASP1</i>	Caspase 1, apoptosis-related cysteine peptidase (interleukin 1 $\beta$ , convertase)	↑ 1.04	↓ 1.12	↓ 1.07
	<i>CASP1</i>	Caspase 1, apoptosis-related cysteine peptidase (interleukin 1 $\beta$ , convertase)	↑ 1.12	↓ 1.01	↑ 1.01
	<i>CASP1</i>	Caspase 1, apoptosis-related cysteine peptidase (interleukin 1 $\beta$ , convertase)	↑ 1.00	↓ 1.09	↑ 1.00
	<i>CASP1</i>	Caspase 1, apoptosis-related cysteine peptidase (interleukin 1 $\beta$ , convertase)	↑ 1.08	↓ 1.14	↓ 1.09
	<i>CASP1</i>	Caspase 1, apoptosis-related cysteine peptidase (interleukin 1 $\beta$ , convertase)	↑ 1.12	↑ 1.15	↑ 1.10
	<i>CASP2</i>	Caspase 2, apoptosis-related cysteine peptidase (neural precursor cell expressed, developmentally down-regulated 2)	↓ 1.35	↓ 1.15	↓ 1.06
	<i>CASP2</i>	Caspase 2, apoptosis-related cysteine peptidase (neural precursor cell expressed, developmentally down-regulated 2)	↓ 1.18	↓ 1.04	↓ 1.01

Categories	Gene Symbol	Gene Title	Fold change		
			SFN	6-MSITC	6-MTITC
	<i>CASP2</i>	Caspase 2, apoptosis-related cysteine peptidase (neural precursor cell expressed, developmentally down-regulated 2)	↑ 1.08	↓ 1.03	↑ 1.01
	<i>CASP2</i>	Caspase 2, apoptosis-related cysteine peptidase (neural precursor cell expressed, developmentally down-regulated 2)	↓ 1.41	↓ 1.42	↓ 1.31
	<i>CASP2</i>	Caspase 2, apoptosis-related cysteine peptidase (neural precursor cell expressed, developmentally down-regulated 2)	↓ 1.25	↓ 1.19	↑ 1.00
	<i>CASP2</i>	Caspase 2, apoptosis-related cysteine peptidase (neural precursor cell expressed, developmentally down-regulated 2)	↓ 1.07	↑ 1.00	↓ 1.00
	<i>CASP2</i>	Caspase 2, apoptosis-related cysteine peptidase (neural precursor cell expressed, developmentally down-regulated 2)	↓ 1.05	↓ 1.00	↑ 1.01
	<i>CASP3</i>	Caspase 3, apoptosis-related cysteine peptidase	↓ 1.02	↓ 1.06	↑ 1.02
	<i>CASP3</i>	Caspase 3, apoptosis-related cysteine peptidase	↓ 1.14	↓ 1.08	↑ 1.12
	<i>CASP4</i>	Caspase 4, apoptosis-related cysteine peptidase	↓ 1.25	↑ 1.14	↓ 1.20
	<i>CASP4</i>	Caspase 4, apoptosis-related cysteine peptidase	↓ 1.02	↓ 1.00	↑ 1.17
	<i>CASP5</i>	Caspase 5, apoptosis-related cysteine peptidase	↑ 1.06	↑ 1.25	↑ 1.19
	<i>CASP6</i>	Caspase 6, apoptosis-related cysteine peptidase	↓ 1.07	↓ 1.37	↓ 1.07
	<i>CASP6</i>	Caspase 6, apoptosis-related cysteine peptidase	↓ 1.06	↓ 1.14	↓ 1.17

Categories	Gene Symbol	Gene Title	Fold change		
			SFN	6-MSITC	6-MTITC
	<i>CASP7</i>	Caspase 7, apoptosis-related cysteine peptidase	↓ 1.11	↑ 1.11	↑ 1.03
	<i>CASP8</i>	Caspase 8, apoptosis-related cysteine peptidase	↓ 1.43	↑ 1.10	↑ 1.07
	<i>CASP8</i>	Caspase 8, apoptosis-related cysteine peptidase	↓ 1.14	↓ 1.03	↓ 1.18
	<i>CASP8</i>	Caspase 8, apoptosis-related cysteine peptidase	↓ 1.10	↓ 1.29	↓ 1.01
	<i>CASP9</i>	Caspase 9, apoptosis-related cysteine peptidase	↓ 1.50	↓ 1.09	↓ 1.31
	<i>CASP9</i>	Caspase 9, apoptosis-related cysteine peptidase	↓ 1.22	↑ 1.07	↓ 1.05
	<i>CASP9</i>	Caspase 9, apoptosis-related cysteine peptidase	↑ 1.06	↑ 1.04	↑ 1.02
	<i>CASP10</i>	Caspase 10, apoptosis-related cysteine peptidase	↓ 1.19	↓ 1.16	↓ 1.38
	<i>CASP10</i>	Caspase 10, apoptosis-related cysteine peptidase	↑ 1.20	↑ 1.08	↓ 1.07
	<i>CASP10</i>	Caspase 10, apoptosis-related cysteine peptidase	↓ 1.02	↑ 1.07	↓ 1.09
	<i>CASP10</i>	Caspase 10, apoptosis-related cysteine peptidase	↑ 1.07	↑ 1.20	↑ 1.13
Death receptor	<i>ADAM17</i>	ADAM metallopeptidase domain 17 (tumor necrosis factor $\alpha$ , converting enzyme)	↑ 1.01	↑ 1.09	↑ 1.18
	<i>ADAM17</i>	ADAM metallopeptidase domain 17 (tumor necrosis factor $\alpha$ , converting enzyme)	↓ 1.16	↑ 1.06	↑ 1.04
	<i>ADAM17</i>	ADAM metallopeptidase domain 17 (tumor necrosis factor $\alpha$ , converting enzyme)	↓ 1.03	↑ 1.07	↑ 1.04
	<i>ADAM17</i>	ADAM metallopeptidase domain 17 (tumor necrosis factor $\alpha$ , converting enzyme)	↑ 1.22	↑ 1.10	↑ 1.06
	<i>AMACR /// C1QTNF3</i>	$\alpha$ -methylacyl-CoA racemase /// C1q and tumor necrosis factor related protein 3	↓ 1.02	↓ 1.18	↓ 1.30

Categories	Gene Symbol	Gene Title	Fold change		
			SFN	6-MSITC	6-MTITC
	<i>AMACR</i> /// <i>C1QTNF3</i>	$\alpha$ -methylacyl-CoA racemase /// C1q and tumor necrosis factor related protein 3	↓ 1.01	↑ 1.02	↑ 1.01
	<i>AMACR</i> /// <i>C1QTNF3</i>	$\alpha$ -methylacyl-CoA racemase /// C1q and tumor necrosis factor related protein 3	↓ 1.07	↓ 1.02	↓ 1.05
	<i>CFLAR</i>	CASP8 and FADD-like apoptosis regulator	↓ 1.13	↓ 1.01	↑ 1.12
	<i>CFLAR</i>	CASP8 and FADD-like apoptosis regulator	↑ 1.02	↓ 1.02	↓ 1.08
	<i>CFLAR</i>	CASP8 and FADD-like apoptosis regulator	↓ 1.12	↓ 1.00	↑ 1.05
	<i>CFLAR</i>	CASP8 and FADD-like apoptosis regulator	↑ 1.16	↑ 1.40	↑ 1.31
	<i>CFLAR</i>	CASP8 and FADD-like apoptosis regulator	↓ 1.02	↓ 1.04	↓ 1.00
	<i>CFLAR</i>	CASP8 and FADD-like apoptosis regulator	↑ 1.27	↑ 1.08	↑ 1.16
	<i>CFLAR</i>	CASP8 and FADD-like apoptosis regulator	↑ 1.05	↑ 1.14	↓ 1.07
	<i>CFLAR</i>	CASP8 and FADD-like apoptosis regulator	↑ 1.10	↑ 1.24	↑ 1.31
	<i>CFLAR</i>	CASP8 and FADD-like apoptosis regulator	↑ 1.18	↑ 1.13	↑ 1.04
	<i>CFLAR</i>	CASP8 and FADD-like apoptosis regulator	↑ 1.65	↑ 1.47	↑ 1.43
	<i>CFLAR</i>	CASP8 and FADD-like apoptosis regulator	↓ 1.13	↓ 1.07	↓ 1.12
	<i>FADD</i>	Fas (TNFRSF6)-associated via death domain	↑ 1.11	↑ 1.19	↑ 1.23
	<i>FAIM2</i>	Fas apoptotic inhibitory molecule 2	↓ 1.10	↑ 1.16	↑ 1.08
	<i>FAIM2</i>	Fas apoptotic inhibitory molecule 2	↑ 1.12	↑ 1.31	↑ 1.21
	<i>FAS</i>	Fas (TNF receptor superfamily, member 6)	↑ 1.04	↑ 1.07	↑ 1.04
	<i>FAS</i>	Fas (TNF receptor superfamily, member 6)	↑ 1.05	↓ 1.04	↑ 1.01
	<i>FAS</i>	Fas (TNF receptor superfamily, member 6)	↓ 1.01	↓ 1.04	↑ 1.07
	<i>FAS</i>	Fas (TNF receptor superfamily, member 6)	↑ 1.20	↑ 1.05	↑ 1.05
	<i>FAS</i>	Fas (TNF receptor superfamily, member 6)	↓ 1.09	↑ 1.02	↓ 1.09
	<i>FASLG</i>	Fas ligand (TNF superfamily, member 6)	↑ 1.27	↓ 1.19	↑ 1.16
	<i>FASLG</i>	Fas ligand (TNF superfamily, member 6)	↑ 1.42	↑ 1.29	↑ 1.14

Categories	Gene Symbol	Gene Title	Fold change		
			SFN	6-MSITC	6-MTITC
	<i>MGC31957</i> /// <i>TNFRSF10C</i>	Tumor necrosis factor receptor superfamily, member 10c, decoy without an intracellular domain /// hypothetical protein MGC31957	↑ 1.07	↑ 1.10	↓ 1.09
	<i>MGC31957</i> /// <i>TNFRSF10C</i>	Tumor necrosis factor receptor superfamily, member 10c, decoy without an intracellular domain /// hypothetical protein MGC31957	↓ 1.05	↓ 1.03	↓ 1.12
	<i>RTEL1</i> /// <i>TNFRSF6B</i>	Tumor necrosis factor receptor superfamily, member 6b, decoy /// regulator of telomere elongation helicase 1	↓ 1.05	↑ 1.13	↑ 1.36
	<i>RTEL1</i> /// <i>TNFRSF6B</i>	Tumor necrosis factor receptor superfamily, member 6b, decoy /// regulator of telomere elongation helicase 1	↑ 1.18	↑ 1.20	↑ 1.17
	<i>TNF</i>	Tumor necrosis factor (TNF superfamily, member 2)	↓ 1.03	↑ 1.27	↑ 1.13
	<i>TNFAIP1</i>	Tumor necrosis factor, $\alpha$ -induced protein 1 (endothelial)	↑ 1.14	↑ 1.05	↑ 1.00
	<i>TNFAIP1</i>	Tumor necrosis factor, $\alpha$ -induced protein 1 (endothelial)	↑ 1.32	↑ 1.40	↑ 1.28
	<i>TNFAIP2</i>	Tumor necrosis factor, $\alpha$ -induced protein 2	↑ 1.00	↓ 1.29	↓ 1.19
	<i>TNFAIP2</i>	Tumor necrosis factor, $\alpha$ -induced protein 2	↓ 1.03	↑ 1.07	↑ 1.29
	<i>TNFAIP3</i>	Tumor necrosis factor, $\alpha$ -induced protein 3	↓ 1.19	↓ 1.52	↓ 1.48
	<i>TNFAIP3</i>	Tumor necrosis factor, $\alpha$ -induced protein 3	↓ 1.38	↓ 1.33	↓ 1.19
	<i>TNFAIP6</i>	Tumor necrosis factor, $\alpha$ -induced protein 6	↓ 1.23	↓ 1.07	↑ 1.08
	<i>TNFAIP6</i>	Tumor necrosis factor, $\alpha$ -induced protein 6	↓ 1.09	↓ 1.15	↓ 1.01
	<i>TNFAIP8</i>	Tumor necrosis factor, $\alpha$ -induced protein 8	↑ 1.02	↓ 1.75	↓ 1.72
	<i>TNFAIP8</i>	Tumor necrosis factor, $\alpha$ -induced protein 8	↓ 1.40	↓ 1.79	↓ 1.78
	<i>TNFRSF10B</i>	Tumor necrosis factor receptor superfamily, member 10b	↑ 1.25	↑ 1.60	↑ 1.32



Categories	Gene Symbol	Gene Title	Fold change		
			SFN	6-MSITC	6-MTITC
	<i>TNFRSF10B</i>	Tumor necrosis factor receptor superfamily, member 10b	↑ 1.11	↑ 1.25	↑ 1.14
	<i>TNFRSF10B</i>	Tumor necrosis factor receptor superfamily, member 10b	↑ 1.19	↑ 1.06	↑ 1.31
	<i>TNFRSF10C</i>	Tumor necrosis factor receptor superfamily, member 10c, decoy without an intracellular domain	↑ 1.14	↓ 1.02	↓ 1.05
	<i>TNFRSF10C</i>	Tumor necrosis factor receptor superfamily, member 10c, decoy without an intracellular domain	↑ 1.03	↑ 1.18	↑ 1.15
	<i>TNFRSF10D</i>	Tumor necrosis factor receptor superfamily, member 10d, decoy with truncated death domain	↑ 1.10	↑ 1.02	↑ 1.08
	<i>TNFRSF10D</i>	Tumor necrosis factor receptor superfamily, member 10d, decoy with truncated death domain	↑ 1.21	↓ 1.06	↓ 1.14
	<i>TNFRSF11A</i>	Tumor necrosis factor receptor superfamily, member 11a, NFKB activator	↓ 1.10	↓ 1.14	↓ 1.10
	<i>TNFRSF11A</i>	Tumor necrosis factor receptor superfamily, member 11a, NFKB activator	↑ 1.19	↑ 1.19	↑ 1.19
	<i>TNFRSF11B</i>	Tumor necrosis factor receptor superfamily, member 11b (osteoprotegerin)	↑ 1.05	↓ 1.03	↓ 1.09
	<i>TNFRSF11B</i>	Tumor necrosis factor receptor superfamily, member 11b (osteoprotegerin)	↓ 1.22	↑ 1.15	↑ 1.01
	<i>TNFRSF13B</i>	Tumor necrosis factor receptor superfamily, member 13B	↑ 1.17	↑ 1.17	↑ 1.46
	<i>TNFRSF14</i>	Tumor necrosis factor receptor superfamily, member 14 (herpesvirus entry mediator)	↓ 1.09	↓ 1.00	↑ 1.21
	<i>TNFRSF17</i>	Tumor necrosis factor receptor superfamily, member 17	↑ 1.13	↑ 1.16	↑ 1.08

Categories	Gene Symbol	Gene Title	Fold change		
			SFN	6-MSITC	6-MTITC
	<i>TNFRSF1A</i>	Tumor necrosis factor receptor superfamily, member 1A	↑ 2.86	↑ 4.57	↑ 4.26
	<i>TNFRSF1B</i>	Tumor necrosis factor receptor superfamily, member 1B	↓ 1.02	↑ 1.06	↑ 1.05
	<i>TNFRSF21</i>	Tumor necrosis factor receptor superfamily, member 21	↓ 1.24	↓ 1.67	↓ 1.25
	<i>TNFRSF21</i>	Tumor necrosis factor receptor superfamily, member 21	↓ 1.15	↓ 1.30	↓ 1.26
	<i>TNFRSF25</i>	Tumor necrosis factor receptor superfamily, member 25	↑ 1.23	↑ 1.16	↑ 1.16
	<i>TNFRSF25</i>	Tumor necrosis factor receptor superfamily, member 25	↓ 1.04	↓ 1.42	↓ 1.30
	<i>TNFRSF25</i>	Tumor necrosis factor receptor superfamily, member 25	↓ 1.08	↓ 1.19	↓ 1.06
	<i>TNFRSF25</i>	Tumor necrosis factor receptor superfamily, member 25	↑ 1.42	↑ 1.18	↑ 1.32
	<i>TNFRSF25</i>	Tumor necrosis factor receptor superfamily, member 25	↓ 1.03	↑ 1.10	↓ 1.01
	<i>TNFRSF25</i>	Tumor necrosis factor receptor superfamily, member 25	↑ 1.01	↑ 1.43	↑ 1.06
	<i>TNFRSF4</i>	Tumor necrosis factor receptor superfamily, member 4	↓ 1.07	↑ 1.14	↑ 1.07
	<i>TNFRSF4</i>	Tumor necrosis factor receptor superfamily, member 4	↑ 1.63	↓ 1.13	↑ 1.35
	<i>TNFRSF8</i>	Tumor necrosis factor receptor superfamily, member 8	↓ 1.06	↑ 1.07	↑ 1.02
	<i>TNFRSF9</i>	Tumor necrosis factor receptor superfamily, member 9	↑ 1.12	↑ 1.12	↑ 1.26
	<i>TNFRSF9</i>	Tumor necrosis factor receptor superfamily, member 9	↑ 1.12	↑ 1.09	↑ 1.11
	<i>TNFSF10</i>	Tumor necrosis factor (ligand) superfamily, member 10	↓ 1.09	↓ 1.17	↓ 1.11
	<i>TNFSF10</i>	Tumor necrosis factor (ligand) superfamily, member 10	↓ 1.02	↓ 1.00	↑ 1.02

Categories	Gene Symbol	Gene Title	Fold change		
			SFN	6-MSITC	6-MTITC
	<i>TNFSF10</i>	Tumor necrosis factor (ligand) superfamily, member 10	↓ 1.00	↑ 1.03	↓ 1.03
	<i>TNFSF11</i>	Tumor necrosis factor (ligand) superfamily, member 11	↓ 1.06	↓ 1.00	↑ 1.07
	<i>TNFSF11</i>	Tumor necrosis factor (ligand) superfamily, member 11	↑ 1.08	↑ 1.29	↑ 1.16
	<i>TNFSF12</i>	Tumor necrosis factor (ligand) superfamily, member 12	↓ 1.01	↑ 1.11	↑ 1.13
	<i>TNFSF12</i> /// <i>TNFSF12-T</i> <i>NFSF13</i> /// <i>TNFSF13</i>	Tumor necrosis factor (ligand) superfamily, member 13 /// tumor necrosis factor (ligand) superfamily, member 12 /// TNFSF12-TNFSF13	↑ 1.35	↑ 1.23	↑ 1.15
	<i>TNFSF12</i> /// <i>TNFSF12-T</i> <i>NFSF13</i> /// <i>TNFSF13</i>	Tumor necrosis factor (ligand) superfamily, member 13 /// tumor necrosis factor (ligand) superfamily, member 12 /// TNFSF12-TNFSF13	↑ 1.21	↑ 1.33	↑ 1.28
	<i>TNFSF12</i> /// <i>TNFSF12-T</i> <i>NFSF13</i> /// <i>TNFSF13</i>	Tumor necrosis factor (ligand) superfamily, member 13 /// tumor necrosis factor (ligand) superfamily, member 12 /// TNFSF12-TNFSF13	↓ 1.28	↓ 1.40	↑ 1.02
	<i>TNFSF13</i>	Tumor necrosis factor (ligand) superfamily, member 13	↓ 1.01	↑ 1.08	↑ 1.17
	<i>TNFSF13</i>	Tumor necrosis factor (ligand) superfamily, member 12	↓ 1.03	↑ 1.18	↑ 1.03
	<i>TNFSF14</i>	Tumor necrosis factor (ligand) superfamily, member 14	↑ 1.02	↑ 1.39	↑ 1.20
	<i>TNFSF4</i>	Tumor necrosis factor (ligand) superfamily, member 4 (tax-transcriptionally activated glycoprotein 1, 34kDa)	↑ 1.07	↑ 1.25	↑ 1.24
	<i>TNFSF8</i>	Tumor necrosis factor (ligand) superfamily, member 8	↓ 1.38	↓ 1.14	↓ 1.04
	<i>TNFSF8</i>	Tumor necrosis factor (ligand) superfamily, member 8	↓ 1.18	↓ 1.01	↓ 1.17

Categories	Gene Symbol	Gene Title	Fold change		
			SFN	6-MSITC	6-MTITC
Apoptosis Inhibitor	<i>TNFSF9</i>	Tumor necrosis factor (ligand) superfamily, member 9	↑ 1.14	↑ 1.17	↑ 1.13
	<i>LOC652755</i> <i>/// NAIP</i>	NLR family, apoptosis inhibitory protein <i>///</i> similar to Baculoviral IAP repeat-containing protein 1 (Neuronal apoptosis inhibitory protein)	↓ 1.22	↓ 1.23	↓ 1.42
	<i>LOC652755</i> <i>/// NAIP</i>	NLR family, apoptosis inhibitory protein <i>///</i> similar to Baculoviral IAP repeat-containing protein 1 (Neuronal apoptosis inhibitory protein)	↑ 1.02	↓ 1.18	↓ 1.08
	<i>BIRC2</i>	Baculoviral IAP repeat-containing 2	↓ 1.03	↓ 1.18	↓ 1.06
	<i>BIRC3</i>	Baculoviral IAP repeat-containing 3	↓ 1.01	↓ 1.08	↓ 1.08
	<i>XIAP</i>	X-linked inhibitor of apoptosis	↑ 1.17	↓ 1.37	↓ 1.21
	<i>XIAP</i>	X-linked inhibitor of apoptosis	↑ 1.20	↓ 1.22	↑ 1.00
	<i>XIAP</i>	X-linked inhibitor of apoptosis	↓ 1.20	↓ 1.18	↓ 1.40
	<i>XIAP</i>	X-linked inhibitor of apoptosis	↓ 1.08	↓ 1.18	↓ 1.03
	<i>XIAP</i>	X-linked inhibitor of apoptosis	↑ 1.04	↑ 1.01	↓ 1.01
	<i>XIAP</i>	X-linked inhibitor of apoptosis	↑ 1.02	↓ 1.07	↓ 1.16
	<i>XIAP</i>	X-linked inhibitor of apoptosis	↓ 1.06	↓ 1.03	↓ 1.03
	<i>BIRC5</i>	Baculoviral IAP repeat-containing 5 (survivin)	↑ 1.19	↑ 1.36	↑ 1.41
	<i>BIRC5</i>	Baculoviral IAP repeat-containing 5 (survivin)	↑ 1.13	↑ 1.22	↑ 1.22
	Anti-apoptosis	<i>BIRC5</i>	Baculoviral IAP repeat-containing 5 (survivin)	↑ 1.09	↑ 1.08
<i>BCL2</i>		B-cell CLL/lymphoma 2	↑ 1.13	↓ 1.02	↓ 1.00
<i>BCL2</i>		B-cell CLL/lymphoma 2	↓ 1.04	↓ 1.38	↓ 1.30
<i>BCL2A1</i>		BCL2-related protein A1	↑ 1.05	↓ 1.01	↓ 1.05
<i>BCL2L1</i>		BCL2-like 1	↑ 1.34	↑ 1.40	↑ 1.21
<i>BCL2</i>		B-cell CLL/lymphoma 2	↑ 1.02	↑ 1.53	↑ 1.15
<i>BCL2</i>		B-cell CLL/lymphoma 2	↓ 1.02	↓ 1.00	↓ 1.06
<i>BCL2L2</i>		BCL2-like 2	↓ 1.26	↓ 1.28	↓ 1.21
<i>BCL2L1</i>	BCL2-like 1	↓ 1.21	↓ 1.25	↓ 1.20	

Categories	Gene Symbol	Gene Title	Fold change		
			SFN	6-MSITC	6-MTITC
	<i>BCL2L1</i>	BCL2-like 1	↓ 1.15	↓ 1.18	↓ 1.28
	<i>BCL2L13</i>	BCL2-like 13 (apoptosis facilitator)	↑ 1.25	↑ 1.48	↑ 1.45
	<i>BCL2L13</i>	BCL2-like 13 (apoptosis facilitator)	↑ 1.13	↑ 1.14	↑ 1.33
	<i>BCL2L13</i>	BCL2-like 13 (apoptosis facilitator)	↓ 1.01	↓ 1.01	↓ 1.03
	<i>BCL2L13</i>	BCL2-like 13 (apoptosis facilitator)	↓ 1.09	↓ 1.12	↑ 1.09
	<i>BCL2L1</i>	BCL2-like 1	↓ 1.20	↑ 1.01	↓ 1.14
	<i>BCL2L2</i>	BCL2-like 2	↓ 1.17	↑ 1.11	↓ 1.05
	<i>MCL1</i>	Myeloid cell leukemia sequence 1 (BCL2-related)	↑ 1.20	↑ 1.23	↑ 1.10
	<i>MCL1</i>	Myeloid cell leukemia sequence 1 (BCL2-related)	↑ 1.09	↑ 1.22	↑ 1.20
	<i>MCL1</i>	Myeloid cell leukemia sequence 1 (BCL2-related)	↑ 1.09	↑ 1.10	↑ 1.22
	<i>MCL1</i>	Myeloid cell leukemia sequence 1 (BCL2-related)	↓ 1.04	↑ 1.01	↑ 1.42
	<i>MCL1</i>	Myeloid cell leukemia sequence 1 (BCL2-related)	↑ 1.04	↑ 1.00	↑ 1.12
Pro-apoptosis	<i>BAX</i>	BCL2-associated X protein	↑ 1.41	↑ 1.23	↑ 1.40
	<i>BAX</i>	BCL2-associated X protein	↑ 1.22	↑ 1.23	↑ 1.30
	<i>BAK1</i>	BCL2-antagonist/killer 1	↓ 1.06	↓ 1.11	↑ 1.08
	<i>BID</i>	BH3 interacting domain death agonist	↑ 1.13	↑ 1.08	↑ 1.14
	<i>BID</i>	BH3 interacting domain death agonist	↑ 1.13	↑ 1.15	↑ 1.10
	<i>BID</i>	BH3 interacting domain death agonist	↑ 1.10	↑ 1.14	↑ 1.17
	<i>BCL2L11</i>	BCL2-like 11 (apoptosis facilitator)	↓ 1.01	↑ 1.07	↑ 1.06
	<i>BCL2L11</i>	BCL2-like 11 (apoptosis facilitator)	↑ 1.21	↓ 1.00	↑ 1.24
	<i>BCL2L11</i>	BCL2-like 11 (apoptosis facilitator)	↓ 1.21	↓ 1.26	↓ 1.21
	<i>BCL2L11</i>	BCL2-like 11 (apoptosis facilitator)	↑ 1.01	↑ 1.10	↑ 1.07
	<i>BCL2L11</i>	BCL2-like 11 (apoptosis facilitator)	↑ 1.25	↑ 1.32	↑ 1.40
	<i>BCL2L11</i>	BCL2-like 11 (apoptosis facilitator)	↓ 1.28	↓ 1.11	↓ 1.00
	<i>BCL2L11</i>	BCL2-like 11 (apoptosis facilitator)	↓ 1.44	↓ 1.11	↓ 1.10
		<i>BAD</i>	BCL2-antagonist of cell death	↓ 1.13	↑ 1.00

Categories	Gene Symbol	Gene Title	Fold change		
			SFN	6-MSITC	6-MTITC
Other proteins	<i>BAD</i>	BCL2-antagonist of cell death	↓ 1.08	↓ 1.03	↓ 1.02
	<i>BAD</i>	BCL2-antagonist of cell death	↑ 1.14	↑ 1.20	↑ 1.21
	<i>BIK</i>	BCL2-interacting killer (apoptosis-inducing)	↑ 1.01	↑ 1.05	↑ 1.02
	<i>HRK</i>	Harakiri, BCL2 interacting protein (contains only BH3 domain)	↓ 1.30	↓ 1.53	↓ 1.42
	<i>HRK</i>	Harakiri, BCL2 interacting protein (contains only BH3 domain)	↓ 1.12	↑ 1.18	↑ 1.05
	<i>PMAIP1</i>	phorbol-12-myristate-13-acetate-induced protein 1	↑ 1.43	↑ 1.64	↑ 1.67
	<i>PMAIP1</i>	phorbol-12-myristate-13-acetate-induced protein 1	↑ 1.49	↑ 1.72	↑ 1.70
	<i>BNIP3</i>	BCL2/adenovirus E1B 19kDa interacting protein 3	↑ 1.34	↑ 1.13	↑ 1.18
	<i>BNIP3</i>	BCL2/adenovirus E1B 19kDa interacting protein 3	↑ 1.27	↑ 1.10	↑ 1.14
	<i>BBC3</i>	BCL2 binding component 3	↑ 1.52	↑ 1.11	↓ 1.23
	<i>APAF1</i>	Apoptotic peptidase activating factor 1	↓ 1.05	↓ 1.07	↓ 1.03
	<i>APAF1</i>	Apoptotic peptidase activating factor 1	↑ 1.12	↑ 1.28	↑ 1.05
	<i>APAF1</i>	Apoptotic peptidase activating factor 1	↑ 1.08	↑ 1.36	↑ 1.01
	<i>HTRA1</i>	HtrA serine peptidase 1	↓ 1.52	↓ 1.44	↓ 1.47
	<i>HTRA2</i>	HtrA serine peptidase 2	↑ 1.04	↑ 1.25	↑ 1.12
	<i>HTRA2</i>	HtrA serine peptidase 2	↑ 1.16	↑ 1.16	↑ 1.09
	<i>AIFM1</i>	Apoptosis-inducing factor, mitochondrion-associated, 1	↓ 1.12	↓ 1.14	↑ 1.00
	<i>ENDOGL1</i>	Endonuclease G	↑ 1.04	↓ 1.00	↓ 1.01
	<i>ENDOGL1</i>	Endonuclease G-like 1	↓ 1.59	↓ 1.55	↓ 1.40
	<i>ENDOGL1</i>	Endonuclease G-like 1	↑ 1.14	↑ 1.07	↓ 1.06
	<i>ENDOGL1</i>	Endonuclease G-like 1	↑ 1.00	↑ 1.03	↑ 1.19
	<i>CYC1</i>	Cytochrome c-1	↓ 1.05	↓ 1.10	↓ 1.11
	<i>CYCS</i>	Cytochrome c, somatic	↓ 1.13	↓ 1.11	↓ 1.04
	<i>CYCS /// CYCSP52</i>	Cytochrome c, somatic /// Cytochrome c, somatic pseudogene 52	↑ 1.12	↓ 1.03	↓ 1.03
	<i>CYCS</i>	Cytochrome c, somatic	↓ 1.59	↓ 1.48	↓ 1.51
	<i>CYCS</i>	Cytochrome c, somatic	↓ 1.17	↓ 1.26	↓ 1.10

**Table 3.7.** List of genes involved in Nrf2-mediated oxidative stress pathway by SFN, 6-MSITC and 6-MTITC in IMR-32 cells

<b>Gene involved</b>	<b>Gene ID</b>	<b>SFN</b>	<b>6-MSITC</b>	<b>6-MTITC</b>
<b>(a) Upstream Regulators</b>				
<i>ACTIN (ACTA1)</i>	NM_001100	1.27	1.05	1.09
<i>ATF4</i>	NM_001675	1.32	1.63	1.57
<i>BACH</i>	NM_001186	1.94	2.08	2.24
<i>c-FOS (FIGF)</i>	NM_004469	-1.66	-2.36	-2.64
<i>c-MAF (MAF)</i>	NM_005360	-1.07	-1.05	1.07
<i>CBP (CREBBP)</i>	NM_004380	1.05	1.21	1.24
<i>ERK1/2 (MAP2K1)</i>	AI571419	1.07	1.18	1.26
<i>FRA1 (FOSL1)</i>	BG251266	1.20	1.39	1.09
<i>JUN</i>	NM_002228	-1.13	-1.11	1.08
<i>MAFF</i>	AL021977	2.21	2.90	2.78
<i>P300 (EP300)</i>	AI459462	-1.20	-1.34	-1.61
<b>(b) Genes coding for antioxidant protein</b>				
<i>CAT</i>	NM_001752	1.04	1.05	1.01
<i>FTH1</i>	AA083483	2.74	3.41	3.48
<i>FTL</i>	BG538564	2.59	2.88	2.86
<i>GPX2</i>	NM_002083	1.08	1.07	1.15
<i>GSR</i>	AI888037	3.63	3.50	3.45
<i>HO1 (HMOX1)</i>	NM_002133	11.50	59.14	54.63
<i>PRDX1</i>	L19184	1.58	1.82	1.74
<i>SOD</i>	NM_000454	1.23	1.43	1.38
<i>SQSTM1</i>	AW293441	3.36	4.66	5.00
<i>TRXD1 (TXNRD1)</i>	NM_003330	4.82	4.82	4.77
<i>TXN</i>	AF065241	1.35	1.32	1.16
<b>(c) Metabolizing enzymes</b>				
<i>AFAR (AKR7A2)</i>	NM_003689	-1.18	-1.26	-1.24
<i>AKR1C1</i>	S68290	10.60	11.02	12.02
<i>AKR1C2</i>	M33376	11.00	11.96	12.23
<i>AKR1C3</i>	AB018580	103.64	103.85	109.70
<i>AOX1</i>	NM_001159	1.09	1.01	1.03
<i>CBR1</i>	BC002511	-1.09	-1.04	-1.12
<i>CYP1A</i>	NM_000499	-1.24	-1.22	-1.07
<i>CYP2A (CYP2A13)</i>	NM_000766	-1.16	-1.03	-1.24
<i>CYP2C (CYP2C18)</i>	NM_000772	-1.06	1.05	1.07
<i>CYP3A (CYP3A4)</i>	NM_017460	1.10	1.10	1.20
<i>CYP4A (CYP4A11)</i>	NM_000778	-1.26	-1.39	-1.10
<i>EPHX1</i>	NM_000120	1.51	1.89	1.67
<i>FMO1</i>	NM_002021	-1.16	1.07	-1.00
<i>GCLC</i>	NM_001498	1.62	1.48	1.54
<i>GCLM</i>	NM_002061	8.44	11.88	5.39
<i>GST (GSTA1)</i>	NM_000846	-1.11	-1.11	-1.05
<i>NQO1</i>	NM_000903	27.37	27.67	28.41

<b>Gene involved</b>	<b>Gene ID</b>	<b>SFN</b>	<b>6-MSITC</b>	<b>6-MTITC</b>
<i>UGT</i>	NM_001072	1.30	1.00	1.11
<i>MRP1 (ABCC1)</i>	NM_004996	-1.01	1.04	1.03
<i>SR-BI (SCARB1)</i>	NM_005505	-1.06	-1.03	-1.02
(d) Genes coding for chaperones and stress response				
<i>HSP22 (HSPB8)</i>	AF133207	-1.39	-1.07	-1.09
<i>CCT7</i>	NM_006429	1.05	1.09	1.11
<i>CLPP</i>	NM_006012	-1.04	1.00	-1.03
<i>ERP29</i>	NM_006817	-1.01	1.10	1.09
<i>FKBP5</i>	NM_004117	1.10	-1.32	-1.16
<i>HERPUD1</i>	AF217990	1.21	1.28	1.31
<i>HSP40 (DNAJB4)</i>	NM_007034	4.30	5.34	5.39
<i>HSP90 (HSP90B1)</i>	AK025862	1.59	1.48	1.59
<i>PPIB</i>	NM_000942	1.20	1.26	1.33
<i>PTPLAD1</i>	NM_016395	-1.01	1.07	1.05
(e) Ubiquitination				
<i>HIP2 (UBE2K)</i>	NM_005339	1.17	1.23	1.33
<i>PSM (PSMA1)</i>	NM_002786	1.04	1.11	1.07
<i>UB2R1 (UBE2R2)</i>	BE221883	1.05	1.11	1.06
<i>UBB (UBA52)</i>	AF348700	-1.09	-1.06	-1.06
<i>USP14</i>	NM_005151	1.12	1.18	1.14
<i>VCP</i>	AF100752	1.29	1.51	1.41



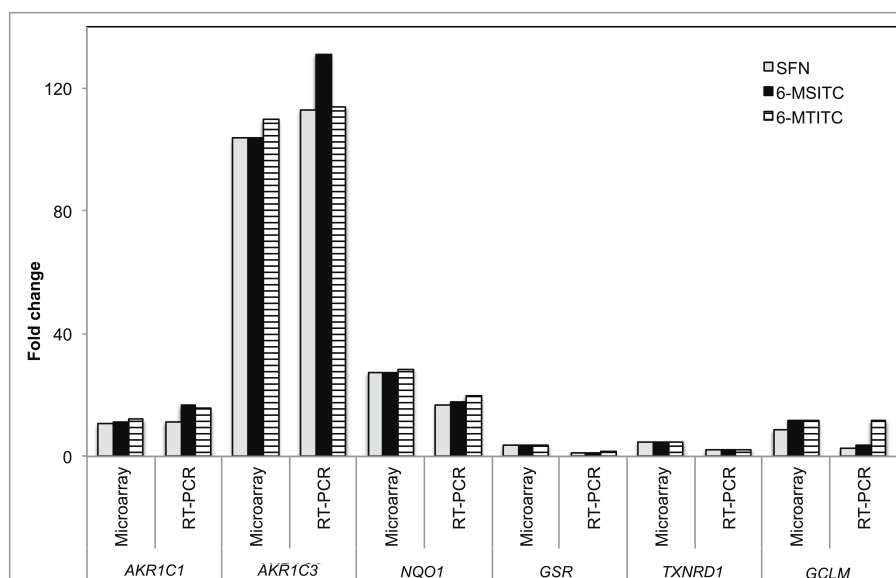


**Figure 3.4.** Validation of differentially expressed genes in Wasabi-derived ITC-treated IMR-32 cells from DNA microarray analysis by real-time PCR. DNA microarray analyses results were compared to real-time PCR results for selected genes. Real-time PCR was performed using dynamo™ SyBR® Green 2-Step qRt-PCR Kit as described in the “**Section 3.3.6**”. Fold changes represented the ratio between the treated samples values to that of the untreated samples. expression changes are depicted as fold change (y-axis). Gene symbols are shown below.

To confirm the results of microarray analyses, the expression levels of six selected genes were further detected by real-time PCR (Figure 3.4). Most of these genes exhibited a similar expression pattern between the microarray and real-time PCR data. For instance, 6-MSITC induced gene expression of *AKR1C1* by 16 folds in the real-time PCR experiment, whereas 11 folds in microarray analysis. The 6-MSITC-induced *AKR1C3* gene expression was 131 folds in real-time PCR while 104 folds in microarray analysis. The effect of 6-MSITC on *NQO1* induction level was found higher in microarray analysis (27 folds) than in real-time PCR (18 folds).

### **3.4.5. Influence of 6-MSITC on Nrf2-mediated protein levels**

To verify the involvement of ITCs in Nrf2-mediated oxidative stress response pathway, 6-MSITC which has the highest bioactive ITC among the three treatments were chosen to investigate the levels of Nrf2-mediated proteins by Western blotting. Dose (Figure 3.5A) and time (Figure 3.5B) experiments showed that treatment with 10  $\mu$ M of 6-MSITC for 12 hours could effectively induce the production of Nrf2 and Nrf2-mediated proteins including NQO1, TXNRD1, AKR1C1, and AKR1C3, but no significant effect on the expression of Keap1. The products of housekeeping gene, GAPDH, was unaltered during such treatment. Moreover, the present results were found to be in agreement with the previous study of 6-MSITC using human hepatoblastoma HepG2 cells (Hou *et al*, 2011). These data suggest that 6-MSITC induced the expressions of antioxidant enzymes through the activation of Nrf2/Keap1 system.

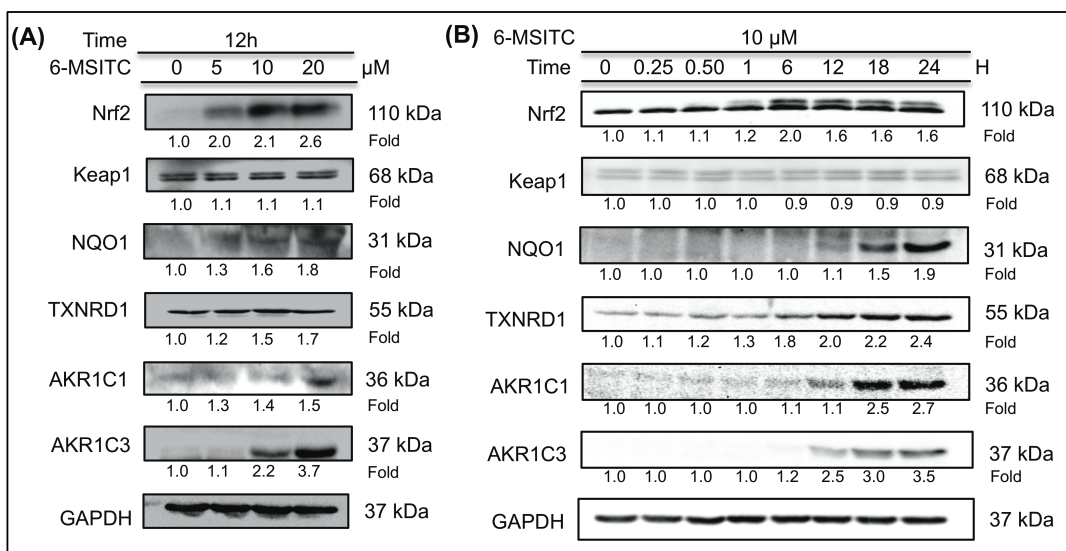


**Figure 3.5.** Effect of 6-MSITC on Nrf2 level and Nrf2-mediated induction of typical proteins. **(A)** IMR-32 cells were treated with 0-20  $\mu$ M of 6-MSITC for 12 hours. **(B)** IMR-32 cells were treated with 10  $\mu$ M of 6-MSITC for 0-24 hours. Nrf2, Keap1, NQO1, TXNRd1, AKR1C1, AKR1C3, and GAPDH were detected using Western blot analysis with their respective antibodies. The induction fold of the protein was calculated as the intensity of the treatment relative to that of control normalized to GAPDH by densitometry. the blots shown are the examples of three separate experiments.

### 3.4.6. Influence of 6-MSITC on Nrf2 protein at transcription and post transcription

The increase in the level of Nrf2 protein by 6-MSITC is possible due to transcriptional and posttranscriptional regulation. Thus, the microarray data was first examined. Cells treated with 10  $\mu$ M of SFN, 6-MSITC, or 6-MTITC for 9 hours upregulated only 1.06-, 1.03-, and 1.07-fold of *Nrf2*, respectively, compared to that without treatment, indicating that ITCs did not regulate the expression *Nrf2* gene in such treatment. Next, the influence of these ITCs on the stability of Nrf2 protein was investigated by adding cycloheximide (CHX), a protein synthesis inhibitor. IMR-32

cells were pretreated with 6-MSITC (10  $\mu$ M) for 3 hours and then treated with CHX (5  $\mu$ g/mL) for 15–60 minutes. As shown in Figure 3.6, the level of Nrf2 protein was decreased to 58% 60 minutes later after stopping the protein synthesis with CHX. On the other hand, pretreatment with 6-MSITC extended Nrf2 stability, showing no degradation even after 60 minutes. The results indicated that 6-MSITC might increase Nrf2 protein level by inhibiting the turnover of Nrf2 protein, rather than by stimulating *Nrf2* gene expression at transcriptional level.

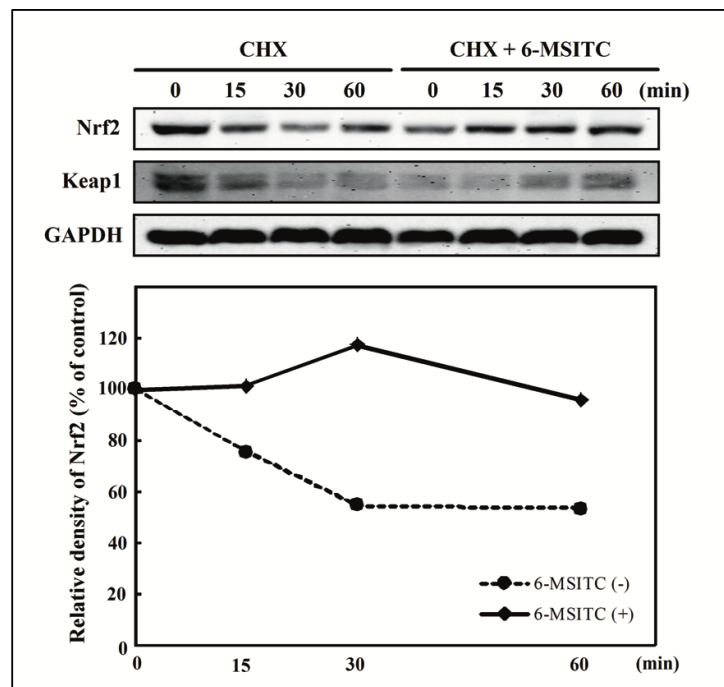


**Figure 3.6.** Effect of 6-MSITC on the stability of Nrf2. IMR-32 cells were pretreated with or without 10  $\mu$ M of 6-MSITC for 3 hours, followed by exposure with 5 mg/ml of CHX for 0–1 hours. Nrf2, Keap1 and GAPDH were detected by Western blot analysis with their respective antibodies. Histograms show the densitometric analysis of Nrf2 compared with the control.

### 3.5. Discussions

ITCs have been reported to exhibit protective effects against oxidative stress in astrocytes, dopaminergic cell death, and traumatic brain injury by inducing the transcriptional factor Nrf2 that activates endogenous defenses of the cell via a battery of cytoprotective genes (Danilov *et al*, 2009; Han *et al*, 2007; Dash *et al*, 2009). Thus, this implies that ITCs may possess neuroprotection, although the exact molecular mechanisms are not fully clarified. In the present study, the gene expression profiles of IMR-32 neuron cells treated by three ITCs (SFN, 6-MSITC, and 6-MTITC) was investigated for the first time to study the neuroprotective mechanisms on a genome-wide level using microarray technology. IMR-32 cell line is an ideal cell model for molecular study of distinct patterns of antioxidant-related pathway because it contains functional ARE capable of inducing endogenous cytoprotective genes (Moehlenkamp & Johnson, 1999). SFN is a major component of broccoli (Zhang *et al*, 1992). 6-MSITC and 6-MTITC are SFN analogs found to be the major bioactive compounds of Japanese Wasabi (Kumagai *et al*, 1994). DNA microarray analysis data revealed that SFN, 6-MSITC, and 6-MTITC could significantly affect the gene expressions of IMR-32 neuron cells. With over 54,000 gene probes on the array, 6-MSITC treatment at 10  $\mu$ M for 9 hours regulated the expression of a total of 263 genes by greater than or equal to 2 folds (Table 3.2). Of the total number of genes regulated by 6-MSITC, 100 are upregulated and 163 are downregulated. The number of genes regulated by 6-MSITC is twice higher than that regulated by the treatment with SFN, suggesting that 6-MSITC elicited a stronger stimulation on gene expression than SFN in the IMR-32 cells. On the other hand, the number of genes regulated by 6-MTITC is close to the number of genes regulated by 6-MSITC, indicating that removal of oxygen atom on the sulfinyl sulfur of the methyl group has no significant

influence on gene regulation among the two SFN analogues derived from Wasabi. Both 6-MSITC and 6-MTITC have the same number of carbon atoms, but differ on the sulfur substituent attached to the methyl group. 6-MSITC is a methylthioalkyl ITC containing S=O substituent in the methyl group, whereas, 6-MTITC is a methylsulfinylalkyl ITC without oxygen atom attached to the sulfur atom of the methyl group (Ina *et al*, 1989; Etoh *et al*, 1990). On the other hand, SFN is two carbon atoms less than 6-MSITC and 6-MTITC. It looks that the capacity of Wasabi-derived ITCs to regulate gene expression depends on the alkyl chain length between the ITC group and the methyl sulfinyl. However, it will be interesting to investigate the effect of longer alkyl chain or aromatic ITCs on the gene expression profile of IMR-32 cells. Furthermore, it will also be valuable to explore the influence of Wasabi-derived ITCs on gene regulation of other types of brain cells by DNA microarray.

It is noticed that most of the genes targeted by SFN, 6-MSITC, and 6-MTITC belonged to oxidative stress response cluster. A total of 14, 17, and 18 differentially expressed genes by SFN, 6-MSITC, and 6-MTITC, respectively, were associated with oxidative stress response. The upregulation of phase 2 metabolizing enzymes such as AKR1C3 and GCLM and antioxidant proteins such as GSR, HO-1, and TXNRD1 by SFN has been reported to protect the cells against oxidative stress, and Wasabi-derived ITCs were also found to upregulate their expressions (Ye *et al*, 2013). In addition, 6-MSITC and 6-MTITC also upregulated the expressions of other oxidative stress-related genes, such as *AKR1C1*, *AKR1C2*, *NQO1*, *FTH1*, *FTL*, and *SQSTM1*. These genes are well documented to be involved in detoxification and antioxidant defense, neuronal proliferation and differentiation, and signal transduction (Li *et al*, 2002). Thus, this suggests that SFN, 6-MSITC, and 6-MTITC might also exert neuroprotective activity via pathways governing the regulation of antioxidant

defense genes. In order to confirm the regulation of these genes in the signal network level, signal pathway analyses by IPA software were performed. Nrf2-mediated oxidative stress response pathway came up to be the most significant pathway modulated by SFN, 6-MSITC, and 6-MTITC. Moreover, detailed evaluation showed that 6-MSITC enhanced higher number of genes associated with Nrf2-mediated stress response pathway than SFN and 6-MTITC, suggesting that 6-MSITC is a stronger inducer of Nrf2-mediated oxidative stress response pathway than SFN and 6-MTITC (Figure 3.3, Table 3.5). 6-MSITC stimulation in animal study exhibited a stronger HO-1 protein expression than the SFN treatment (Mizuno *et al*, 2011). Recent cancer cell model study demonstrated that lengthening the carbon chain between the sulfinyl sulfur and the ITC group from 4 to 6 carbon atoms has a beneficial effect on Nrf2 activation, whereas the increasing steric size of the substituent on the sulfur atom contributes a negative effect on the biological activity (Elhalem *et al*, 2014). On the other hand, SFN was observed to not affect the gene regulation of other upstream transcription factors similar to what 6-MSITC and 6-MTITC did. The TR/RXR activation pathway was also noted to rank the second significantly regulated pathway for ITC-induced gene expression, and the expressions of *AKR1C1*, *AKR1C2*, and *AKR1C3* linked to this pathway were highly upregulated by the SFN, 6-MSITC, and 6-MTITC. However, an understanding of how these ITC interactions with TR/RXR activation is linked to neuroprotection will require further study. Other significantly regulated pathways include metabolism of xenobiotics by cytochrome P450, GSH metabolism, and C21-steroid hormone metabolism. These denote that Wasabi-derived ITCs also act as xenobiotics, causing induction of metabolizing enzymes and intracellular GSH.

Finally, the products of these genes were confirmed at the protein level using

6-MSITC, a representative of these Wasabi-derived ITCs. 6-MSITC treatment induced a higher level of Nrf2 protein, but no significant effect on Keap1 protein (Figure 3.5A & Figure 3.5B). These data are in agreement with the results in primary cortical neurons, in which SFN enhanced Nrf2 protein level in a time-dependent manner, but no effect on Keap1 protein (Vauzour *et al*, 2010). On the other hand, Wasabi-derived ITCs could covalently modify Keap1, preventing Nrf2 ubiquitination and promoting Nrf2 stability to mediate the ARE-driven activation in human hepatoblastoma cells, HepG2 (Korenori *et al*, 2013; Hou *et al*, 2011). These data suggest that Wasabi-derived ITCs may have different actions on Keap1 protein in different cell types. As indicated in Figure 3.5A & Figure 3.5B, the activation of Nrf2 followed increase in the levels of NQO1, TXNRD1, AKR1C1, and AKR1C3 protein expressions. These data further demonstrated that Wasabi-derived ITCs exert the neuroprotective effects in IMR-32 cells via activating Nrf2-mediated oxidative stress response pathway until the protein level. Furthermore, *in vivo* experiment showed that ITC could penetrate the blood brain barrier and deliver its neuroprotective function in the central nervous system (Tarozzi *et al*, 2013). In addition, ITCs such as 6-phenethyl isothiocyanate and SFN are also rapidly accumulated in various types of cell lines with intracellular concentration within millimolar level (Zhang, 2001). In rats and humans, pharmacokinetic data revealed that SFN can be absorbed in the body and reach micromolar concentration in the blood. Specifically in rats, detectable amount of SFN was evident after an hour and peaked at ~20  $\mu\text{M}$  after four hours, following 50  $\mu\text{M}$  gavages of SFN (Hu *et al*, 2004). On the other hand, single doses of 200  $\mu\text{M}$  broccoli sprouts ITC preparation given to human subjects showed that ITC plasma concentrations peaked between 0.943 and 2.27  $\mu\text{M/L}$  one hour after intake (Ye *et al*, 2002). Thus, the dose of 10  $\mu\text{M}$  ITCs used in this study maybe achievable *in*



*vivo*.

In summary, the DNA microarray data revealed for the first time the gene expression profiles of Wasabi-derived ITCs in a neuronal cell model, IMR-32. 6-MSITC had the strongest regulation on gene expression among the three ITCs, showing a positive relationship in a carbon chain length of ITCs. Specifically, 6-MSITC could stimulate Nrf2-mediated gene expressions through the stabilization of Nrf2 protein at post-transcription. Taken together, the present data and previous findings, 6-MSITC can exert the neuroprotective effect by activating the Nrf2-mediated oxidative stress response pathway (Figure 3.7).

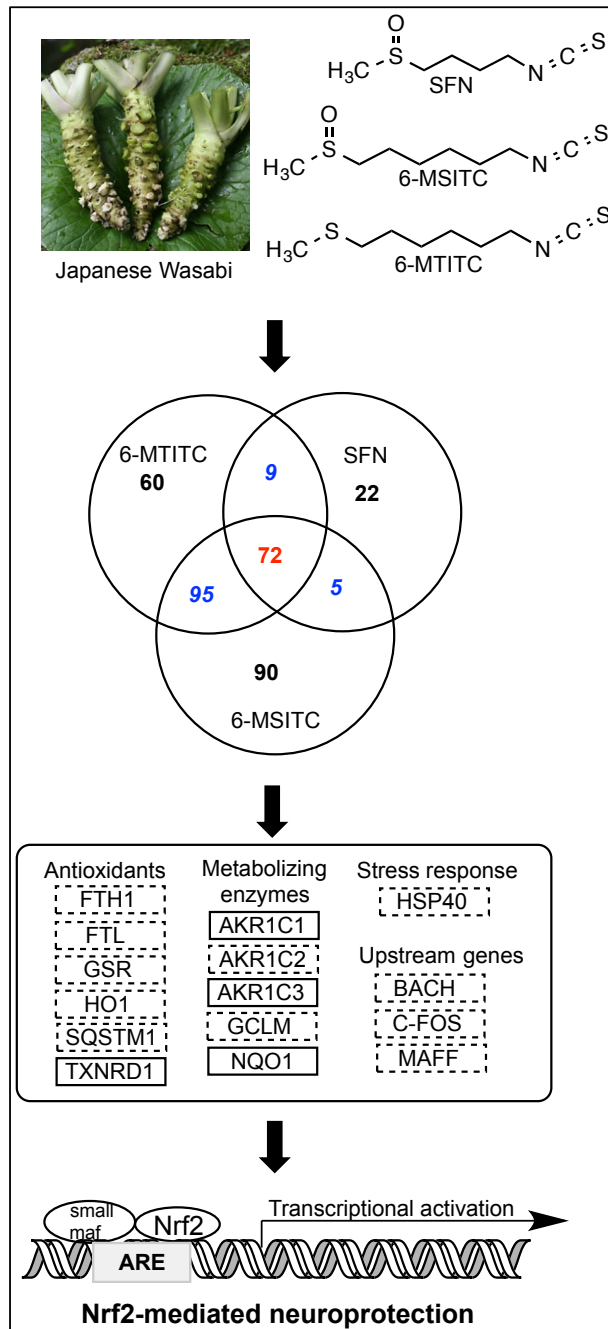


**Figure 3.7.** Proposed mechanisms for the neuroprotective effects by Wasabi-derived 6-MSITC in IMR-32 cells. Wasabi-derived ITCs activate Nrf2-mediated oxidative stress pathway and subsequently induce the expression of antioxidant proteins/enzymes to exert the neuroprotective effects. The mRNA and protein of marker in solid box were confirmed by RT-PCR and Western blotting.

## CHAPTER IV

### Discussion and Conclusions

#### 4.1. Discussions

Microarray-based gene transcription profiling was performed in the present study to contrast the genome wide-gene expression changes associated with Wasabi SFN, 6-MSITC and 6-MTITC stimulation in HepG2 cells with that of IMR-32 cells. Thereafter, biologically important information from the vast amount of microarray data were extracted using GO and IPA software to detect significantly regulated genes, identify global patterns of gene expression and determine biological meaning of both individual genes and group of genes between different ITC treatments and cell types. Finally, biologically meaningful genes were confirmed by real-time PCR and post transcription analyses were performed using Western blot to study the molecular mechanism accompanying the protective effects of Wasabi ITCs in various cell types. Combining all the obtained data from different steps have provided information how isothiocyanates targets specific cell tissue.

##### ***4.1.1. Effect of Wasabi-derived isothiocyanates on gene expression profile changes in HepG2 and IMR-32 cells***

SFN have been widely reported to exhibit different protective effects such as anti-proliferative, neuroprotective, anti-inflammatory and anti-cancer activities (Chaudhuri *et al*, 2007; Tarrozi *et al*, 2013; Sun *et al*, 2015; Chung *et al*, 2015). However, microarray-based method of determining Wasabi-derived ITCs biological effects is rare. This is the

first study to simultaneously analyze the protective effect of SFN and its analogues in hepatic and neuronal cell models using microarray-based transcriptional profiling.

In Chapters II and III, gene expression profiling revealed the genome-wide gene expression patterns in HepG2 and IMR-32 treated by 10  $\mu$ M of ITCs for 9 hours. In Chapter II, 6-MTITC was highlighted as the strongest inducer of gene expression changes based on the total number of differentially altered gene expressions, followed by 6-MSITC and SFN, respectively (Table 2.2). Further assessment of the significantly up- and downregulated genes demonstrated that ITCs caused upregulation of most genes in HepG2 cells over downregulation. Whereas, Chapter III showed that 6-MSITC had greater influence than 6-MTITC and SFN in the gene expression regulation of IMR-32 cells (Table 3.2). Comparison of the direction of regulation showed that Wasabi-derived ITCs, 6-MSITC and 6-MTITC, had stronger effect towards the downregulation of IMR-32 genes. Data showed that the longer the carbon chain backbone linking the ITC group and the methyl sulfinyl group, the more potent the Wasabi-derived ITCs as an inducer of gene expression changes in both cell lines. Both 6-MSITC and 6-MTITC have six methylene groups linking the methyl sulfur and isothiocyanate group as compared with SFN that has only four methylene groups between the methyl sulfur and isothiocyanate group (Figure 4.1). However, no direct correlation can be derived when it comes to the effect of sulfur substituent attached to methyl group of Wasabi-derived ITCs. Sulfide-containing ITC, 6-MTITC, was more potent than 6-MSITC in HepG2 cells whereas sulfoxide-containing ITC, 6-MSITC, was stronger in IMR-32 cells. This observation seemed to be inconsistent with the published studies that change of the oxidation state of the sulfur atom attached to the methyl group from sulfide to sulfoxide enhanced the potency of alkyl ITCs (Zhang *et al*,

1992; Vasanthi *et al*, 2009). Yet, it should be noted that the reported studies evaluated structure-bioactivity relationship of different kinds of ITC and not the genome-wide expression effect. This is vital since this is the first report to demonstrate global gene expression of changes induced by SFN and SFN analogues and this inconsistency could be possibly attributed to the cell variation effect. Also, Venn diagrams (Figures 2.1 and 3.7) demonstrated that the common genes shared by the three ITCs in HepG2 and IMR-32 cells were comparable to that shared by SFN analogues, suggesting that SFN analogues may possess similar strength as stimulator of gene expression alteration in HepG2 and IMR-32 cell models compared with SFN.

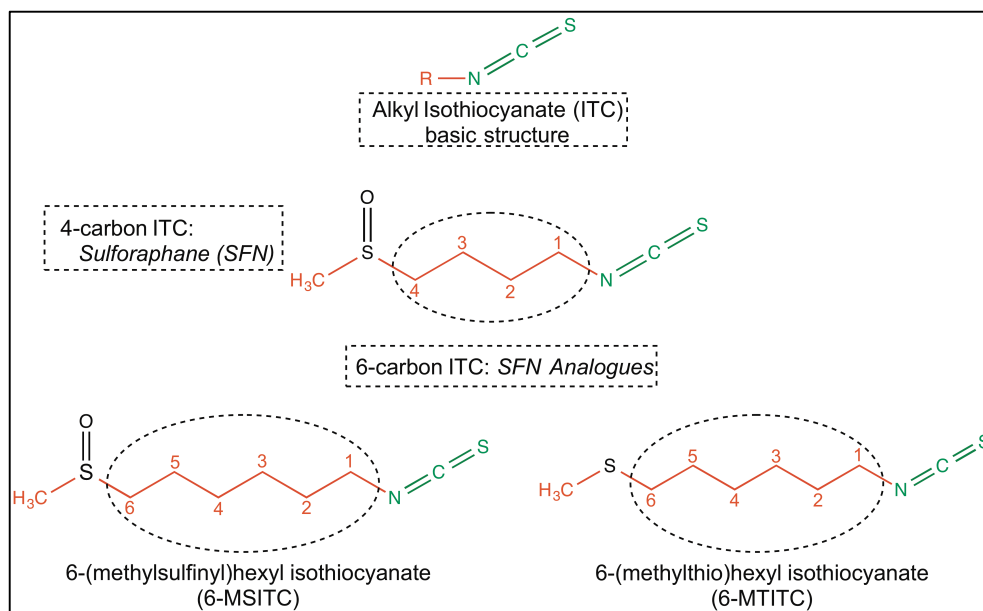


**Figure 4.1.** Structure-gene expression profile relationship of SFN and SFN analogues. The methylene groups bridging the methyl sulfur group and isothiocyanate group showed to be the essential component in the potency of ITCs as regulator of gene expression changes in HepG2 and IMR-32 cell culture models. However, not much difference is observed in the potency of sulfur and sulfoxide groups.

The data obtained is the first report that SFN and its analogues from Wasabi have dissimilar degree of potency towards regulating global genome-wide gene expression changes. The structure-gene expression profile relationship study demonstrated that Wasabi-derived ITCs were the most potent inducer of transcriptional changes at a genome-wide level irrespective of the kind of cell culture model being used. From these observations, the following could be inferred: (a) ITC compounds with six methylene groups bridging the methyl sulfur and isothiocyanate functional group are more potent than those containing only three methylene groups; (b) no significant correlation on potency of ITC compounds with varying sulfur oxidation state at the methyl sulfinyl group provided the number of methylene groups connecting the methyl sulfur group and isothiocyanate group remain constant; and (c) sulfide is more potent in hepatic cell model than sulfoxide while sulfoxide is more potent in neuron cell model than sulfur, which seemed to be a cell-type dependent response.

#### ***4.1.2. Influence of cell type variations on gene expression profiles following isothiocyanates treatment***

Previous discussion indicated that SFN analogues, 6-MSITC and 6-MTITC, were more potent inducers of altered gene expressions in HepG2 and IMR-32 cell models than SFN. However, some discrepancies were observed in the gene expression profiles of SFN analogues between the two cell culture models. Thus, this subsection will focus on the effects of cell type variation on gene expression profile changes in response to ITCs stimulation. The need to investigate the functional capacities and responses of each cell

types is important to ascertain the effect of dietary intake components or bioactive agents such as ITCs in the pathology or treatment of certain diseases.

As a whole, IMR-32 ITC-treated cells had higher total number of differentially altered genes than HepG2 ITC-treated cells (Figure 4.2). In 6-MSITC treatment, the IMR-32 cells gene expression profile was 83 % greater than HepG2 cells in terms of the total number of differentially altered genes. A similar relationship is also observed between HepG2 cells and IMR-32 cells treated with 6-MTITC wherein IMR32-treated cells was 23 % higher than HepG2 cells. Surprisingly, HepG2 and IMR-32 produced no significant variation (1% difference) in response to SFN treatment. Assessment of the up- and downregulated genes showed that the two cell lines responses to Wasabi-derived ITCs have opposing direction of regulation wherein most genes were upregulated in HepG2 and downregulated in HepG2 cells. However, SFN was found to trigger upregulation of most genes regardless of what cell type used. These observations suggest that cell type influenced the number of genes turned on or shut off in response to ITCs. Different kinds of cells have different specialized roles to perform (Mazzarello, 1999) but the knowledge of cellular diversity still remains incomplete and have been subjected to continuous debate. HepG2 is a hepatoblastoma-derived cell line commonly used for various field of investigation such as liver metabolism and development, chemocarcinogenesis, mutagenesis and hepatotoxicity. HepG2 genetic profile revealed losses of the chromosome 4q3 region and other typical hepatoblastoma chromosomal abnormalities, which includes trisomies 2 and 20 (Lopez-Terrada *et al*, 2009). In contrast, IMR-32 is of human origin and mimics large projection of neurons of the cerebral cortex. It has been

generally used in studies related to the stability of the amyloid precursor protein (Lahiri, 1993).

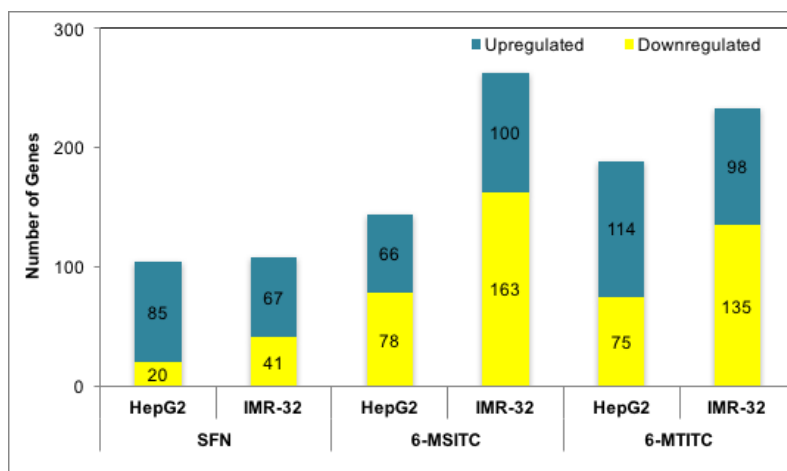


**Figure 4.2.** Comparative total number of genes regulated by ITCs in HepG2 and IMR-32 cells lines using Affymetrix HG UG133 plus 2.0 oligonucleotide arrays containing 54,000 probe sets. Between different ITC compounds, Wasabi-derived ITC stimulation exhibited the highest number of altered gene expressions. Between different types of cell model, IMR-32 cell model showed the highest number of regulated genes in response to ITC treatments.

Furthermore, gene expressions pattern analysis revealed that the differentially expressed genes common between HepG2 and IMR-32 cells in response to ITCs stimulation were mostly belonging to the group of antioxidant-related genes (Figure 4.3A-C). However, SFN analogues were observed to contribute to a higher number of common genes between HepG2 and IMR-32 cells. Observed data supported previous findings that the presence of oxygen on sulfur enhances the antioxidant inducing potency of ITCs (Zhang *et al*, 1992). Evidence indicated that ITCs with six methylene groups in the bridge linking the methyl sulfinyl group and isothiocyanate group were more potent regulator of



antioxidant gene expression changes than those with 4 methylene groups. Also, the sulfoxide enhanced antioxidant genes more than sulfide. Fold changes of the selected antioxidant-related genes obtained via microarray analyses demonstrated substantial agreement with the fold change values determined via real-time PCR, thereby confirming the microarray data (Figures 2.3 and 3.4). Surprisingly, gene expression patterns showed that the number of differentially altered genes common between HepG2 and IMR-32 cells in response to 6-MSITC and 6-MTITC treatments were almost alike. This observation supported the previous findings that there was no significant effect on the biological activity of sulfoxide and sulfur attached to the methyl group when the number of methylene groups bridging the methyl sulfur and isothiocyanate group are equal. However, expression levels of antioxidant genes between two cell lines varied significantly. Furthermore, this seemed to indicate that 6-MSITC and 6-MTITC shared common gene targets. Not surprisingly, HepG2 and IMR-32 cell lines had not much difference in the number of uniquely altered genes in response to SFN treatment (Figure 4.3A). Evidences have shown that SFN is capable of inducing antioxidant-related genes in both cell lines (Li *et al*, 2002; Gan *et al*, 2010). Interestingly, in response to 6-MSITC treatment, a higher number of unique altered genes were observed in IMR-32 than HepG2 cells (Figure 4.3B). A similar trend of cellular response was also observed for treatment of 6-MTITC (Figure 4.3C). These gene associations were identical with the categories of genes found in 6-MSITC treatment.

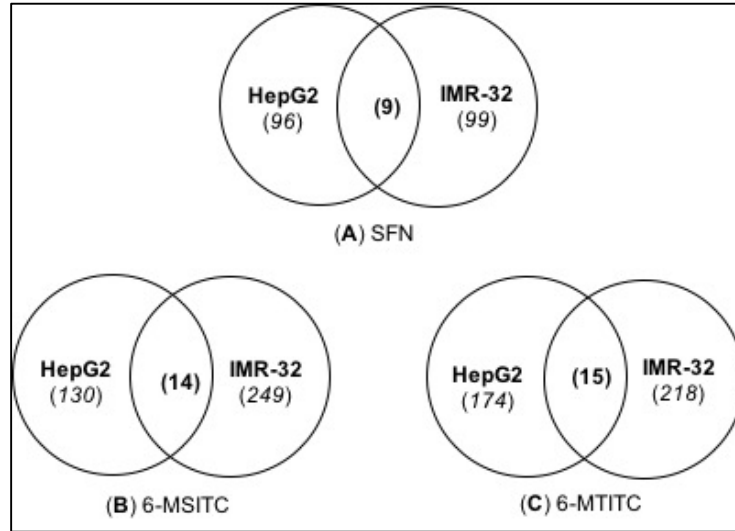


**Figure 4.3.** Comparative Venn diagram representation of HepG2 and IMR-32 cells gene expression profile from microarray data in response to Wasabi-derived ITCs, **(A)** SFN, **(B)** 6-MSITC and **(C)** 6-MTITC stimulations. Common genes between two cell lines is represented by overlapping circles. Unique genes between two cell lines is displayed in non-overlapping part of the circle.

GO enrichment analysis revealed a number of overexpressed biological processes in HepG2 and IMR-32 cells. Specifically, they corresponded to cell proliferation and inflammatory response were distinct to HepG2 in response to ITCs stimulation, while CNS specific function was unique to IMR-32 cells (Table 4.1). *ADAMTS1*, *ADM*, *CCL14*///*CCL15*, *DAB2*, *FOSL1*, *HMOX1*, *IHH*, *IL11*, *JAG1*, *KITLG*, *KLF4*, *PROX1*, and *TRIB1* were overexpressed genes related to cell proliferation in HepG2. Meanwhile, the overexpressed genes linked with inflammatory response were *CCL20*, *CYP4F11*, *FOS*, *LY96*, *SCYE1*, *TLR6*, and *TNFRSF1A*. Some of the overexpressed CNS-specific function-related genes in IMR-32 cells were also expressed in HepG2 cells but *CCDC50*, *NGEF*, *PDGFC*, and *PRCD* genes were specific to IMR-32 cells. With that observation, it

can be said that genes and processes related to carcinogenesis or tumorigenesis were intrinsically active in HepG2 cell line while genes and processes associated to neuro response function were inherently functional in IMR-32 cell line (Lopez-Terrada *et al*, 2009; Lahiri, 1993). The extent of activation of the cell proliferation and inflammatory response-associated genes by ITCs in HepG2 cells makes them an ideal cell type for identification of other signal transduction cascade involved in cell proliferation and inflammation by ITCs. Additionally, the ability of IMR-32 cells to actively express genes related to CNS specific function marks this cell line to be suitable for neuroprotective mechanism studies by ITCs.

**Table 4.1.** Comparative classification of genes annotated for biological processes targeted by Wasabi-derived ITCs in HepG2 and IMR-32 cell lines.

Category	HepG2			IMR-32		
	SFN	6-MSITC	6-MTITC	SFN	6-MSITC	6-MTITC
Adhesion	3	7	9	1	4	4
Apoptosis	7	14	17	2	7	5
Autophagy	0	0	0	1	1	1
Binding	0	1	1	5	26	15
Biogenesis	2	4	3	0	1	0
Catabolic process	6	11	12	2	3	3
Catalytic activity	0	0	0	0	2	1
Cell cycle	2	2	6	0	2	1
Cell growth	1	2	2	1	1	1
Cell proliferation	5	10	12	0	1	2
CNS specific function	0	0	0	3	10	5
DNA repair	1	1	1	1	1	1

Category	HepG2			IMR-32		
	SFN	6-MSITC	6-MTITC	SFN	6-MSITC	6-MTITC
Inflammatory response	4	6	5	0	1	0
Metabolic process	12	21	23	9	22	17
Oxidoreductase activity	4	5	7	10	15	16
Response to stimuli	7	7	8	0	2	2
Signal transduction	12	33	29	10	22	21
Stress response	6	8	14	5	7	8
Transcription	13	26	36	16	41	36
Transferase activity	5	12	16	5	10	9
Translation	2	4	7	2	2	4
Transport	16	33	30	9	20	19

This result is the first to show that though ITC treatments on different types of cell lines can result to dissimilar gene expression profiles, they can still share similar target genes. The obtained data confirmed the following: (a) IMR-32 cell line is more sensitive to Wasabi-derived ITCs treatment than HepG2 cell line as indicated by the higher number responsive genes; (b) biological processes that were associated with antioxidant-related functions were the most common gene annotation for the differentially expressed genes of HepG2 and IMR-32 in response to ITC treatments; (c) Genes associated with cell proliferation were cell-specific genes to HepG2 cells in response to ITCs treatment while CNS specific function genes were specific to IMR-32 cells; (d) application of microarray technology is a rapid and versatile method to identify the unique genes in a given type of

cell culture model; and (e) microarray-based transcription profiling is capable of screening gene activity in biological systems.

#### ***4.1.3. Pathway network and global functional analyses by ITCs stimulation in HepG2 and IMR-32 cell lines***

Previous sections explored and uncovered the influence of varied cell type to gene expression profile changes in response to SFN, 6-MSITC and 6-MTITC treatments. Cell variation was identified as one factor that could lead to dissimilar number activated or deactivated genes. However, to fully extract the essence of this huge genomic data from microarray analysis, the significantly modulated genes are needed to be subjected to pathway and global functional analyses. By using IPA, the function of cell-specific genes targeted by Japanese wasabi-derived ITCs in HepG2 and IMR-32 cell lines would be understood.

##### ***4.1.3.1. Isothiocyanates effect***

As highlighted in Chapters 2 and 3, ITCs treatment highly affected the expressions of a number of antioxidant-related genes. IPA canonical pathway analyses confirmed the key regulators of these antioxidant gene expressions and the canonical antioxidant pathways targeted by these ITCs in HepG2 and IMR-32 cell lines. Nrf2-mediated oxidative stress response pathway turned out to be the main pathway targeted by SFN, 6-MSITC and 6-MTITC (Figures 2.2 and 3.3). Other antioxidant-associated pathways such as glutamate metabolism, glutathione metabolism, and metabolism of xenobiotics by cytochrome P450-related pathways were also significantly perturbed pathways by the

three ITCs (Figures 2.2 and 3.3). These results showed that SFN, 6-MSITC and 6-MTITC indirectly targeted multiple antioxidant pathways by directly targeting Nrf-2 pathway which is the master regulator of antioxidant response (Figure 4.4). Nrf2 is a transcription factor that crucially regulates gene expressions having antioxidant functions within the cell (Sporn and Liby, 2012). Nrf2 drives the expression of the glutamate-cysteine ligase modifier subunit (GCLM) and glutamate-cysteine ligase catalytic (GCLC) subunit that leads to the formation of glutamate-cysteine ligase (GCL) complex. GCL catalyzes the reaction of glutamate with cysteine, which is the rate-limiting step in the synthesis glutathione (GSH), the most abundant antioxidant cofactor within the cell (Lu, 2009). Nrf2 controls the amount of cysteine within the cell that is necessary for GSH production (Taguchi *et al*, 2011; Meister, 1983). Nrf2 also supports utilization of GSH by controlling the expression of detoxification enzymes (McGrath-Morrow *et al*, 2009; Thimmulappa *et al*, 2002). Aside from its direct involvement in reactive oxygen species (ROS) detoxification through GSH metabolism, Nrf2 indirectly modulates the amount of ROS by controlling free  $Fe^{2+}$  homeostasis. Majority of the free  $Fe^{2+}$  comes from the breakdown of heme molecule by HO-1 and Nrf2 stabilizes this by upregulating HO-1 transcription (Gozzelino *et al*, 2010; Alam *et al*, 1999). As a result of HO-1 upregulation, Nrf2 enhances the transcription of genes encoding FTL and FTH which are constituents of the ferritin complex (Chorley *et al*, 2012). Then ferritin complex converts  $Fe^{2+}$  to  $Fe^{3+}$  and stores it within the complex so that it cannot be used for Fenton reaction (Orino *et al*, 2001). Therefore, Nrf2 diminishes the production of damaging  $\bullet OH$  radicals by stimulating the release of  $Fe^{2+}$  from heme molecules followed by its sequestration.

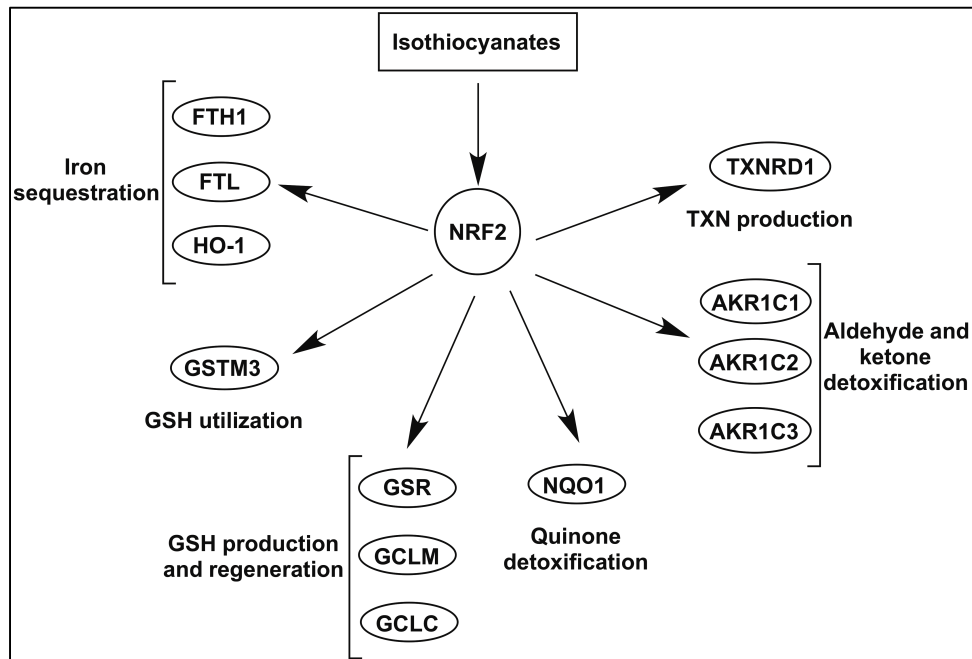


**Figure 4.4.** Wasabi-derived isothiocyanates multitargeted pathways. ITCs directly targeted Nrf2-mediated oxidative stress response pathway and indirectly targeted several antioxidant pathways controlled by Nrf2. Genes were grouped based on their antioxidant functions.

Furthermore, gene ratio comparative analyses were also performed for the significantly modulated by ITCs in HepG2 and IMR-32 cells (Tables 2.4 and Table 3.5). Gene ratio signified the number of statistically differentially regulated genes divided by the number of genes associated to the pathways. 6-MSITC had the highest gene ratio for Nrf2-mediated oxidative stress pathway across the treatment for both cell lines and SFN had the least. This further implies that the functions of methylene groups and the oxidation state of sulfur of the thiomethyl group were critical in not only the ITCs antioxidant inducing capabilities but also in other biological activities (Zhang *et al*, 1992; Li *et al*, 2013). However, this finding was more pronounced in HepG2 cells than in IMR-32 cells. This inconsistency could be attributed to the difference in cell type models.

Structure-canonical pathway modulation analyses among SFN, 6-MSITC and 6-MTITC highlighted (a) Nrf2-mediated oxidative stress response as the key pathway targeted by ITC compounds in HepG2 and IMR-32 cell lines; and (b) downstream pathways controlled by Nrf2 were also activated in response to ITCs treatment in both cell lines.

#### **4.1.3.2. Cell type effect**

The use of *in vitro* cell lines has become an ideal model since they offer a cost-effective solution for measuring and mapping out phytochemical response, and gene-gene interaction. As seen from the previous discussions, not all cells expressed all or similar genes as characterized by their varied response to ITC treatments indicating the wide-ranging biochemical properties of individual cell lines.

The data presented herein indicate that aside from modulation of signaling pathway by ITCs in HepG2 cells is significantly different from the signal pathway modulation in IMR-32 cells (Figure 4.5). The extent of regulation of the Nrf2-mediated oxidative stress response pathway by ITCs is higher in IMR-32 cells than HepG2 cell which correlates with the higher induction of antioxidants in IMR-32 cells. Genes associated with Nrf2-mediated oxidative stress pathway were observed to have different induction levels in HepG2 and IMR-32 cells. These could be associated with the cell-specific differences in ARE/EpRE activation which is necessary together with Nrf2 for the induction of antioxidant genes (Moehlenkamp *et al*, 1999). Although both cell types activated Nrf2 in response to ITCs, the cell lines showed differences in the secondary pathways that are significantly modulated. These may be due to the dissimilarities in the



up- and downregulated transcription factors between HepG2 and IMR-32 cells. For instance, gene expression profiles of unstimulated HepG2 showed that *Wnt*, cell growth and cell survival pathways were deregulated (Adesina *et al*, 2009). Interestingly, TR/RXR pathway was predominant in IMR-32 cells as a results of ITCs treatment. Activation of transcription factors PPAR/RXR and RAR/RXR have been explored for neuro therapeutic strategy but studies implicating activation TR/RXR transcription factor remain elusive. Although PPAR/RXR and RAR/RXR relevance to neurological disease is far from conclusive but studies have shown promising results. PPARs and RARs display anti-inflammatory which could be very useful for pathological processes involving microglia, macrophages and astrocytes and of particular importance to most neurodegenerative diseases (Neerven *et al*, 2008). Thus, the finding of this study could provide preliminary evidence about the possible neuroprotective effect of ITCs via the TR/RXR signal transduction. This also implies that TR/RXR signal transduction could also a promising target for neuroprotective function and it will be interesting to know the molecular mechanism behind.

When cell-type was considered the variable in pathway network and global functional analysis by ITC the following findings were observed (a) Nrf2 pathway is active in both cell types; (b) TR/RXR signal pathway is dominant in IMR-32 cells in response to ITCs treatment.

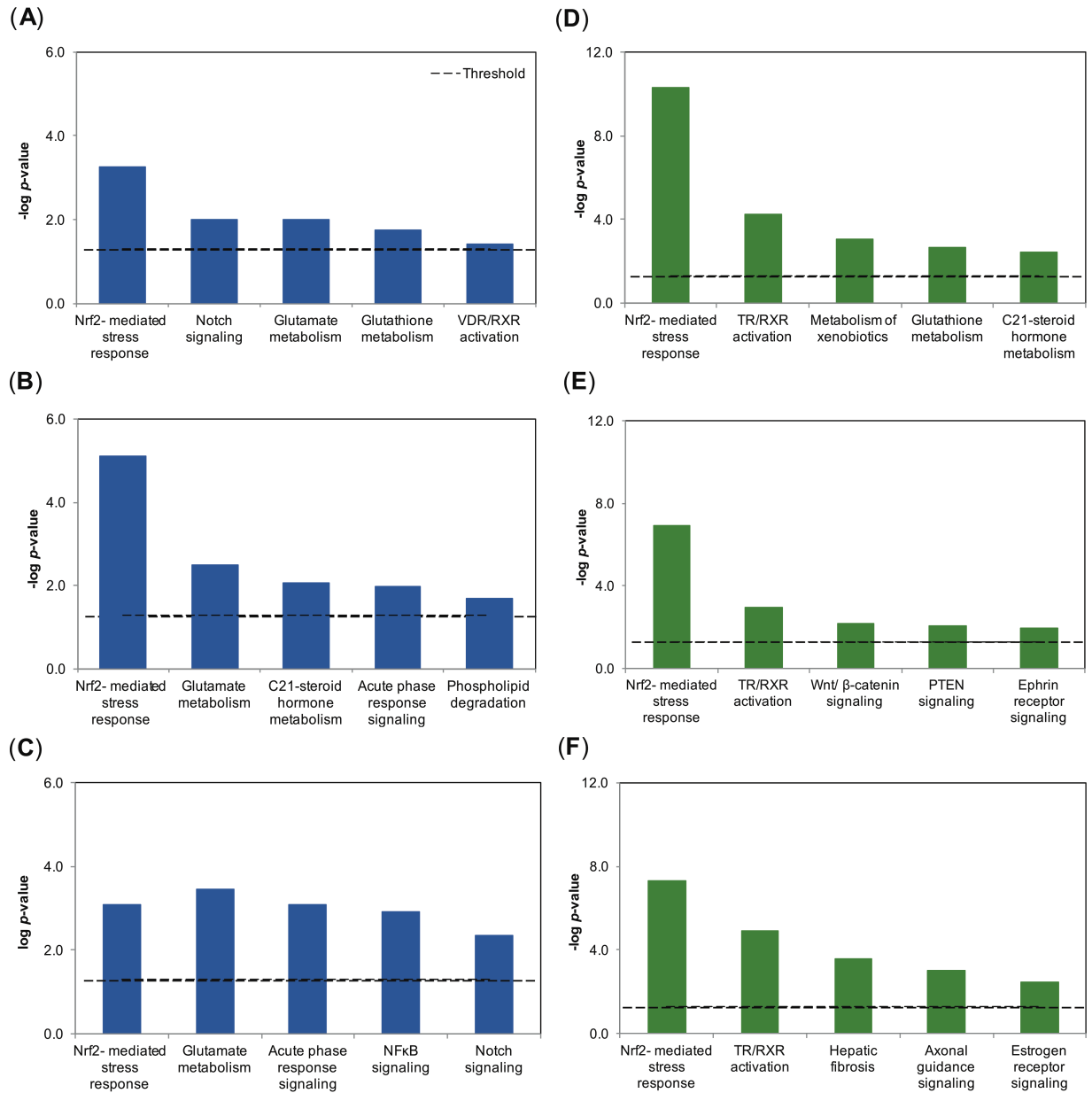


**Figure 4.5.** Comparative analyses of significantly modulated pathways by ITCs in HepG2 and IMR-32 cell lines. **(A)** SFN-treated HepG2 cells; **(B)** 6-MSITC-treated HepG2 cells; **(C)** 6-MTITC-treated HepG2 cells; **(D)** SFN-treated IMR-32 cells **(E)** 6-MSITC-treated IMR-32 cells; **(F)** 6-MTITC-treated IMR-32 cells.

#### 4.1.4. Nrf2-ARE pathway activation underlying mechanisms as the major target of Wasabi-derived ITCs in hepatic and neuron cell models

As discussed earlier, Wasabi-derived ITCs can modulate Nrf2 pathway and significantly upregulate antioxidant-related genes at the transcriptional levels in HepG2 and IMR-32 cell lines (Tables 2.4 and 3.5). However, no significant change in the *Nrf2* gene at the transcriptional level (Table 4.2). Thus, the effects of ITCs at the posttranscriptional level was investigated using 6-MSITC since it was the most potent inducer of antioxidant genes at the transcriptional level.

**Table 4.2.** Nrf-2 gene expression changes by SFN, 6-MSITC, and 6-MTITC in HepG2 and IMR-32 cell lines.

Gene ID	SFN		6-MSITC		6-MTITC	
	HepG2	IMR-32	HepG2	IMR-32	HepG2	IMR-32
AF323119	-1.01	1.06	-1.01	-1.02	-1.03	1.04
AF323119	-1.08	1.11	-1.14	1.04	-1.10	-1.06
AF323119	-1.25	1.06	-1.21	1.14	-1.20	1.13
NM_006164	-1.06	1.06	-1.10	1.04	-1.09	1.10

At the post transcriptional analysis, molecular evidence showed that 6-MSITC could activate Nrf2 at the protein level while keeping the expression of Keap1 at a steady state (Vauzour *et al*, 2010). Wasabi-derived ITCs could covalently modify Keap1; thereby, inhibiting Nrf2 ubiquitination and enhancing Nrf2 stability leading to ARE-driven activation (Korenori *et al*, 2013; Hou *et al*, 2011). In response to Nrf2-ARE activation, an increase in the expression of cytoprotective proteins could follow. The data demonstrated that Wasabi-derived ITCs exert antioxidant function by activating Nrf2 leading to upregulation of downstream antioxidant proteins which was also reported by Hou *et al* (2011). However,

in cancer cells, 6-MTITC was observed to be a stronger antioxidant inducer per concentration than 6-MSITC since 6-MTITC has a higher maximal attainable response (Itoh *et al*, 1997). In contrast, 6-MSITC had a longer effective window but of late response than 6-MTITC since 6-MSITC had late induction of antioxidant protein expression which continuously increase. Another study using the cancer cell model reported that lengthening the carbon chain between the sulfinyl sulfur and the ITC group from 4 to 6 carbon atoms has a beneficial effect on Nrf2 activation, whereas the increasing steric size of the substituent on the sulfur atom contributes a negative effect on the biological activity (Elhalem *et al*, 2014). Additionally, ITCs has been found to accumulate rapidly in various cell lines and can penetrate the blood brain barrier to deliver its neuroprotective function in the central nervous system (Zhang, 2001; Tarozzi *et al*, 2013). ITCs can even be absorbed by the body and remain at micromolar amount in the blood suggesting that the concentration used in this study is achievable to deliver protective effects and activation of the cellular targets.

The molecular data of this study showed that 6-MSITC could (a) induce upregulation of Nrf2 at the posttranscriptional level in HepG2 and IMR-32 cell lines; (b) stabilize Nrf2 via inhibiting of the Nrf2 protein turn over and by stimulating Nrf2 gene transcriptional expression; and that (c) 6-MTITC was potent antioxidant in cancer cell but 6-MSITC had a longer protective effect.

## 4.2. Conclusions

The concluded DNA gene expression profiling in hepatic and neuronal cell lines was performed to investigate the genome-wide gene expression changes associated to Wasabi-derived isothiocyanates and to determine the underlying mechanism towards its targets to exert biological effects.

From the results of the study, the following conclusions were derived:

1. The number of methylene groups bridging the methyl sulfur and isothiocyanate functional group is correlated with the potency of ITCs as gene expression changes inducer in HepG2 and IMR-32 cells but the oxidation state of sulfur at the methyl sulfinyl group had no significant influence;
2. Both the number of methylene groups and sulfur oxidation states enhanced the strength of ITCs as antioxidant gene and gene products inducer;
3. IMR-32 cells were more sensitive gene expression changes in response to ITCs treatments than HepG2 cells;
4. Genes associated with cell proliferation were specific to HepG2 while CNS specific function-related genes were distinct to IMR-32 cells;
5. Nrf2-mediated oxidative stress response pathway were the main signal pathway targeted by ITCs in HepG2 and IMR-32 cells;
6. Nrf2 signal pathway were upregulated by ITCs at the posttranscriptional level in HepG2 and IMR-32 cells through inhibition of Nrf2 protein turn over resulting to the stabilization of Nrf2 and induction of Nrf2 mediated genes; and
7. Lastly, aside from Nrf2 pathway, TR/RXR signal pathway was also activated by ITCs in IMR-32 cells.

## Chapter V

### References

1. Adesina AM, Lopez-Terrada D, Wong KK, Gunaratne P, Ngyuyen Y, Pulliam J, Margolin J, and Finegold M: Gene expression profiling reveals signatures characterizing histologic subtypes of hepatoblastoma and global deregulation in cell growth and survival pathways. *Hum Pathol* **40**, 843–853, 2009.
2. Alam J, Stewart D, Touchard C, Boinapally S, Choi AM, and Cook JL: Nrf2, a cap'n'collar transcription factor, regulates induction of the heme oxygenase-1 gene. *J Biol Chem* **274**, 26071–26078, 1999.
3. Atwell LL, Beaver LM, Shannon J, Williams DE, Dashwood RH, and Ho E: Epigenetic regulation by sulforaphane: Opportunities for breast and prostate cancer chemoprevention. *Curr Pharmacol Rep* **1**, 102–111, 2015.
4. Babish JG, Pacioretty LM, Bland JS, Minich DM, Hu J, and Tripp ML: Antidiabetic screening of commercial botanical products in 3T3-L1 adipocytes and *db/db* mice. *J Med Food* **13**, 535–547, 2010.
5. Barrett JC, and Kawasaki ES: Microarrays: the use of oligonucleotides and cDNA for the analysis of gene expression. *Drug Discov Today* **8**, 134–141, 2003.
6. Berard A, Kroeker AL, and Coombs KM: Transcriptomics and quantitative proteomics in virology. *Future Virol* **7**, 1193–1204, 2012.

7. Bergantin E, Quarta C, Nanni C, Fanti S, Pession A, Cantelli-Forti G, Tonelli R, and Hrelia P: Sulforaphane induces apoptosis in rhabdomyosarcoma and restores TRAIL-sensitivity in aggressive alveolar subtype leading to tumor elimination in mice. *Cancer Biol Ther* **15**, 1219–1225, 2014.
8. Botstein D, Butler H, Cherry M, Davis AP, Dolinski K, Dwight SS, Eppig JT, Harris MA, Hill DP, Issel-Taver L, Kasarskis A, Lewis S, Matese JC, Richardson JE, Ringwald M, Rubin GM, and Sherlock G: Gene Ontology: tool for the unification of biology. *Nat Genet* **25**, 25–29, 2000.
9. Brown RH, Reynolds C, Brooker A, Talalay P, and Fahey JW: Sulforaphane improves the bronchoprotective response in asthmatics through Nrf2-mediated gene pathways. *Respir Res* **16**, 1–12, 2015.
10. Calkins MJ, Johnson DA, Townsend JA, Vargas MR, Dowell JA, Williamson TP, Kraft AD, Lee JM, Li J, and Johnson JA: The Nrf2/ARE pathway as a potential therapeutic target in neurodegenerative disease. *Antioxid Redox Signal* **11**, 497–508, 2009.
11. Cantor CR, Mirzabekov A, and Southern E: Report on the sequencing by hybridization workshop. *Genomics* **13**, 1378–1383, 1992.
12. Chadwich CI, Lumpkin TA, and Elbertson LR: The botany, uses and production of *Wasabia Japonica* (Miq.) (Cruciferae) Matsum. *Econ Bot* **47**, 113–135, 1993.
13. Chaudhuri D, Orsulic S, and Ashok BT: Antiproliferative activity of sulforaphane in Akt-overexpressing ovarian cancer cells. *Mol Cancer Ther* **6**, 334–345, 2007.

14. Chen J, Qin S, Xiao J, Tanigawa S, Uto T, Hashimoto F, Fujii M, and Hou DX: A genome-wide microarray highlights the anti-inflammatory genes targeted by oolong tea theasinensin A in macrophages. *Nutr Cancer* **63**, 1064–1073, 2011.
15. Chen J, Uto T, Tanigawa S, Kumamoto T, Fujii M, and Hou DX: Expression profiling of genes targeted by bilberry (*Vaccinium myetillus*) in macrophages through DNA microarray. *Nutr Cancer* **60**, 43–50, 2008.
16. Chen J, Uto T, Tanigawa S, Yamada-Kato T, Fujii M, and Hou DX: Microarray-based determination of anti-inflammatory genes targeted by 6-(methylsulfinyl)hexyl isothiocyanate in macrophages. *Exp Ther Med* **1**, 33–40, 2010.
17. Choi P, Jordan CD, Mendez E, Houck J, Yueh B, Farwell DG, Futran N, and Chen C: Examination of oral cancer biomarkers by tissue microarray analysis. *Arch Otolaryngol Head Neck Surg* **134**, 539–546, 2008.
18. Chorley BN, Campbell MR, Wang X, Karaca M, Sambandan D, Bangura F, Xue P, Pi J, Kleeberger SR, and Bell DA: Identification of novel Nrf2-regulated genes by ChIP:Seq: influence on retinoid X receptor alpha. *Nucleic Acid Res* **40**, 7416–7429, 2012.
19. Chung YK, Or RCH, Lu CH, Ouyang WT, Yang SY, and Chang CC: Sulforaphane down-regulates SKP2 to stabilize p27KIP1 for inducing anti-proliferation in human colon adenocarcinoma cells. *J Biosci Bioeng* **119**, 35–42, 2015.
20. Clarke JD, Hsu A, Williams DE, Dashwood RH, Stevens JF, Yamamoto M, and Ho E: Metabolism and tissue distribution of sulforaphane in Nrf2 knockout and wild-type mice. *Pharm Res*, **28**, 3171–3179, 2011.



21. Colombo PE, Milanezi F, Weigelt B, and Reis-Fiho J: Microarray in the 2010s: the contribution of microarray-based gene expression profiling to breast cancer classification, prognostication and prediction. *Breast Cancer Res* **13**, 212–227, 2011.
22. Danilov C, Chandrasekaran K, Racz J, Soane L, Zielke C, and Fiskum G: Sulforaphane protects astrocytes against oxidative stress and delayed death caused by oxygen and glucose deprivation. *Glia* **57**, 645–656, 2009.
23. Dash PK, Zhao J, Orsi SA, Zhang M, and Moore AN: Sulforaphane improves cognitive function administered following traumatic brain injury. *Neurosci Lett* **460**, 103–107, 2009.
24. Depree JA, Howard TM, and Savage GP: Flavour and pharmaceutical properties of the volatile sulphur compounds of Wasabi. *Food Res Int* **31**, 329–337, 1999.
25. DeRisi J, Penland L, Brown PO, Bittner ML, Meltzer PS, Ray M, Chen Y, Su YA, and Trent JM: Use of a cDNA microarray to analyse gene expression patterns in human cancer. *Nat Genet* **14**, 457–460, 1996.
26. Dwivedi S, Rajaseker N, Hanif K, Nath C, and Shukla R: Sulforaphane ameliorates okadaic acid-induced memory impairment in rats by activating the Nrf2/HO-1 anti-oxidant pathway. *Mol Neurobiol* **53**, 5310–5323, 2016.
27. Elhalem E, Recio R, Werner S, Lieder F, Calderon-Montaña JM, Lopez-Lazaro M, Fernandez I, and Khair N: Sulforaphane homologues: Enantiodivergent synthesis of both enantiomers, activation of the Nrf2 transcription factor and selective cytotoxic activity. *Eur J Med Chem* **87**, 552–563, 2014.
28. Endo Y, Fu Z, Abe K, Arai S, and Kato H: Dietary protein quantity and quality affect

- rat hepatic gene expression. *J Nutr* **132**, 3632–3637, 2002.
29. Etoh H, Nishimura A, Takasawa R, Yagi A, Saito K, Sakata K, Kishima I, and Ina K:  $\omega$ -Methylsulfinylalkyl isothiocyanates in wasabi, *Wasabia japonica* Matsum. *Agric Biol Chem* **54**, 1587–1589, 1990.
  30. Fahmideh L, Kord H, and Shiri Y: Importance of microarray technology and its application. *J Curr Res Sci* **4**, 24–28, 2016.
  31. Fenwick GR, Heaney RK, Mullin WJ, and VanEtten CH: Glucosinolates and their breakdown products in food and plants. *Crit Rev Food Sci Nutr* **18**, 123–201, 1982.
  32. Freiberg C, Fischer HP, and Brunner NA: Discovering the mechanism of action of novel antibacterial agents through transcriptional profiling of conditional mutants. *Antimicrob Agent Chemother* **49**, 749–759, 2005.
  33. Frohlich DA, McCabe MT, Arnold RS, and Day ML: The role of Nrf2 in increased reactive oxygen species and DNA damage in prostate tumorigenesis. *Oncogene* **27**, 4353–4362, 2008.
  34. Fuentes F, Paredes-Gonzales X, and Kong AT: Dietary glucosinolates sulforaphane, phenethyl isothiocyanate, indol-3-carbinol/3,3'-diindolylmethane: Antioxidative stress/inflammation, Nrf2, epigenetics/epigenomics and *in vivo* cancer preventive efficacy. *Curr Pharm Reports* **1**, 179–196, 2015.
  35. Fuke Y, Ohishi Y, Iwashita K, Ono H, and Shinohara K: Growth suppression of MKN-28 human stomach cancer cells by wasabi (*Eutrema wasabi* Maxim.). *J Jap Soc Food Sci* **41**, 709–711, 1994.
  36. Gan N, Mi L, Sun X, Dai G, Chung FL, and Song L: Sulforaphane protects microcystin-LR-induced toxicity through activation of the Nrf2-mediated defense

- response. *Toxicol Appl Pharmacol* **247**, 129–137, 2010.
37. Gerhold DL, Jensen RV, and Gullan SR: Better therapeutics through microarrays. *Nat Genet* **32**, 547–552, 2002.
  38. Gozzelino R, JeneY V, and Soares MP: Mechanisms of cell protection by heme oxygenase-1. *Annu Rev Pharmacol Toxicol* **50**, 323–254, 2010.
  39. Han J, Lee YJ, Lee SY, Kim Em, Moon Y, Kim HW, and Hwang O: Protective effect of sulforaphane against dopaminergic cell death. *J Pharmacol Exp Ther* **321**, 249–256, 2007.
  40. Hedge P, Qi R, Abernathy K, Gay C, Dharap S, Gaspard R, Hughes JE, Snesrud E, Lee N, and Quackenbush J: A concise guide to cDNA microarray analysis. *BioTechniques* **29**, 548–562, 2000.
  41. Hodge WH: Wasabi – Native condiment plant of Japan. *Econ Bot* **28**, 118–129, 1974.
  42. Holst B and Williamson G: A critical review of the bioavailability of glucosinolates and related compounds. *Nat Prod Rep* **21**, 425–447, 2004.
  43. Hong Y, Yan W, Chen S, Sun CR, and Zhang JM: The role of Nrf2 signaling in the regulation of antioxidants and detoxifying enzymes after traumatic brain injury in rats and mice. *Acta Pharmacol Sin* **31**, 1421–1430, 2010.
  44. Hou DX, Fukuda M, Fujii M, and Fuke Y: Transcriptional regulation of nicotinamide adenine dinucleotide phosphate: quinone oxidoreductase in murine hepatoma cells by 6-(methylsulfinyl)hexyl isothiocyanate, an active principle of wasabi (*Eutrema wasabi* Maxim.). *Cancer Lett* **20**, 195–200, 2000.

45. Hou DX, Korenori Y, Tanigawa S, Yamada-Kato T, Nagai M, He X, and He J: Dynamics of Nrf2 and Keap1 in ARE-mediated NQO1 expression by Wasabi-6-(methylsulfinyl)hexyl isothiocyanate. *J Agr Food Chem* **59**, 11975–11982, 2011.
46. Hsuan SW, Chyau CC, Hung HY, Chen JH, and Chou FP: The induction of apoptosis and autophagy by *Wasabi japonica* extract in colon cancer. *Eur J Nutr* **55**, 491–503, 2016.
47. Hu R, Hebbar V, Kim BR, Chen C, Winnik B, Buckley B, Soteropoulos P, Tolias P, Hart RP, and Tony Kong AN: *In vivo* pharmacokinetics and regulation of gene expression profiles by isothiocyanate sulforaphane in the rat. *J Pharmacol Exper* **310**, 263–271, 2004.
48. Hu R, Xu C, Shen G, Jain M, Khor TO, Gopalkrishnan A, Lin W, Reddy B, Chan JY, and Kong ANT: Gene expression profiles induced by cancer chemopreventive isothiocyanate sulfuraphane in liver of C57BL/6J mice and C57BL/6J/Nrf2 (-/-) mice. *Cancer Lett* **243**, 170–192, 2006.
49. Ina K, Ina H, Ueda M, Yagi A, and Kishima I:  $\omega$ -Methylthioalkyl isothiocyanates in Wasabi. *Agric Biol Chem* **53**, 537–538, 1989.
50. Isshiki K and Tokouka K: Allyl Isothiocyanate and wholesomeness of food. *Jpn J Food Microbiol* **12**, 1–6, 1993.
51. Itoh K, Chiba T, Takahashi S, Ishii T, Igarashi K, Katoh Y, Oyake T, Hayashi N, Satoh K, Hatayama I, Yamamoto M, and Nabeshima Y: An Nrf2/small Maf heterodimer mediates the induction of phase II detoxifying enzyme genes through antioxidant response element. *Biochem Biophys Res Commun* **236**, 313–322, 1997.

52. Jung KA, and Kwak MK: The Nrf2 System as a Potential Target for the Development of Indirect Antioxidants. *Molecules* **15**, 7266–7291, 2010.
53. Kawakami Y, Yamanaka-Okumura H, Sakuma M, Mori Y, Adachi C, Matsumoto Y, Sato T, Yamamoto H, Taketani Y, Katayama T, and Takeda E: Gene expression profiling in peripheral blood cells in response to the intake of food with different glycemic index using DNA microarray. *J Nutrigen Nutrigenomics* **6**, 154–168, 2013.
54. Keum Y, Jeong W, and Tony Kong, A: Chemoprevention by isothiocyanates and their underlying molecular signaling mechanisms. *Mutat Res* **555**, 191–202, 2004.
55. Khor TO, Huang MT, Prawan A, Liu Y, Hao X, Yu S, Cheung WKL, Chan J, Reddy BS, Yang CS, and Kong AN: Increase susceptibility of Nrf2 knockout mice to colitis-associated colorectal cancer. *Cancer Prev Res* **1**, 187–191, 2008.
56. Kim YJ, Lee DH, Ahn J, Chung WJ, Kang YJ Seong KS, Moon JH, Ha TY, and Jung CH: Pharmacokinetics, tissue distribution, and anti-lipogenic/adipogenic effects of allyl isothiocyanates metabolites. *PLOS ONE* **10**, e0132151, 2015.
57. Konstantinopoulos P, Spentzos D, and Cannistra SA: Gene-expression profiling in epithelial ovarian cancer. *Nat Clin Pract Oncol* **5**, 577–587, 2008.
58. Korenori Y, Tanigawa S, Kumamoto T, Qin S, Daikoku Y, Miyamori K, Nagai M, and Hou DX: Modulation of Nrf2/Keap1 system by Wasabi 6-methylthiohexyl isothiocyanate in ARE-mediated NQO1 expression. *Mol Nutr Food Res* **57**, 854–864, 2013.
59. Kramer A, Green J, Pollard J Jr, and Tugendreich S: Causal analysis approaches in Ingenuity Pathway Analysis. *Bioinformatics* **30**, 523–530, 2014.

60. Kumagai H, Kashima N, Seki T, Sakurai H, Ishii K, and Ariga T: Analysis of components in essential oil of upland Wasabi and their inhibitory effects on platelet aggregation. *Biosci Biotech Biochem* **58**, 2131–2135, 1994.
61. Kumagai K, Kashima N, Seki T, Sakurai H, Ishii K, and Ariga T: Analysis of volatile components in essential oil of upland wasabi and their inhibitory effects on platelet aggregation. *Biosci Biotech Biochem* **58**, 2131–2135, 1994.
62. Kuno T, Hirose Y, Yamada Y, Imaida K, Tatematsu K, Mori Y, and Mori H: Chemoprevention of 1,2-dimethylhydrazine-induced colonic preneoplastic lesions in Fischer rats by 6-methylsulfinylhexyl isothiocyanate, a wasabi derivative. *Oncol Lett* **1**, 273–278, 2010.
63. Lahiri DK: The stability of beta-amyloid precursor protein in nine different cell types. *Biochem Mol Biol Int* **29**, 849–858, 1993.
64. Lee CK, Klopp RG, Weindruch R, and Prolla TA: Gene expression profile of aging and its retardation by caloric restriction. *Science* **285**, 1390–1393, 1999.
65. Lee JM, Calkins MJ, Chan K, Kan YW, and Johnson JA: Identification of the NF-E2-related factor-2-dependent genes conferring protection against oxidative stress in primary cortical astrocytes using oligonucleotide microarray analysis. *J Biol Chem* **278**, 12029–12038, 2003.
66. Lee YS: Anti-oxidant effect of *Wasabi Japonica* extracts. *Korean J Oriental Prev Medical Soc* **12**, 119–126, 2008.
67. Li J, and Johnson JA: Time-dependent changes in ARE-driven gene expression by use of a noise-filtering process for microarray. *Physiol Genomics* **9**, 137–144, 2002.

68. Li B and You L: Predictive power of cell-to-cell variability. *Quant Biol* **1**, 131–139, 2013.
69. Lopez-Terrada D, Gunaratne PH, Adesina AM, Pulliam J, Hoang DM, Nguyen Y, Mistretta TA, Margolin J, and Finegold MJ: Histologic subtypes of hepatoblastoma are characterized by the differential canonical Wnt and Notch pathway activation in DLK+ precursors. *Hum Path* **40**, 783–794, 2009.
70. Lu S: Regulation of glutathione synthesis. *Mol Aspects Med* **30**, 42–59, 2009.
71. Mazzarello P: A unifying concept: the history of cell theory. *Nat Cell Bio* **1**, E13–E15, 1999.
72. McGrath-Morrow SA, Lauer T, Yee M, Neptune E, Podowski M, Thimmulappa R, O'Reilly M, and Biswal S: Nrf2 increases survival and attenuates alveolar growth inhibition in neonatal mice exposed to hyperoxia. *Am J Physiol Lung Cell Mol Physiol* **296**, L565–L573, 2009.
73. Meister A, and Anderson ME: Glutathione. *Annu Rev Biochem* **52**, 711–760, 1983.
74. Mizuno K, Kume T, Muto C, Takada-Takatori Y, Izumi Y, Sugimoto H, and Akaike A: Glutathione biosynthesis via activation of the nuclear factor E2–related factor 2 (Nrf2)–antioxidant-response element (ARE) pathway is essential for neuroprotective effects of sulforaphane and 6-(methylsulfinyl)hexyl isothiocyanate. *J Pharmacol Sci* **115**, 320–328, 2011.
75. Moehlenkamp J, and Johnson JA: Activation of antioxidant/electrophile-responsive elements in IMR-32 human neuroblastoma cells. *Arch Biochem Biophys* **363**, 98–106, 1999.
76. Morroni F, Sita G, Tarozzi A, Cantelli-Forti G, and Hrelia P: Neuroprotection by 6-

- (methylsulfinyl)hexyl isothiocyanate in a 6-hydroxydopamine mouse model of Parkinson's disease. *Brain Res* **1589**, 93–104, 2014.
77. Myzak MC, Dashwood WM, Orner GA, Ho E, and Dashwood RH: Sulforaphane inhibits histone deacetylase in vivo and suppresses tumorigenesis in Apcmin mice. *FASEB J* **20**, 506–508, 2006.
  78. Nagai M, and Okunishi I: The effect of Wasabi rhizome extract on atopic dermatitis-like symptoms in HR-1 hairless mice. *J Nutr Sci Vitaminol* **55**, 195–200, 2009.
  79. Naranayan BA, Naranayan NK, Simi B, and Reddy BS: Modulation of inducible nitric oxide synthase and related pro-inflammatory genes by the omega-3 fatty acid docosahexaenoic acid in human colon cancer cells. *Cancer Res* **63**, 972–979, 2003.
  80. Neerven SV, Kampmann E, and Mey J: RAR/RXR and PPAR/RXR signaling in neurological and psychiatric diseases. *Prog Neurobiol* **85**, 433–451, 2008.
  81. Nguyen T, Huang HC, and Pickett CB: Transcriptional regulation of the antioxidant response element: Activation by Nrf2 and repression by MafK. *J Biol Chem* **275**, 15466–15473, 2000.
  82. Okamoto T, Akita N, Nagai M, Hayashi T, and Suzuki K: 6-Methylsulfinylhexyl isothiocyanate modulates endothelial cell function and suppresses leukocyte adhesion. *J Nat Med* **68**, 144–153, 2013.
  83. Okamoto T, and Akita N: 6-Methylsulfinylhexyl isothiocyanate modulates endothelial cell function and suppress leukocyte adhesion. *J Nat Med* **68**, 144–153, 2013.
  84. Ono H, Adach K, Fuke Y, and Shinohara K: Purification and structural analysis of



- substances in Wasabi (*Eutrema Wasabi* Maxim.) that suppress the growth of MKN-28 human stomach cancer cells. *J Jap Food Sci Technol* **43**, 1092–1097, 1996.
85. Ono H, Tesaki S, Tanabe S, and Watanabe M: 6-Methylsulfinylhexyl isothiocyanate and its homologues as food-originated compounds with antibacterial activity against *Escherichia coli* and *Staphylococcus aureus*. *Biosci Biotechnol Biochem* **62**, 363–365, 1998.
86. Orino K, Lehman L, Tsuji Y, Ayaki H, Torti SV, and Torti FM: Ferritin and the response to oxidative stress. *Biochem J* **357**, 241–247, 2001.
87. Otterbein LE, Soares MP, Yamashita K, and Bach FH: Heme oxygenase-1: unleashing the protective properties of heme. *Trends Immunol* **24**, 449–455, 2003.
88. Petri S, Korner S, and Kiaei M: Nrf2/ARE signaling pathway mediator in oxidative stress and potential therapeutic target in ALS. *Neurol Res Int* **2012**, 878030, 2012.
89. Poustka A, Pohl T, Barlow DP, Zehetner G, Craig A, Michiels F, Ehrlich E, Frischauf AM, and Lehrach H: Molecular approaches to mammalian genetics. *Cold Spring Harb Symp Quant Biol* **51**, 131–139, 1986.
90. Qin S, Chen J, Tanigawa S, and Hou DX: Gene expression profiling and pathway network analysis of hepatic metabolic enzymes targeted by baicalein. *J Ethnopharmacol* **140**, 131–140, 2012.
91. Qin S, Chen J, Tanigawa S, and Hou DX: Microarray and pathway analysis highlight Nrf2/ARE-mediated expression profiling by polyphenol myrcetin. *Mol Nutr Food Res* **57**, 435–446, 2013.

92. Ramsey CP, Glass CA, Montgomery MB, Lindl KA, Ritson GP, Chia LA, Hamilton RL, Chu CT, and Jordan-Sciutto KL: Expression of Nrf2 in neurodegenerative diseases. *J Neuropathol Exp Neurol* **66**, 75–85, 2007.
93. Rhee SY, Wood V, Dolinski K, and Draghici S: Use and misuse of gene ontology annotations. *Nat Gen* **9**, 509–515, 2008.
94. Rushmore TH, and Kong ANT: Pharmacogenomics, regulation and signaling pathways of phase I and II drug metabolizing enzymes. *Curr Drug Metab* **3**, 481–490, 2002.
95. Ryu HY, Kyung HB, Eun JK, Sang JP, Bong L, and HO YS: Evaluation for the antimicrobial, antioxidant and antithrombosis activity of natural spices for fresh cut yam. *J Life Sci* **17**, 652–657, 2007.
96. Schena M, Shalon D, Davis RW, and Brown PO: Quantitative monitoring of gene expression patterns with a complementary DNA microarray. *Science* **270**, 467–470, 1995.
97. Seow A, Shi CY, Chung FL, Jiao D, Hankin JH, Lee HP, Coetzee GA, and Yu MC: Urinary total isothiocyanate (ITC) in a population-based sample of middle-aged and older Chinese in Singapore: relationship with dietary total ITC and glutathione S-transferase M1/T1/P1 genotypes. *Cancer Epidemiol Biomarkers Prev* **7**, 775–781, 1998.
98. Shapiro TA, Fahey JW, Wade KL, Stephenson KK, and Talalay P: Human metabolism and excretion of cancer chemopreventive glucosinolates and isothiocyanates of cruciferous vegetables. *Cancer Epidemiol Biomarkers Prev* **7**, 1091–1100, 1998.

99. Shih AY, Imbeault S, Barakauskas V, Erb H, Jiang L, Li P, and Murphy TH: Induction of the Nrf2-driven antioxidant response confers neuroprotection during mitochondrial stress *in vivo*. *J Biol Chem* **280**, 22925–22936, 2005.
100. Shin IS, Masuda H, and Naohide K: Bactericidal activity of wasabi (*Wasabia japonica*) against *Helicobacter pylori*. *Int J Food Microbiol* **94**, 255–261, 2004.
101. Shin SW, Ghimeray AK, and Park CH: Investigation of total phenolic, total flavonoid, antioxidant and allyl isothiocyanate content in the different organs of *Wasabi japonica* grown in an organic system. *Afr J Tradit Complement Altern Med* **11**, 38–45, 2014.
102. Sidransky H, Ito N, and Verney E: Influence of alpha-naphthyl-isothiocyanate on liver tumorigenesis in rats ingesting ethionine and N-2-flourenylacetamide. *J Natl Cancer Inst* **37**, 677–686, 1966.
103. Siegel D, Gustafson DL, Dehn DL, Han JY, Boonchoong P, Berliner LJ, and Ross D: NAD(P)H:quinone oxidoreductase 1: role as a superoxide scavenger. *Mol Pharmacol* **65**, 1238–1247, 2004.
104. Solis WA, Dalton TP, Dieter MZ, Freshwater S, Harrer JM, He L, Shertzer HG, and Nebert DW: Glutamate-cysteine ligase modifier subunit: mouse *Gclm* gene structure and regulation by agents that cause oxidative stress. *Biochem Pharmacol* **63**, 1739–1754, 2002.
105. Sørensen KD and Ørntoft FT: Discovery of prostate cancer biomarkers by microarray gene expression profiling. *Expert Rev Mol Diagn* **10**, 49–64, 2010.
106. Sparks LM, Xie H, Koza RA, Mynatt R, Bray GA, and Smith SR: High-fat/low-carbohydrate diets regulate glucose metabolism via a long-term transcriptional

- loop. *Metab Clin Exp* **55**, 1457–1463, 2006.
107. Sporn MB, and Liby KT: Nrf2 and cancer: the good, the bad and the important of context. *Nat Rev Cancer* **12**, 564–571, 2012.
  108. Sumida, K, Igarash Y, Toritsuka N, Matsushita T, Abe-Tomizawa K, Aoki M, Urushidani T, Yamada H, and Ohno Y: Effects of DMSO on gene expression in human and rat hepatocytes. *Hum Exp Toxicol* **30**, 1701–1709, 2011.
  109. Sun CC, Li SJ, Yang CL, Xue RL, Xi YY, Wang L, Zhao QL, and Li DJ: Sulforaphane attenuates muscle inflammation in dystrophin-deficient mdx mice via NF-E2-related factor 2 (Nrf2)-mediated inhibition of NF- $\kappa$ B signaling pathway. *J Biol Chem* **290**, 17784–17795, 2015.
  110. Taguchi K, Motohashi H, and Yamamoto M: Molecular mechanisms of the Keap1-Nrf2 pathway in stress response and cancer evolution. *Genes Cells* **16**, 123–140, 2011.
  111. Tanida N, Kawaura A, Takahashi A, Sawada K, and Shimoyama T: Suppressive effect of wasabi (pungent Japanese spice) on gastric carcinogenesis induced by MNNG in rats. *Nutr Cancer* **16**, 53–58, 1991.
  112. Tarozzi A, Angeloni C, Malaguti M, Morroni F, Hrelia S, and Hrelia P: Sulforaphane as a potential protective phytochemical against neurodegenerative diseases. *Oxid Med Cell Longev* **2013**, 415078, 2013.
  113. Thimmulappa RK, Mai KH, Srisuma S, Kensler TW, Yamamoto M, and Biswal S: Identification of Nrf2-regulated genes induced by chemopreventive agent sulforaphane by oligonucleotide microarray. *Cancer Res* **62**, 5196–5203, 2002.
  114. Trio P, Fujisaki S, Tanigawa S, Hisaniga A, Sakao K, and Hou DX: DNA microarray

- highlights Nrf2-mediated neuron protection targeted by Wasabi-derived isothiocyanates in IMR-32 cells. *Gene Regul Syst. Bio* **10**, 73–83, 2016.
115. Tsai MF, Wang CC, Chang GC, Chen CY, Chen HY, Cheng CL, Yang YP, Wu CY, Shih FY, Li CC, Lin HP, Jou YS, Lin SC, Lin CW, Chen WJ, Chan WK, Chen JJK, and Yang PC. A new tumor suppressor DnaJ-like heat shock protein, HLJ1, and survival of patients with non-small-cell lung carcinoma. *J Natl Cancer Inst* **98**, 825–838, 2006.
116. Uto T, Fuji M, and Hou DX: Effects of 6-(methylsulfinyl)hexyl isothiocyanate on cyclooxygenase-2 expression induced by lipopolysaccharide, interferon- $\gamma$  and 12-O-tetradecanoylphorbol-13-acetate. *Oncol Rep* **17**, 233–238, 2007.
117. Uto T, Fujii M, and Hou DX: Inhibition of lipopolysaccharide-induced cyclooxygenase-2 transcription by 6-(methylsulfinyl) hexyl isothiocyanate, a chemopreventive compound from *Wasabia japonical* (Miq.) Matsumura, in mouse macrophages. *Biochem Pharmacol* **70**, 1772–1784, 2005a.
118. Uto T, Fujii M, and Hou DX: 6-(Methylsulfinyl)hexyl isothiocyanate suppresses inducible nitric oxide synthase expression through the inhibition of Janus kinase 2-mediated JNK pathway in lipopolysaccharide-activated murine macrophage. *Biochem Pharmacol* **70**, 1211–1221, 2005b.
119. Uto T, Fujii M, and Hou DX: Effects of 6-(methylsulfinyl)hexyl isothiocyanate on cyclooxygenase-2 expression induced by lipopolysaccharide, interferon- $\gamma$  and 12-O-tetradecanoylphorbol-13-acetate. *Oncol Rep* **17**, 233–238, 2007.

120. Uto T, Hou DX, Morinaga O, and Shuyama Y: Molecular mechanisms underlying anti-inflammatory actions of 6-(methylsulfinyl)hexyl isothiocyanate derived from Wasabi (*Wasabi japonica*). *Adv Pharmacol Sci* **2012**, 614046, 2012.
121. Vasanthi HR, Mukherjee S, and Das DK: Health benefits of broccoli- a chemico-biological overview. *Min Rev Med Chem* **9**, 749–759, 2009.
122. Vauzour D, Buonfiglio M, Corona G, Chirafisi J, Vafeiadou K, Angeloni C, Hrelia S, Hrelia P, and Spencer JPE: Sulforaphane protects cortical neurons against 5-S-cysteinyl-dopamine-induced toxicity through the activation of ERK1/2, Nrf-2 and the upregulation of detoxification enzymes. *Mol Nutr Food Res* **54**, 532–542, 2010.
123. Wang L, Tian Z, Yang Q, Li H, Guan H, Shi B, Hou P, and Ji M: Sulforaphane inhibits thyroid cancer cell growth and invasiveness through the reactive oxygen species-dependent pathway. *Oncotarget* **6**, 25917–25931, 2015.
124. White TE and Ford BD: Gene interaction hierarchy analysis can be an effective tool for managing big data related to unilateral traumatic brain injury. In Kobeissy FH (Ed), *Brain neurotrauma: molecular, neuropsychological and rehabilitation aspects* **28**, 1–17, 2015. Boca Raton, Florida: CRC Press/ Taylor and Francis.
125. Wild A, Moinova HR, and Mulcahy T: Regulation of  $\gamma$ -glutamylcysteine synthetase subunit gene expression by the transcription factor Nrf2. *J Biol Chem* **274**, 33627–33636, 1999.
126. Wiltgen M and Tilz GP: DNA microarray analysis: principle and clinical impact. *Hematology* **12**, 271–287, 2007.
127. Wu X, Zhou QH, and Xu K: Are isothiocyanates potential anti-cancer drugs? *Acta Pharmacol Sin* **30**, 501–512, 2009.

128. Xiang CC and Chen Y: cDNA microarray technology and its application. *Biotechnol Adv* **18**, 35–46, 2000.
129. Xiang J, Alesi GN, Zhou N, and Keep RF: Protective effects of isothiocyanates on blood-CSF barrier disruption induced by oxidative stress. *Am J Physiol Regul Integr Comp Physiol* **303**, R1–R7, 2012.
130. Xu C, Huang MT, Shen G, Yuan X, Lin W, Khor TO, Conney AH, and Kong ANT: Inhibition of 7,12-dimethylbenz(a)anthracene-induced skin tumorigenesis in C57BL/6 mice by sulforaphane is mediated by nuclear factor E2-related factor 2. *Cancer Res* **66**, 8293–8296, 2006.
131. Yamasaki M, Ogawa T, Wang L, Katsube T, Yamasaki Y, Sun X, and Shiwaku K: Anti-obesity effects of hot water extract from Wasabi (*Wasabi japonica* Matsum.) leaves in mice fed high-fat diets. *Nutr Res Pract* **7**, 267–272, 2013.
132. Ye L, Dinkova-Kostova AT, Wade KL, Zhang Y, Shapiro TA, and Talalay P: Quantitative determination of dithiocarbamates in human plasma, serum, erythrocytes and urine: pharmacokinetics of broccoli sprout isothiocyanates in humans. *Clin Chim Acta* **316**, 43–53, 2002.
133. Ye L, Yu T, Li Y, Chen B, Zhang J, Wen Z, Zhang B, Zhou X, Li X, Li F, Cao W, and Huang Z: Sulforaphane enhances the ability of human retinal pigment epithelial cell against oxidative stress, and its effect on gene expression profile evaluated by microarray analysis. *Oxid Med Cell Longev* **2013**, 413024, 2013.
134. Zhang Y, Talalay P, Cho CG, and Posner GH: A major inducer of anticarcinogenic protective enzymes from broccoli: isolation and elucidation of structure. *Proc Natl Acad Sci U S A* **89**, 2399–2403, 1992.

135. Zhang Y: Molecular mechanism of rapid cellular accumulation of anticarcinogenic isothiocyanates. *Carcinogenesis* **22**, 425–431, 2001.